# ISOTOPIC AND GEOCHEMICAL STUDIES OF GEOTHERMAL SPRINGS OF NORTH WEST HIMALAYA, INDIA: IMPLICATION FOR SOURCE AND DEGASSING OF METAMORPHIC $CO_2$

By

**SAMEER K. TIWARI**

**WADIA INSTITUTE OF HIMALAYAN GEOLOGY**

**DEHRADUN**

Submitted

**IN PARTIAL FULFILLMENT OF THE REQUIREMENT OF**

**THE DEGREE OF DOCTOR OF PHILOSOPHY**

TO

**UNIVERSITY OF PETROLEUM AND ENERGY STUDIES**

**DEHRADUN**

DECEMBER, 2014

*DEDICATED*

*TO*

*MY PARENTS*

*&*

*MY WIFE 'MANJU'*

# DECLARATION

I hereby declare that this submission is my own work and that, to the best of my knowledge and belief, it contains no material previously published or written by another person nor material which has been accepted for the award of any other degree or diploma of the university or other institute of higher learning, except where due acknowledgment has been made in the text.

**Sameer K. Tiwari**

UPES
THE NATION BUILDERS UNIVERSITY

## ACKNOWLEDGEMENTS

*This thesis has benefited from the encouragement and help of many individuals and I take the immense pleasure in writing this acknowledgement.*

*Firstly, I thank my supervisors* ***Dr. Santosh K. Rai and Dr. S. K. Bartarya*** *for their guidance and advice to complete this work. Dr. Santosh K. Rai had always kept his doors open to introduce me in the field of aqueous geochemistry. Dr. Rai helped me in getting acquainted with the analysis of the samples at the Ion-chromatography and Stable isotope lab of Wadia Institute of Himalayan Geology, Dehradun. This was highly required to carry out the work pertaining to the origin and composition variation in the Himalayan geothermal systems and associated degassing process of* $CO_2$*. Sincere guidance, involvement, and concerns from Dr. S.K. Bartarya are highly appreciable which helped me to complete this thesis. His scientific suggestions and in-depth discussions were of immense help to me in shaping this thesis to its present form.*

*I sincerely express my deep sense of gratitude to* ***Prof. Anil K. Gupta*** *(Director, Wadia Institute of Himalayan Geology) for his valuable scientific suggestions,*

*support, and encouragement during the entire research period. I am also thankful to* ***Dr. P. P. Khanna, Dr. S. K. Ghosh, Dr. Kishor Kumar, Dr. H. K. Sachan, Dr. Rafikul Islam, Dr. D.P. Dobhal, Dr. A. K.L Asthana*** *and* ***Dr. Pradeep Srivastava*** *for their help and kind support at different stages of this study.*

*I also express my gratitude to Prof. S. Krishnaswami and Dr. Sunil Singh of P.R.L., Ahmedabad for their scientific discussion which helped me to improve my understanding on the research work during the analytical session. Encouragement received from* ***Dr. Bhoop Singh*** *(Advisor, DST Govt. of India) on the topic of geothermal energy has helped this work immensely.*

***Dr. Pradeep Joshi*** *and* ***Dr. D. K. Gupta*** *have been very helpful and instrumental throughout the thesis period. They suggested suitable ways to structure the thesis as per the norms of the University of Petroleum and Energy Studies, Dehradun.*

*I thankfully acknowledge the help provided by* ***Mr. Rajendra Prasad*** *during the analysis in Ion-Chromatography and Autotitrator lab at the Institute. I am highly thankful to* ***Mr. Satheesh Deekshith, Mr. Ram Mhatre (Thermo Scientific)*** *and* ***Mr. Girish Dhar*** *for their technical help during the smooth functioning of stable isotope ratio mass spectrometer at WIHG.*

*I acknowledge the help of my friends namely* ***Dr. Kavita, Dr. Amit, Matsyendra, Bhanu, Akshaya, Souvick, Mayank, Kaushik, Aditya, Tanuj, Manju, Divya,*** *and* ***Nikita*** *for their support during my Ph D thesis. I sincerely thank the staff of the*

*library, documentation unit and computer section of the Institute for their help and support for my work. I am highly indebted to my parents for their moral support, best wishes and encouragement in tough time without which this work would not have been possible. Last but not the least; I thank my wife* ***Manju*** *for her endless and unconditional support so that I could complete this work to its present form.*

**Sameer K. Tiwari**

# EXECUTIVE SUMMARY

Internal heat of the Earth has been emanating since its formation which is manifested in forms of volcanism and out gassing of volatiles from its surface. The major emphasis of this thesis is aimed at the understanding of the degassing process in the northwest Himalayan geothermal belt using isotopic and geochemical proxies of geothermal springs. The study makes an attempt to estimate the temperatures of geothermal reservoirs that give rise to geothermal springs which could be utilized for energy exploration in future. The studied springs are mainly situated close to the major tectonic boundaries (Thrust zone) which are associated with high heat flow reasons and therefore make a potential target to be explored for geothermal energy. This goal has been achieved through detailed geochemical and stable isotopic investigations of thermal spring waters. Based on these measurements, efforts have been made to assess the annual degassing flux of carbon dioxide ($CO_2$) in the Himalayan region. Findings of this study have also been used to addresses the source and origin of these geothermal fluids in terms of magmatic vs. meteoric. Chemical compositions of these springs have been used to estimate the reservoirs temperature which may be helpful in utilizing the geothermal energy as future energy source in this region.

As part of this work, forty active geothermal springs were sampled from the entire stretch of northwest Himalayan geothermal belt covering the Garhwal, Himachal and Ladakh regions of India. The surface temperatures of these springs are found to be as hot as 95˚C (i.e. Manikaran, Himachal Pradesh) in the study region. Detail geochemical and isotopic studies were undertaken through an integrated measurement of major ions, trace elements, and stable isotopes of oxygen, hydrogen and carbon in these springs. Geothermal fields sampled in this study are located around the junction of the Indian and the Asian plates where rapid uplift and erosion of the Himalayan Mountains have induced the hot rocks to move near the surface. Under such regime, interaction of hot rocks and meteoric waters has a possibility to produce thermally charged springs with elevated surface temperature up to boiling points which are found in the Himalayan region. This seems to indicate that the geothermal activities have significant controls in terms of tectonics and operational heat flow under varying setup.



These springs are mainly found around the globe in two major configurations in form of storage type and cyclic type. Geothermal springs of the Himalaya fall in the category of cyclic system where hot waters are mostly of meteoric origin and have suffered a complex cycling at various depths. These include heating, migration and upwelling of water masses to the surface. However, there may be the other possibility of the storage system, where water is stored in the rocks in isolation for geologically long periods and warmed in situ due to the accumulated heat produced by radioactive decay of uranium and thorium elements.

Geochemical studies of these springs were also employed to infer about suitable mechanisms for their origin. This suggests a way in which infiltrating water percolates through faults, joints, fractures etc., and is heated by a steep geothermal gradient before it rises to surface through the permeable zones. As a result of this process its solute composition is partially modified during ascend of fluids. Major anions chemistry of these springs shows different natures of water which indicate about the possible mixing of deep thermal fluids with meteoric waters. Their composition shows that $Na^+$ and $K^+$ are the dominant major cations in region along with elevated concentrations of trace elements. This observation reveals that these springs contain a mixture of waters associated with significant leaching of cations from the host rocks at high temperatures.

Stable isotopes (δD, $\delta^{18}O$ and $\delta^{13}C$) were measured in these springs which show similarities with surface water. However, $\delta^{13}C$ composition of these samples indicates that few of them could have resulted due to the mixing of waters other than meteoric sources. Such a scenario may involve suitable rock formations through which water penetrates up to certain depths, source of heat and sufficient availability of water, adequate time and surface area for heat exchange for water to get it thermally charged. In addition, it also requires a favourable return path to the surface. The sources of recharge in thermal springs from the study area are mainly surface waters, ground waters and precipitation excepting few of them, which bear input from deeper fluids. This is inferred from the two isotope plot (between δD and $\delta^{18}O$, which defines a linear relationship and called the Global

Meteoric Water Line, GMWL) for these springs which have yielded a slope and deuterium excess quite similar to the surface and river waters of the region. This indicates that majority of these spring waters are of meteoric origin however some of them fall off the GMWL (i.e. Chumathang and Puga samples from Ladakh) indicating their origins involve non-meteoric components. This is also evident from the carbon isotope compositions of the dissolved inorganic carbon ($\delta^{13}C_{DIC}$) in these springs which show a wide range varying from -8.4‰ to +4.1‰. The $\delta^{13}C_{DIC}$ values of geothermal springs are among the highest reported from the geothermal springs from the northwest Himalaya. However these are similar to the values of $\delta^{13}C_{DIC}$ in geothermal springs reported from Central Nepal, Himalaya, Yellowstone waters and associated travertine's from Utah, USA. This study has also estimated the metamorphic $CO_2$ flux using geochemical composition of forty geothermal springs covering Ladakh, Himachal and Garhwal regions. It has yielded a value of $2x10^8$ moles of $CO_2$/year and hence indicates that the degassing of $CO_2$ from Himalayan orogen is a significant contributor to the global carbon budget of the atmosphere on longer time scale. The altitude effect of stable isotopes has also been observed in these springs which provide an indirect tool for deducing the long time average composition of moisture in the region. This approach is robust than those which are inferred on the basis of limited flash rains in the region.

Based on chemical composition (major ion & silica) of springs, an attempt has been made to estimate the reservoir temperature for these springs using suitable

geothermometers. In the studied area, covering Garhwal, Himachal, and Ladakh regions of northwest Himalaya, it yielded the estimated reservoirs temperatures in the range of (135±15˚C) which are supposed to be minimum temperatures on the surface. Further, these springs from the Himalaya provide an abundant resource of energy through the Earth's internal heat accumulated over a longer period of time. It is relatively unpolluted and reusable in nature and hence becoming a preferred choice for an alternative energy resource worldwide. However it is yet to be explored in India for its full potential that can be exploited using state of the art technologies.

# TABLE OF CONTENTS

## List of Figures

## List of Tables

# CHAPTER 1


# INTRODUCTION

# CHAPTER 1:

# INTRODUCTION

## 1.1 INTRODUCTION

The atmosphere of Earth is a gaseous envelope which protects life by absorbing ultraviolet solar radiation and warming the surface through heat retention under greenhouse conditions. The rise in atmospheric $CO_2$ and its linkage with global climate change have provided a mechanism to understand the processes controlling the carbon cycle. Over geological time scales, Earth's degassing has been reported to have a significant impact on atmospheric $CO_2$ concentrations (Kerrick & Caldeira, 1998; Evans et al., 2008). In the Himalayan region, geological conditions and associated geothermal systems have led to release of $CO_2$ during upward movement of geothermal fluid and volatiles. Therefore, these springs can be used as an object to infer about the release of heat inside the Earth.

The natural carbon cycle includes the conversion and migration of lithospheric, atmospheric, hydrospheric and biospheric carbon, primarily in the form of carbon dioxide ($CO_2$), carbonate ($CO_3^{2-}$), bicarbonate ($HCO_3^-$), methane ($CH_4$), and ($CH_2O$). $CO_2$ being an important atmospheric greenhouse trace gas has been shown to be sourced from the deep crust (Becker et al., 2008) which emanates to the surface as volatiles and dissolved components. The geothermal systems play a key role in mediating the crustal $CO_2$

degassing to the atmosphere. Modern researches are directed towards regional and global-scale $CO_2$ degassing from the deep crust (Kerrick & Caldeira, 1998; Evans et al., 2008). Over the time, a number of studies have shown that $CO_2$ release from both volcanic eruptions and non-eruptive systems affect the global atmospheric composition (Chaidoni et al., 2004; Sano & Marty, 1995). The non-eruptive systems are generally associated with geomagnetic anomaly zones, shallow earthquake zones, gravity anomalies and high heat flow zones (Rawat, 2012) which could be the potential source of volatiles to the atmosphere.

The Himalayan orogeny, produced by the continent-continent collision, is an ongoing tectonic process across the broad region of south Asia since the last 50 million years. It has resulted from the process of under thrusting of the Indian crust beneath southern Tibet (Hochstein & Regenauer, 1998). During this process, a part of the Indian crust was scraped off which underwent crustal thickening by tectonic imbrications (Molnar et al., 1987; Bilham et al., 1997) with metamorphic reactions and crustal melting (Searle et al., 1997; Henry et al., 1997). The India-Asia collision has induced major topographic and drainage evolutions which in turn have modified the dynamics of the processes affecting the carbon cycle. The rise of the Himalaya has contributed to erosion fluxes through silicate weathering and organic carbon burial as major atmospheric sinks for $CO_2$. However, certain processes operating within the Himalaya tend to release $CO_2$ to the atmosphere. These include $CO_2$ degassing due to metamorphism of deeply subducted carbonate rocks and the oxidation of fossil organic carbon exposed to the surface during fluvial

erosion. The degassing of metamorphic $CO_2$ from the active orogeny has been suggested as the process in Earth's carbon cycle having noteworthy controls on the global climate (Kerrick & Caldeira, 1998). Such degassing processes are manifested as geothermal springs continuously emanating volatiles and are noticed mainly along the major structural discontinuity planes in the Himalaya. Thus the Himalaya provides a natural laboratory to study the various aspects of collisional orogeny (Newell et al., 2008) and their consequences in Earth system. The long-term budget of $CO_2$ in the ocean-atmosphere system is controlled by inputs from different sources including volcanism, metamorphic de-volatilization and the oxidation of sedimentary organic carbon (Molnar & England, 1990; Evans et al., 2008). Therefore this dynamic balance is maintained by outputs to the sedimentary reservoir, through the processes of chemical weathering of silicate minerals, their subsequent precipitation in form of carbonates and the burial of organic matter in flood plains and coastal seas.



In the Himalayan orogeny, the geothermal springs occur in the deeply incised valleys along the Main Central Thrust (MCT) and Indus Tsangpo Suture Zone (ITSZ) which cause significant release of metamorphic $CO_2$ (Evans, 2002, 2004, 2008; Becker et al., 2008) to the atmosphere. Earlier studies in the Himalayan region (Gyanprakash & Raina, 1975; Tong & Zhang, 1981) have documented ~600 geothermal springs occurring along its ~3000 km long belt, stretching from Pamir to the Yunnan through Tibet. These geothermal systems have been studied for geochemical features and magnitude of heat transfer properties (Hochstein & Yang, 1995). Though the distribution of geothermal

springs is not over all symmetric with respect to the axial part of the Himalaya, several of these, especially those with surface temperatures $T_s$>90˚C in the northwest Himalaya, fall along the major thrust zones. This shows that these are structurally controlled (Hochstein & Regenauer, 1998; Newell et al., 2008). However their genesis is yet to be understood fully in terms of meteoric vs. deep sources etc.

In the year 1991, Geological survey of India (GSI) has documented about 340 geothermal springs and identified more than 300 sites as plausible utilization sites for geothermal energy. Most of these geothermal spring are located in the northwestern Himalayan region and are characterised by high thermal gradient (>100˚C/km) and heat flow (>468 mW/$m^2$). The present thesis attempts: (1) to understand plausible mechanisms for the origin of geothermal waters in terms of meteoric vs. deep sources; 2) to address the issue of degassing of metamorphic $CO_2$ in the Himalayan orogenic belt; and 3) to estimate the reservoir temperature of geothermal reservoirs giving rise to thermal springs of the northwestern Himalaya. This study is expected to throw light on the degassing of metamorphic $CO_2$ from Himalaya and its contribution in the global carbon cycle, and to estimate the reservoir temperature for evaluating their potential for the geothermal energy source.

## 1.2 GEOTHERMAL SPRING

A type of spring having water above the local mean air temperature is termed as geothermal springs (Bates & Jackson, 1987). Generally a geothermal system can be found in regions with slightly above normal geothermal

gradient. Such regions could be around plate margins where, in general, the geothermal gradients are higher than the average value.

Geothermal spring can be understood as the manifestation of convecting water in the upper crust within a confined space where it transfers heat from a source to sink, usually the free surface (Hochstein, 1990). It mainly consists of three major components: a heat source, a reservoir and a carrier fluid that transfers the heat to the surface. The heat source could be either a very high temperature (>600°C) magmatic intrusion that has reached relatively shallow depths (2 to 5 km; Harinarayana et al., 2006) or as a low-temperature systems, which increases with depth. The reservoir could be a volume of hot permeable rocks from which the circulating fluids extract heat. The reservoir is usually overlain by a cover of impermeable rocks and it is connected to a surface recharge area where the meteoric water can partly replace the fluids escaping from the reservoir. The geothermal fluid is water, in the majority of cases meteoric water, which exists in form of liquid or vapour phase depending on its temperature and pressure. This water often carries the chemical constituents and gases such as $CO_2$, $H_2S$, $SO_2$, He, $CH_4$ etc.

These springs discharge heated groundwater and steam continuously from deep seated faults that describe tectonic boundaries between the Himalaya and Asia (ITSZ) between the Higher and Lesser Himalaya (MCT) and between the Lesser Himalaya and Himalayan Foreland domain (MBT). Based on their heat characteristics, these geothermal springs may have the potential to be exploited for future source of energy. Earlier reports show that India has the potential of an estimated geothermal power of ~10,600 MW (Ravishankar,

1988) which is yet to be developed to generate power. The striking feature of geothermal energy lies with the fact that it is clean, renewable and does not produce hazardous emissions (Smith, 2007; Younger & Gluyas, 2012). Further, generating energy from geothermal system is three folds economical than the hydroelectric power and therefore it is worth exploring the possibilities of developing geothermal systems as objects of energy for future.

## 1.3 PREVIOUS WORK

Atmospheric abundance of $CO_2$ is a crucial component that influences the heat budget and the climate on various time scales. It is regulated by the processes like photosynthesis, chemical weathering of silicate rocks, oxidative weathering of organic matter, burial of organic carbon (in flood plains, and oceanic basins) and metamorphic degassing along the orogenic belts on geological time scales (Gaillardet et al., 1997; France Lanord & Derry, 1997; Krishnaswami et al., 1999; Dalai et al., 2002; Galy et al., 2007, 2008; Evans et al., 2002, 2004, 2008). Therefore the magnitude and rate of degassing of metamorphic $CO_2$ along the major Himalayan tectonic zones is important to understand the global carbon cycle.

Though these processes have been studied intensively, their relative roles in regulating the atmospheric $CO_2$ budget are needed to be quantified. Earlier studies (Bickle, 1996; Evans et al., 2002, 2004, & 2008) are based on the geochemical analyses of fluids and volatiles emanating from the natural geothermal springs along the Main Central Thrust (MCT) zone of the Nepal Himalaya. They have indicated that these zones could be the plausible source of $CO_2$ to the atmosphere with a flux comparable to that by $CO_2$ consumption

via chemical weathering of silicate rocks. Therefore it is important to study these fluxes in a quantitative fashion. The mechanism for this $CO_2$ flux is suggested to be induced by metamorphic reactions (decarbonation and decarboxylation) occurring in the subducted Lesser Himalayan sediments beneath the Himalayan front. Further, this process may also have implications on the carbonate-silicate weathering cycle in the Himalaya which is against the paradigm that suggests Himalaya as an important $CO_2$ sink. However such finding are based on the limited data sets representing only a ~150 km long section of the Nepal Himalaya and southern Tibet against its total stretch of ~3000 km and their generalization for whole of the Himalayan region remains unclear. Therefore it is important to address the degassing of metamorphic $CO_2$ in the Indian Himalaya for a better and representative estimate of the process. Such an estimate may be useful in quantifying the extent of $CO_2$ emanating though the northwestern Himalayan region. Further, the origin of these springs has also been contested in terms of meteoric vs. deep sourced volatiles and hence it needs to be tested in Himalayan set up. This work uses the geochemistry and stable isotopic study of the geothermal springs from the northwest Himalaya (India) to address these issues under certain assumptions as follows:

(1) Extrapolation from a measurement of the short-term flux to the geological long-term flux for the whole mountain ranges (Evans et al., 2008). Due to changes occurring over of the thermal history, an orogenic belt could well be a source or a sink of $CO_2$.

(2) The organic sub-cycle of carbon in the Himalaya does not differ from the whole organic sub-cycle of carbon and is not a major flux of $CO_2$ consumption. This has recently been challenged by the workers (Galy et al., 2007), who have shown that the Himalaya scavenges a factor of 10 more $CO_2$ by organic burial than by chemical weathering.

(3) Questions about the time scale at which a mountain range becomes carbon neutral. This means that the $CO_2$ degassed by the Himalaya eventually reacts with silicate minerals and leads to the formation of carbonate in ocean followed by their heating and degassing to complete the carbon cycle. On the time scale of this geological loop (typically 20 to 50 million years; Gaillardet & Galy, 2008) the net effect of metamorphic $CO_2$ on the global carbon cycle, at steady state, is null. However, if steady state is not achieved and a fraction of sedimentary carbon is re-injected into the mantle and subsequently degassed at mid-oceanic ridge or hot spots, mountain ranges only become carbon neutral on time scales of billions of years (Gaillardet & Galy, 2008).



(4) Therefore, in light of above, mountain ranges appear to have several impacts on the global carbon cycle and hence global climate. Whether they are net sources or sinks of atmospheric $CO_2$, it can only be assesses by considering the importance of different processes at their relevant time scales: the consumption of $CO_2$ by rock weathering (silicate and carbonate), the balance between organic matter burial and oxidation of sedimentary organic matter, and the fluxes of $CO_2$

degassing. Further, reconstructing the evolution of atmospheric $CO_2$ over geological time would depend on how these mechanisms and their respective time scales interact among them.

## 1.4 OBJECTIVES OF THE THESIS

The present study is attentive on the geochemical (including isotopic) characteristics of geothermal springs in the northwest Himalaya through the following main objectives:

1. ***To study the isotopic and geochemical characteristics of the geothermal springs in the northwest Himalaya to get insights into their source of origin and degassing of metamorphic $CO_2$.***
2. ***To study the altitude effect on stable isotopes of oxygen ($\delta^{18}O$) if these geothermal springs having meteoric affinity.***
3. ***To estimate the reservoir temperature of these springs.***

## 1.5 CONTRIBUTION OF RESEARCH

This work attempts to address some important issues pertaining to the origin of geothermal springs in the northwest Himalaya and their contribution in $CO_2$ budget to the atmosphere. In addition, majority of the springs, taken up in this study have been demonstrated to be sourced from meteoric waters. These results have facilitated the use of isotopic data to trace the altitude effect of stable isotopes in the Himalayan region. The importance of estimating altitude

effect in this study lies with the fact that it represents an average precipitation (integrated over the residence time of waters in these springs) which could be a better estimate than those based on a single rain sample.

This work focuses on Indian Himalaya to estimate the metamorphic $CO_2$ flux and the nature of geothermal fluids in terms of their origin. These issues have significant bearing on the on going research whether Himalaya serves as sink or source of $CO_2$ in global model of climate change. Results obtained in this work may be used for the understanding of the geothermal reservoirs to provide inputs to further energy exploration attempts from the Himalayan region.

## 1.6 OUTLINE OF THESIS CHAPTERS

This thesis is divided into the eight chapters covering major aspects of northwest Himalayan springs which are briefed as follows.

*Chapter 1* Presents the current state of the knowledge of these topics through a brief description of introduction, motivation, and previous studies of the geothermal springs in the Himalayan region.

*Chapter 2* Describes the regional geological setup of the Himalaya and geological setup of geothermal springs of the northwest Himalaya. First part of the chapter provides a brief account of the overall geologic and tectonic setup of the Himalaya whereas the second outlines the details of geological and structural attributes of the geothermal springs with discussion on the major tectonic boundaries of the northwest Himalaya.

*Chapter 3* Outlines about the sampling details and different analytical techniques adopted for the measurements of various parameters of geothermal springs. It contains information on the isotopic and geochemical analysis. In addition, it describes the field work and sampling strategies of geothermal springs. All the analytical techniques used for their physical, chemical and stable isotopic parameters are presented in a flow diagram, given in the chapter.

*Chapter 4* Presents the data on major ions, trace elements, and physical parameters (pH, EC, Temperature, and TDS) in geothermal springs and river waters from the study area. These measurements have been utilized to determine the distribution of major and trace elements and their sources in geothermal waters. These data have also been used to infer about the nature of fluids presents in these springs and to estimate the metamorphic $CO_2$ flux of the degassing process.



*Chapter 5* Presents and discusses the data on stable isotopes of ($\delta^{18}O$, $\delta D$) composition of the geothermal springs. These results have been used to discuss the $\delta^{18}O$ and $\delta D$ relationship and to infer on their altitude effect. It also describes the origin of geothermal waters in terms of meteoric vs. magmatic or deep sources.

*Chapter 6* Presents the data on $\delta^{13}C_{DIC}$ of geothermal springs which dwells upon the origin of geothermal springs and degassing process of metamorphic $CO_2$ using as an independent proxy. In this chapter, schematic diagrams are also presented to explain the

enrichment process in $\delta^{13}C$ composition of thermal springs and their possible link to magmatic or deeply sourced fluids.

*Chapter 7* Presents the data on dissolved silica in the water samples from the study area. First part of this chapter discusses about the geochemical thermometry and dissolved silica thermometry using abundance of dissolved silica to estimate the reservoir temperature of individual springs. In the second part, estimates of the reservoir temperature for the individual geothermal springs have been given which may be used to utilization towards geothermal energy.

*Chapter 8* Contains the syntheses of the results from this study and major conclusions drawn from them. At the end, with the scopes of future work, it addresses some of the issue that has been borne out of this study. In addition, limitation of this work has also been presented in this chapter.

# *CHAPTER 2*

# *REGIONAL SETTING AND GEOLOGY*

# CHAPTER 2:

# REGIONAL SETTING AND GEOLOGY

## 2.1 OVERVIEW

This chapter deals with the geological setup of geothermal springs from the Garhwal (Uttarakhand), Himachal and Ladakh (Jammu Kashmir) regions of the northwest Himalaya, India. Locations with their places of occurrence of these geothermal fields are given in (Figs. 2.1 & 2.2).

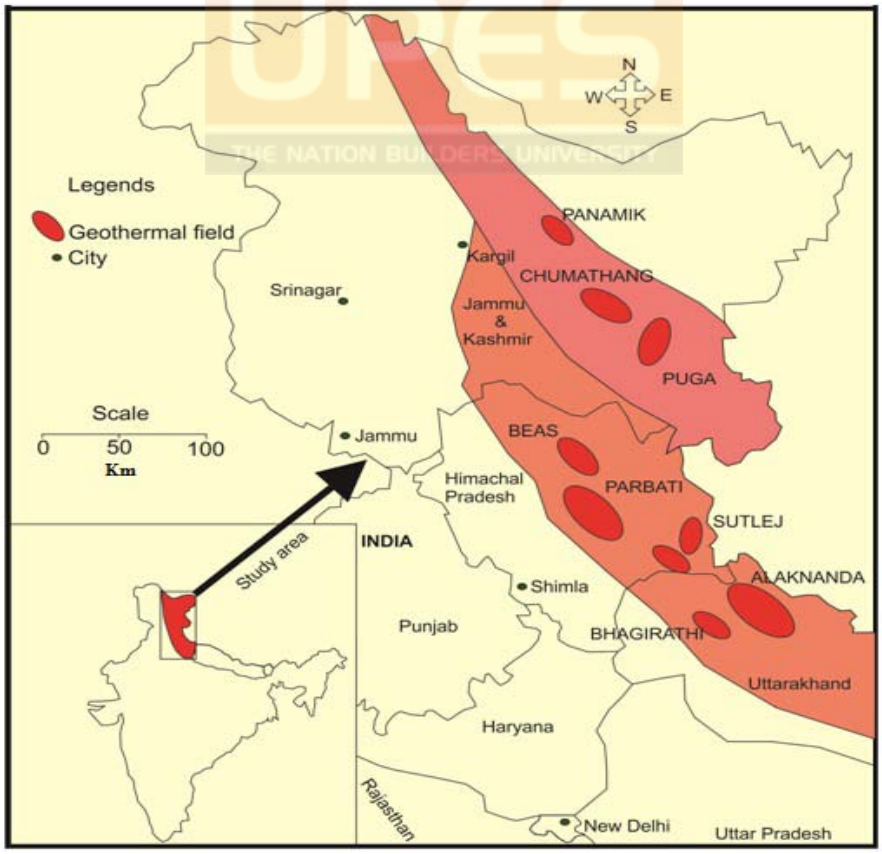


***Fig. 2.1:*** *Geothermal fields of northwest Himalaya modified after (*Craig, *2013).*

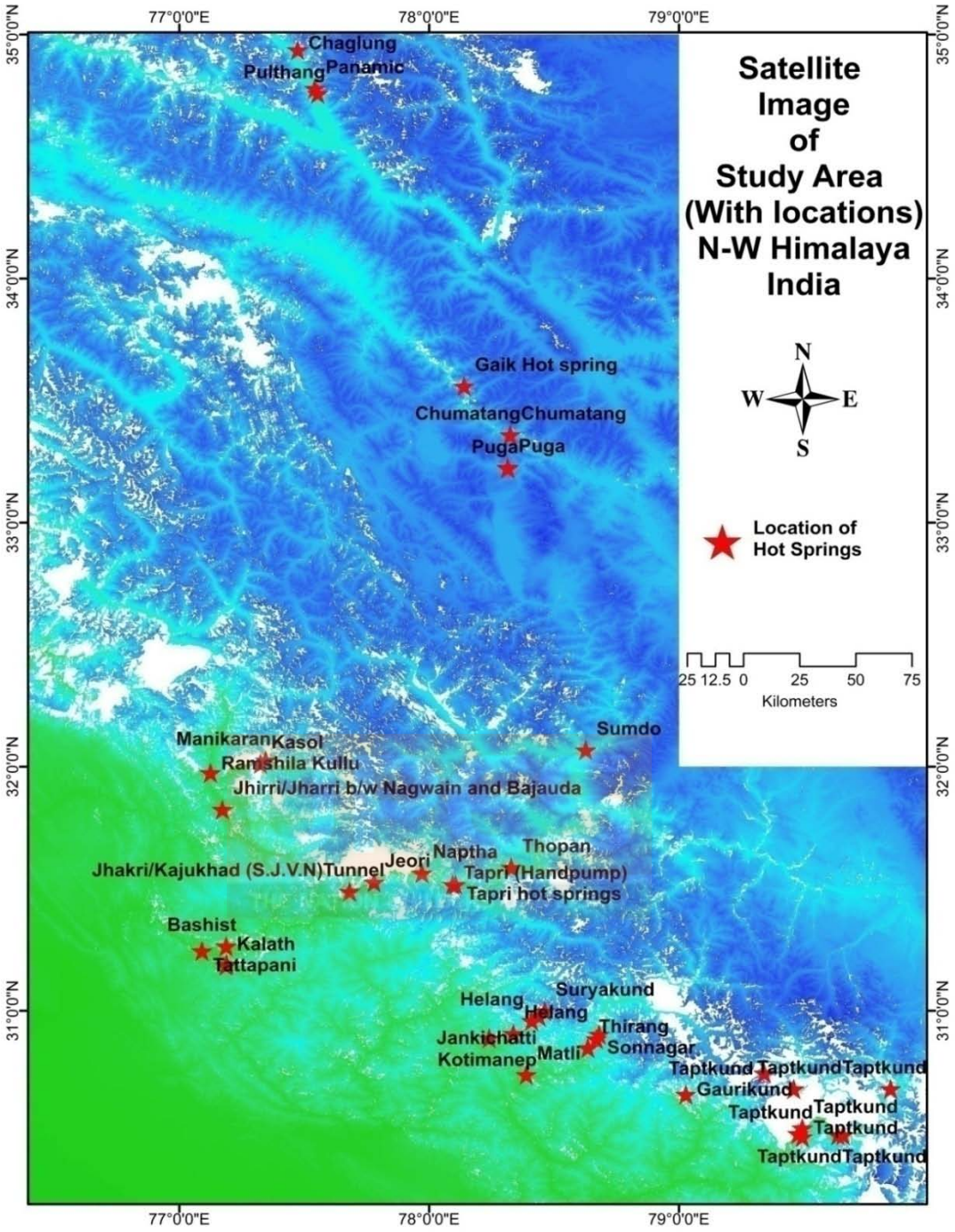


***Fig. 2.2:*** *Shuttle Radar Topography Mission (SRTM) image of the study area showing location of geothermal springs.*

## 2.2 EVOLUTION OF THE HIMALAYA

The Himalayan Mountains range represents a classical example of continental-continental collisional set up (Dewey & Bird, 1970; Dewey & Burke, 1973). It

frames the Indian subcontinent in large arc of ~2400 km with icy wall between the Tropical highlands of India and the Central Asia. The northwest and northeast Himalayan syntaxes are the marked bands of strike on the both ends of the Himalaya. The orogen is characterized by Indus Tsangpo Suture Zone (ITSZ) in the north, the Chaman fault in west, the Sagging fault in the east, and Main Frontal Thrust (MFT) in the south (LeFort, 1975).

Himalaya is a geologically young and collisional orogen and therefore it makes an ideal site for studying the diverse geological processes related to mountain building. Its potential to decode the feedback processes between lithospheric deformation and atmospheric circulation as a driver of global climate change has inspired many researchers in recent years (e.g., Harrison et al., 1992, 1998a; Molnar et al., 1987; Royden et al., 1997; Ramstein et al., 1997; Tapponnier et al., 2001; Beaumont et al., 2000; Yin et al., 2002).

To perceive the evolution of the Himalayan mountain chain is a challenging task in itself owing to the past configurations and the present positions of the Indian plate. Therefore it requires a suitable way which could throw an ample light on the journey of the Indian plate since the Proterozoic time. During the Late Paleozoic, the Indian continent was a part of the Pangaea supercontinent which broke at ~200 Ma, in three major phases (Early-Middle Jurassic ~175 Ma, Early Cretaceous: ~145 Ma and Cenozoic: 65–55 Ma), Merali et al., (2009).

The first phase of braking of Pangaea resulted due to the rifting between Tethys Ocean in the east and the Pacific Ocean at the west. It began to separate at ~175 Ma (Early-Middle Jurassic period) that rose in to two

supercontinents namely, Laurasia to the north and Gondwana to the south. The second phase took place at ~145 Ma (Early Cretaceous) during which, the Gondwana supercontinent divided further into two major continents namely West Gondwana (together with Africa and South America) and East Gondwana (a group of India, Australia, and Antarctica). Finally, India was broken off from the East Gondwana (Australia and Antarctica), and began its journey towards northward direction to collide with the Asian plate (moving @ 18.5 cm/year) which induced the closing of Tethys ocean (Meng et al., 2012).

The third and the last phase of brake-up in the Pangaea that took place in Cenozoic period (~60-55, Ma) during which the Laurasia was further fragmented into North America and Greenland. It is suggested that during the second phase of break-up of Pangaea, the Indian continental plate moved towards the Asian plate and is considered to be the beginning of the Himalayan orogeny. After the collision, Himalaya began to rise and gradually attained considerable height which gave rise to the Indian monsoon system.

### 2.2.1 MAJOR DIVISIONS OF THE HIMALAYA

The Himalayan tectonic system is a complex combination of processes that operate on different time scales. It combines the Himalayan orogen, the active foreland basin and major depositional system like Indus and Bengal fans. The description of major Himalayan division goes from south to north; starting from the foothills and proceeding to the Lesser, High, and Tethys Himalayas and finally the Indus Suture Zone, which is connected with the Trans-Himalaya. These geographic and geologic zones are assumed to continue

along the entire Himalayan orogen (Gansser, 1964; LeFort, 1975). These include as follows:

**A.** Sub-Himalaya (Tertiary strata).

**B.** Lesser Himalaya (mostly unfossiliferous, diagenetically altered. sedimentary strata and low-grade metamorphics).

**C.** Greater Himalaya or (Crystalline complex).

**D.** Tethyan Himalaya (mostly marine, fossiliferous strata).

### 2.2.2 GEOGRAPHIC DIVISION

The Himalayan mountain range is situated between its eastern and western syntaxes, symbolized by the Namche Barwa and Nanga Parbat peaks. The northern boundary of the Himalayan range is demarcated by the east flowing Yalu Tsangpo and the west flowing Indus River. The southern boundary of the Himalayan mountain belts is the Main Frontal Thrust (MFT) that touches the northern limit of Indo-Gangetic plain. Himalayan orogen is also described by the Indus Tsangpo suture zone (ITSZ) in the north and left-slip Chaman fault in the west, the right slip Sagging fault in the east and Main Frontal Thrust in the south. From the north to south, Himalayan orogen can be divided in to two major sections namely north Himalaya and south Himalaya partitioned by its high crest line (Yin, 2006). The geography of northern part is equivalent to Tethyan Himalaya or the Tibetan part of the Himalaya (LeFort; 1975). The southern slope of the Himalayan mountain belt is divided from north to south into Higher, Lower, and Sub-Himalaya. The boundary between the Lower and Sub Himalaya situated along the axis of the lowest inter montane valley is

parallel to its range (Yin, 2006). However, some parts of the Lower Himalaya are altitude wise higher than lower parts of the Higher Himalaya. Vertically, the Himalayan mountain range can be divided into mainly three groups namely the basal (<1500m), the middle (1500-3000m) and the upper Himalaya (>3500).

### 2.2.3 STRATIGRAPHIC DIVISION

Stratigraphically, the Himalayan orogen is divided in mainly five major parts (Fig. 2.3) from south to north namely the Neogene Siwalik Group, the Proterozoic Lesser Himalaya, Greater Himalayan Crystalline complex, and the Tethyan Himalayan sequence. The Siwalik range (250-800 m high) rises above the Indo-Gangetic Plain along the (MFT). It consists predominately of Tertiary and Quaternary sediments and is bounded to the north by northward dipping Main Boundary Thrust (MBT) which separates it from the overlying Lesser Himalaya. The Lesser Himalaya consists of Precambrian and Cambrian sequence of unfossiliferous low grade metamorphic, metasedimentary, and metavolcanic rocks. The Higher Himalayan Crystalline (HHC) is separated from the Lesser Himalaya along the Main Central Thrust (MCT). The HHC is enormously rouged with perennial streams fed by snow and glacier capped peaks covering elevation of 3000 m to more than 8000 m.

It consists of high grade metamorphic rocks of Cambrian to Early Ordovician period (800-480 Ma). The HHC in the western Himalaya is characterized by the Chail, Jutogh, and Vaikrita Groups of rocks. It passes into the Tethyan Himalayan Sequence, which is demarcated as the northern most part of the Indian subcontinent.

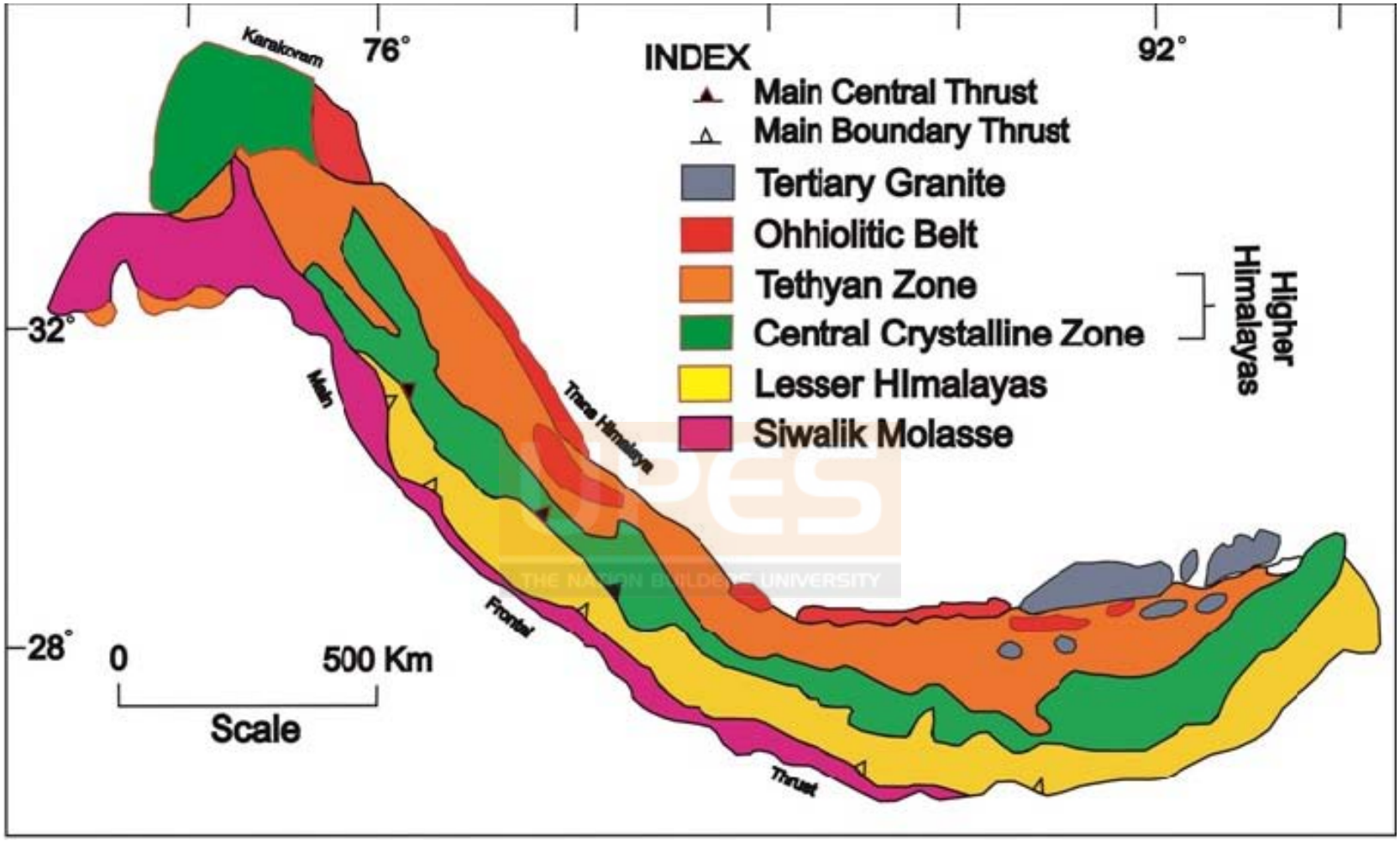


***Fig. 2.3:*** *Outline geological map of the Himalayan mountain belt showing its major tectonic subdivisions across the range (Modified after Gansser, 1964).*

The Tethyan unit is a rugged terrain with sculptured landscape developed in sedimentary sequences ranging from Late Precambrian (>600 Ma) to Cretaceous and Eocene (Valdiya, 1999). The HHC acts as a barrier for the wet monsoon clouds to go further north up to the Tethyan Himalayan sequence which has developed into cold and dry deserts. The Himalayan province ends in the Ladakh-Kohistan range along the Indus Tsangpo suture zone where the Indian plate collided with Asian (Tibetan) plate at about 55 Ma (LeFort, 1975). Indus Tsangpo Suture Zone is characterized by the remnants of the Neo-Tethys Ocean; the major part of which was subducted during the period when India moved north with respect to Asia.

## 2.3 GEOTHERMAL SPRINGS OF LADAKH REGION: GEOLOGICAL BACKGROUND

Ladakh is an example of dry and cold climate with winter temperatures touching as low as (-40°C). This area lies along the collided junction of the Indian and Asian plates that were involved in the Himalayan orogeny along the Indus Suture zone (ISZ). It consists of ophiolites and basic to ultra-basic rocks resulted from plutonic and submarine volcanism of middle to upper Cretaceous age. It has witnessed several phases of widespread acid igneous activities extending from the upper Cretaceous to upper Tertiary periods. The ophiolite suites of rocks, presented all along the Indus Suture Zone from Puga in the south east to Dras/Kargil in the north-west, corresponds to the abducted oceanic crust which now lies compressed between the collided continental

masses. Detail of the locations and geological setup of geothermal springs of Ladakh region are given in the (Fig. 2.4 & Tables 2.1, & 2.2).

### 2.3.1 GEOTHERMAL FIELDS

#### (A) PUGA VALLEY

Puga geothermal field is situated in the Indus valley in the eastern Ladakh (India) region of the northwest Himalaya. Puga is located 20 km upstream of the Mahe Bridge on river Indus which itself is about 20 km upstream of Chumathang on the Leh-Chishul road. It lies close to the south of Indus Suture Zone whereas the Chumathang geothermal field lies in north of Indus Tsangpo Suture Zone (ITSZ). The geothermal activities are confined along the faulted crest of the anticline having the Precambrian sequence of para-gneisses and schist, with lenses of patchy crystalline limestone. In the central part of the ITSZ, abundant thermal activities are present with their surface manifestation in form of sulphur condensates. These condensates represent an old fumarole activity along the fault covered by valley fill deposits. The deep seated faults encircling the (ITSZ) and the other faults act as channel for the transfer of heat and thermal fluids from deeper depths to shallow and subsurface heat reservoirs present in the vicinity of the Puga valley. The local as well as regional geo-tectonic settings suggest that the heat is probably obtained from the intrusive rocks lying close to the zone of major collision and subduction.

The other major geothermal spring, *Chumathang* is situated 150 km southeast of the Leh. It is located along the Chumathang fault which marks the contact between the middle and lower members of the Indus Formation. The lithology

of Chumathang geothermal field comprises of hornblende granite, pegmatite and quartz veins intruded into the Basal conglomerate where ~1 km-long quartz vein containing fluorite is also seen along the sheared contact. Copper and pyrite mineralization is also visible in the pegmatite near Chumathang whereas beryl is found in pegmatite traversing the Ladakh granite around Kiari-Gaik area.

### (B) SHYOK VALLEY

The Shyok valley contains three major geothermal springs namely, *Panamik, Changlung, and Pulthang*. It is composed of relatively younger rocks separating the Eurasian plate from the Indian plate. It could be divided into three litho-tectonic units namely (i) the Indus suture zone following Indus river valley, (ii) the Shyok ophiolitic melange or the Shyok suture zone following the Shyok River and (iii) the Ladakh batholiths or Ladakh magmatic arc in the axial part that acts as a barrier between Indus and Shyok valleys.

The northwest-southeast trending rock sequences of the Shyok Suture Zone occur between strongly deformed tectonic segments of the Ladakh batholiths in the south-west and the Karakoram batholiths in the north-east. These tectonic segments contain sedimentary, metamorphic and volcano-plutonic rocks which are defined as an accretionary complex (Upadhyay, 2001). The Shyok ophiolitic mélange belt is intruded by granodiorites of Cretaceous-Tertiary age. In addition, there are three major plutons exposed in this valley along the Leh-Siachen road between Khardung and Panamik.

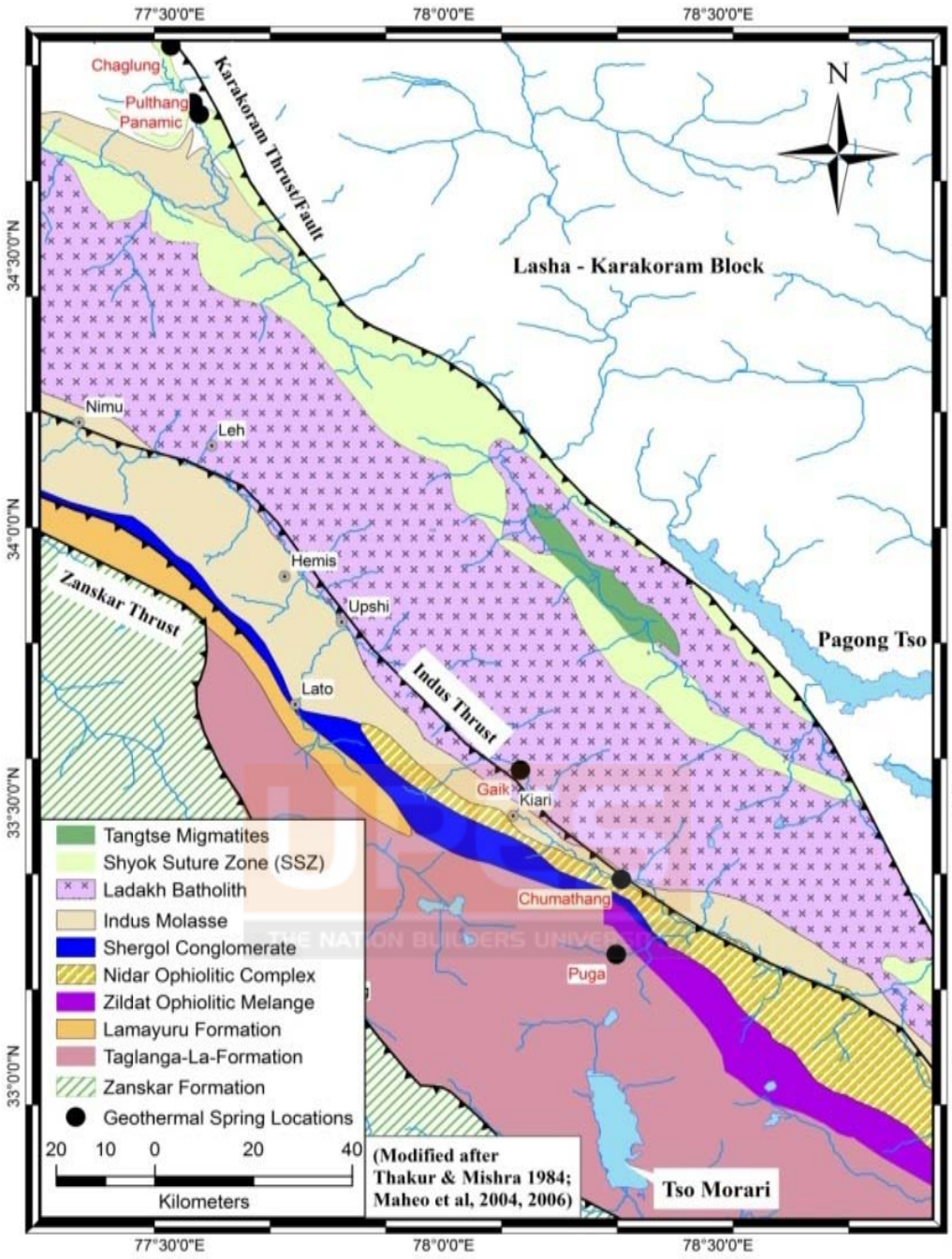


***Fig. 2.4:*** *Geological map of Ladakh Himalaya showing location of geothermal springs, modified after (Thakur & Mishra, 1984; Maheo et al., 2004; 2006).*

***Table 2.1:*** *Sampling and geographical distribution of geothermal springs, Ladakh region.*

| Sr. No | Sample No | Sites name | Date of Sampling | Lat. | Long. | Elevation (m, asl) |
|---|---|---|---|---|---|---|
| 1 | HS-21 | *Changlung* | 26-9-2011 | 34˚56'13″ | 77˚28'25″ | 3410 |
| 2 | HS-22 | *Pulthang* | 26-9-2011 | 34˚45'30″ | 77˚33'15″ | 3175 |
| 3 | HS-23 | *Panamic* | 27-9-2011 | 34˚46'45″ | 77˚32'33″ | 3225 |
| 4 | HS-24 | *Gaik* | 29-9-2011 | 33˚33'34″ | 78˚08'24″ | 3770 |
| 5 | HS-25 | *Chumathang* | 29-9-2011 | 33˚21'35″ | 78˚19'26″ | 4029 |
| 6 | HS-26 | *Puga* | 30-9-2011 | 33˚13'22″ | 78˚18'53″ | 4410 |

***Table 2.2:*** *Places of occurrence of geothermal springs, Ladakh region.*

| Sites name | Discharge (L/min) | Places of Occurrence | Geological Settings |
|---|---|---|---|
| *Changlung* | *180* | *100 meter above of the road level, north of the Changlung village (Nubra valley).* | *(Ophiolite/volcanics/ Flysch Melange)* |
| *Pulthang* | *160* | *Right side of the road, 1km form Pulthang village towards Panamik (Nubra valley).* | *(Ophiolite/volcanics/ Flysch Melange)* |
| *Panamic* | *600* | *Above of the road side in the south of the Panamik village (Nubra Valley).* | *(Ophiolite/volcanics/ Flysch Melange)* |
| *Gaik* | *200* | *Northwest along the Indus Valley towards Leh.* | *Granite and Indus formation of the Trans Himalayan sub division* |
| *Chumathang* | *200* | *Various geothermal springs occur along the southern bank of Indus river.* | *Granite and Indus formations* |
| *Puga* | *18000** | *More than 100 outlets are situated in this geothermal field along the Puga nala.* | *Para gneiss and quartz-mica schist and gneiss.* |

(*Craig et al., 2013)

## 2.4 GEOTHERMAL SPRINGS OF HIMACHAL REGION: GEOLOGICAL BACKGROUND

Geothermal field of Himachal Pradesh is a part of the large Himalayan geothermal province where geothermal activities along Sutlej, Spiti, Parbati, Beas, and Kullu valleys are known for their high surface temperatures. Earlier workers (Sehgal, 1963; Jangi et al., 1976; Gupta et al., 1976; Giggenbach et al., 1983; GSI, 1991; Alam, 2002) have reported the geological setup of this region in details and therefore a brief about the location and geological setup of these springs are given in the Fig. 2.5, and Tables 2.3 & 2.4. The salient features of thermal activities of this region are given basin wise as follow.

### 2.4.1 GEOTHERMAL FIELDS

### (A) SUTLEJ AND SPITI VALLEY

The locations of geothermal springs of Sutlej and Spiti valley fall in Survey of India toposheet nos.-53E/11,14; 53I/2, 3, 6 and 53 L. The major rock types of this area are the gneiss, schist, and quartzite which belong to Central Crystallines. Geothermal springs namely, *Jhakri, Tattapani, Jeori, Naptha, Tapri, Thopan* and *Sumdo* are located in these valleys Fig. 2.5, which are described as follows:

*Jeori* geothermal spring is situated on the right bank of Raikhad nala, a tributary of Sutlej River, at Jeori village. Country rocks around the geothermal springs are amphibolites intruding the gneiss and schist of the Central Crystallines.

*Jhakri* geothermal spring lies inside the tunnel of Naphtha Jhkari hydropower project which is built on the Sutlej River. Country rocks around this spring are gneiss and schist intruded by pegmatite and granite. There are numerous outlets of the springs present inside the main tunnel.

*Naptha* geothermal spring is situated on the right bank of Sutlej River in the premises of Nag Devta temple. Source rocks near this spring are the gneiss and schist intruded by pegmatite and granite.

*Tapri* geothermal spring is located on the hill slope about 2m above the road side on the right bank of Sutlej River near the Tapri village. The country rocks are gneiss and schist intruded by granites having joints and fractures.

*Thopan* geothermal spring is situated 10 m above the road level along the Sutlej valley where water emerges through the joint planes in the gneiss rocks which are the part of the central crystallines.



*Sumdo* geothermal spring occurs in the catchment of the tributary of Spiti River. Country rock types of this area comprising gneiss, schist, and quartzites.

**(B) BEAS VALLEY**

Earlier studies have reported the occurrences of geothermal springs in the Beas valley (Oldham, 1882; Middlemiss, 1910; Bhatnagar, 1961). There are five active geothermal springs located in the Beas valley namely *Jhiri, Karalbihal, Kalath, Bashist* and *Kullu Ramshila* which are spread over the stretch of ~70 Km from Bashist in the north to Thalaut in the south. Geological sequence of the rocks of the valley has been classified into

Vaikrita, Kullu, Larji and Rampur Groups. The Vaikrita Group consists mainly of gneisses with kyanite, sillimanite and schist. Kullu Group is relatively less metamorphosed than Vaikrita group and consists of gneisses, schists, shales, phylites, amphibolites and quartzites. The associated rocks with Rampur Group include phylite, quartzite and green schist whereas the Larji groups of rocks have dolomite and limestone as major lithology.

*Jharar* geothermal spring lies ~ 2.5 km downstream from Bhuntar on Garsa road on the left bank of Beas River. Algae and brown precipitates were seen around the spring. The country rocks near the Jharar geothermal springs are mainly gneisses, schists, and quartzites which are the part of Central Crystalline group.

*Kharal Bihal* geothermal spring is situated at ~1.5 km upstream of Kalath on the either sides of the river bank where carbonate deposits and red staining can be seen around them. Country rocks near the springs are mainly gneisses, schist, and quartzite of Central Crystalline Group.

*Kalath* geothermal spring, occurring in form of many outlets, is located ~500 m, downstream of the main village on the right bank of Beas River. The main rock types, around these springs are gneisses, boulder and mica schist of Central Crystallines.

*Bashist* is another geothermal spring situated on the hill slope and ~150 m above river bed with gneisses as country rock from which geothermal water comes out continuously. *Kulu-Ramshila* spring is situated in the Kulu-Akhara market on the right bank of the Beas River where geothermal water emerges out from the quaternary deposits.

## (C) PARBATI VALLEY

Geothermal field of Parbati valley falls in Survey of India (SOI) toposheet no-52H and 53E and situated in the inner Himalayan range covering altitudes from 1300 m to 3000 m above mean sea level. *Khir Ganga, Pulga, Manikaran, Kasol,* and *Jan* are the major geothermal springs located in the valley. Out of these only *Manikaran* and *Kasol* were sampled where quartzite and phylite rocks are exposed as major rocks. The phylite in this region is mainly carbonaceous and contains lenses of quartz veins.

*Kasol* geothermal spring is situated on the right bank of Parbati River, where the exposed rocks belong to Kullu and Rampur Groups and are separated by Kullu thrust. Thermal activities in the area are mainly associated with quartzite of Rampur Group. A strong $H_2S$ smell and yellowish deposits of carbonates were found around Kasol spring.



*Manikaran* geothermal spring is located on the right bank of Parbati River in form of many outlets. These have also been used for religious activities inside a Gurudwara. The major rock types exposed between the Manikaran and Kasol villages are highly fractured and jointed. These are white to grayish in colour with thick sequence of quartzites (Manikaran quartzite), phylites and slates. The main surface features of Manikaran were its significant discharge, $H_2S$ smell, and high temperature (94˚C) which could also be used for cooking food. The yellowish carbonates deposit could also be seen around the Manikaran geothermal field.

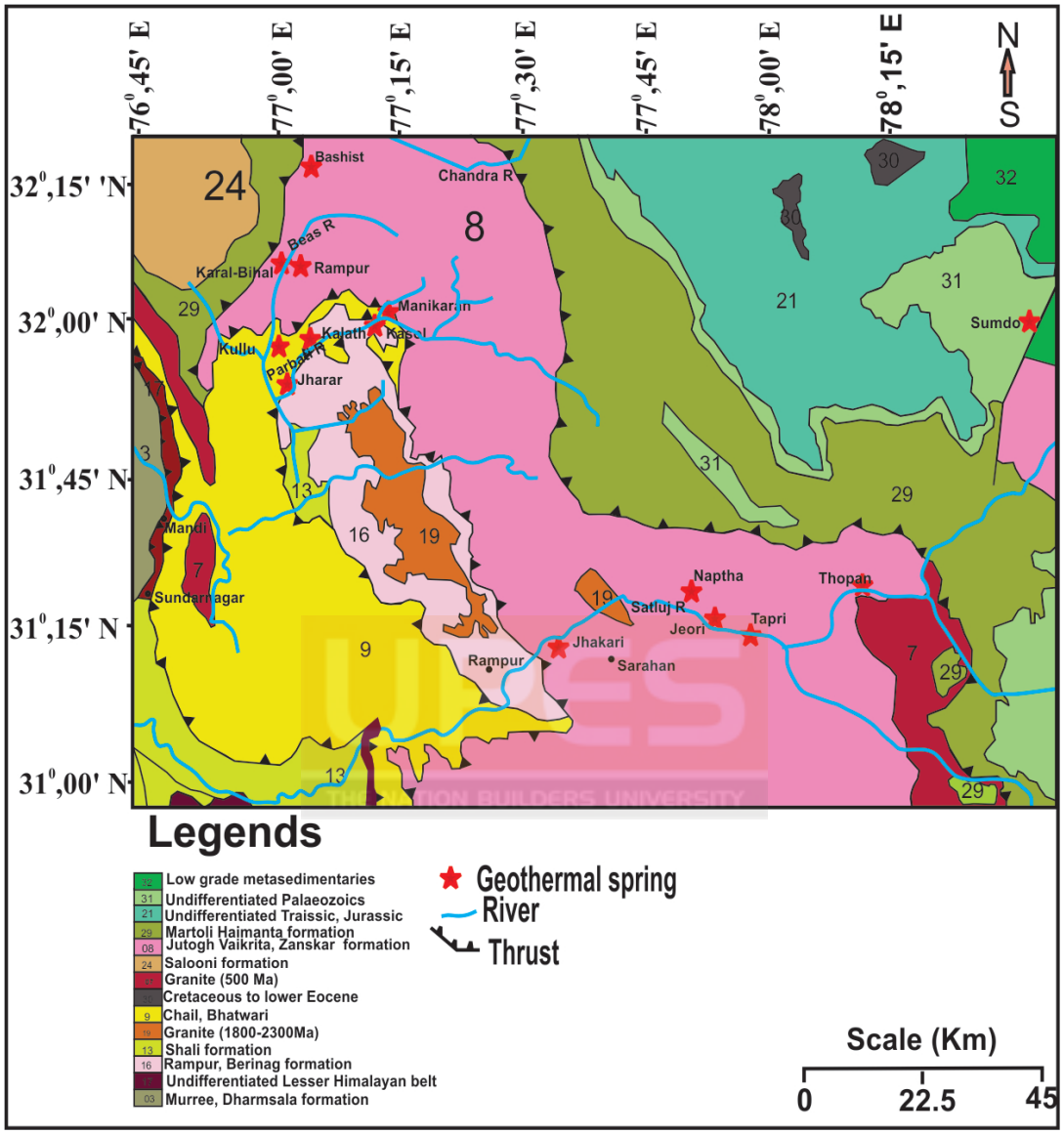


***Fig.2.5:*** *Outline geological map of Himachal Himalaya showing locations of geothermal springs, modified after Thakur & Rawat, (1992).*

***Table 2.3:*** *Sampling and geographical distribution of geothermal springs, Himachal region.*

| Sr. No | Sample No | Sites name | Date of Sampling | Lat. | Long. | Elevation (m, asl) |
|---|---|---|---|---|---|---|
| 7 | HS-27 | *Sumdo* | 04-10-2011 | 32˚04'06″ | 78˚37'37″ | 3270 |
| 8 | HS-28 | *Thopan* | 05-10-2011 | 31˚35'16″ | 78˚19'44″ | 2180 |
| 9 | HS-29 | *Tapri* | 07-10-2011 | 31˚31'02″ | 78˚06'21″ | 1702 |
| 10 | HS-29-B | *Tapri (Handpump)* | 07-10-2011 | 31˚31'01″ | 78˚05'40″ | 1762 |
| 11 | HS-30 | *Naptha* | 08-10-2011 | 31˚33'50″ | 77˚58'17″ | 1793 |
| 12 | HS-31 | *Jeori* | 08-10-2011 | 31˚31'38″ | 77˚46'45″ | 1793 |
| 13 | HS-32 | *Jhakri* | 08-10-2011 | 31˚29'19″ | 77˚40'53″ | 1130 |
| 14 | HS-33/34 | *Jharar* | 10-10-2011 | 31˚49'31″ | 77˚10'22″ | 1033 |
| 15 | HS-35 | *Bashist* | 11-10-2011 | 31˚15'52″ | 77˚11'15″ | 2110 |
| 16 | HS-36 | *Khiral Bihal* | 11-10-2011 | 31˚11'28″ | 77˚11'23″ | 1750 |
| 17 | HS-37 | *Kalath* | 11-10-2011 | 31˚11'08″ | 77˚11'11″ | 1730 |
| 18 | HS-38 | *Ramshila(Kullu)* | 11-10-2011 | 31˚58'31″ | 77˚07'28″ | 1228 |
| 19 | HS-39 | *Manikaran* | 13-10-2011 | 32˚01'35″ | 77˚20'45″ | 1662 |
| 20 | HS-40 | *Kasol* | 13-10-2011 | 32˚00'45″ | 77˚19'30″ | 1600 |

***Table 2.4:*** *Places of occurrence of geothermal springs, Himachal region.*

| Sites name | Discharge (L/min) | Places of Occurrence | Geological Settings |
|---|---|---|---|
| *Sumdo* | 80 | Situated in the Spiti valley, at the right bank of tributary stream of Spiti river near Sumdo village | Gneiss, schist and quartzite. |
| *Thopan* | 50 | Situated at 10 m above from the road site in the southeast of the Thopan village of Sutlej valley. | Geothermal spring emerges through the joint planes in the gneiss rocks of the central crystalline. |
| *Tapri* | 40 | Situated on the hill slope and about 2m above the road side near the Tapri village in the Sutlej valley. | Mainly gneiss and schist intruded by (jointed and fractured) granites. |
| *Tapri (Handpump)* | 100 | This Handpump is discharging geothermal water, and situated on the thermal anomaly in the main market of Tapri village. | The country rocks are gneiss and schist intruded by granites (jointed and fractured). |
| *Naptha* | 200 | Situated on the right bank of Sutlej river and present in the premises of the Nag Devta temple. | Gneiss and schist intruded by pegmatite and granite. |
| *Jeori* | 60 | Situated on the right bank of Raikhad nala, a tributary of Sutlej river. | Amphibolites intruding the gneiss and schist of Central Crystalline. |
| *Jhakri* | 100 | Situated inside the tunnel of Naphtha Jhakri hydropower project of Sutlej river | Country rocks |
| *Jharar* | 50 | Situated 2.5 km downstream from Bhuntar on Garsa road along the left bank of Beas river | Mainly gneisses, schist, and quartzite are found in this area |
| *Bashist* | 100 | Situated on hill slope about 150 m above Beas river bed. | Gneisses and mica schist of Central Crystalline |
| *Khiral Bihal* | 50 | Situated at 1.5 km upstream of Kalath village on the both side of Beas river bank. | Gneisses boulder and mica schist of Central Crystalline. |
| *Kalath* | 350 | Located on the right river bank, and ~500 m, south of Kalath village. | Gneisses boulder and mica schist of Central Crystalline. |
| *Ramshila(Kullu)* | 100 | Situated in the Kullu-Akhara market on the left bank of the river Beas. | Gneisses boulder and mica schist of Central Crystalline. |
| *Manikaran* | 300 | Located on the right bank of Parbati river inside the Gurudwara. | Quartzite and phylite |
| *Kasol* | 100 | Situated on the right bank of Parbati river. | Mainly quartzite and phylite. |

## 2.5 GEOTHERMAL SPRINGS OF GARHWAL REGION: GEOLOGICAL BACKGROUND

Geothermal field of Garhwal Himalayan belt contains spring activities which are common along the Alaknanda, the Bhagirathi, the Mandakani, and Yamuna valleys. These are known for their high surface temperature with Tapoban (Shaldhar) being the hottest. These springs occur in the four major litho-tectonic units which include the Munsiari, Joshimath, Pindari, and Pandukeshwar formations. Locations and details of geological setup of these springs are presented in Fig. 2.6, and Tables 2.5 & 2.6. It consists mainly of meta-sediments of Precambrian to Palaeozoic age which are intensely deformed up to the MBT (Gansser, 1964). Further south to the MBT, the sub-Himalaya consists of Tertiary molasse sequences which have involved in thin skinned tectonics induced by thrusting of the Himalaya over Indian basements in the Siwalik Hills (Gansser, 1964). The present study covers the thermal springs mostly along the major thrust zones which were first recognized by Heim & Gansser (1939) near the localities of Badrinath and Joshimath. The important tectonic plane in this region is the MCT. It is traceable all along the Himalayan stretch in terms of broken crustal blocks that moved up southward along the deep faults. It is the response of an inclined fault which got detached from the upper crust along a sub horizontal zone at an inclination of 30° to 40° northward. It has also suffered a thrusting up to a depth of ~125 km which brought basement rocks up to the surface through ductile deformation (Roy &Valdiya, 1988). Nearby the (MCT) in the lesser Himalayan zone, the

metamorphic and associated granite rocks are found severely deformed and compressed (Bhattacharya et al., 1985).

### 2.5.1 GEOTHERMAL FIELDS

### (A) ALAKNANDA VALLEY

Alaknanda Valley hosts many geothermal activities in range of exposed rocks (Auden, 1936; Heim & Gansser, 1939) which include gneiss and schist with bands of calc-silicate, calc-schist, marble and quartzites of Central Crystallines. These rocks are folded into a symmetrical anticline and syncline with variable strikes and dips. The thermal springs sampled from this valley have characteristics as follows:

*Badrinath* geothermal spring, also known as Taptkund, is situated on the right bank of river Alaknanda at an altitude of ~ 3000 m. It emerges through old morainic deposits where its outlet is covered by the permanent structure in the vicinity of the temple. Sulphurous odour with gas bubbles could also be seen associated with this spring.

*Khiroi* geothermal spring is located along the Khiroi Ganga, a tributary of river Alaknanda, about 15 Km upstream from its confluence. There are many outlets of this thermal spring seen emerging out on the surface. Rock types exposed around the springs are gneiss and schist of Pandukeshwar Formation.

*Bhapkund* geothermal spring is situated near the Malari locality along Dhauliganga River, a tributary of Alaknanda and has the lithological characteristics similar to the central crystalline rocks.

*Tapoban* geothermal spring is located close to a local stream on the left bank of Dhauliganga River at the elevation of ~1920 m, asl. It is underlain by sericitic and fine-grained quartzite with considerable thickness. The quartzite is associated with thin bands of garnet mica schist and overlies the gneisses and schists with occasional bands of quartzite exposed further downstream Bilagarh. To the east of Bilagarh basic rocks (amphibolite) are found associated with gneiss and schist. The quartzite exposed around Tapoban seems to be the southeastern extension of Pandukeshwar quartzite. This spring discharges very hot water and also emanates hot volatile and steam in form of a jet.

*Shaldhar* geothermal spring emerges through the overburden of talus material of quartz and is situated on hill slope on the left bank of river Dhauliganga. Around the thermal spring, a thin encrustation of carbonate deposits can be seen in the vicinity. It is very close to the Tapoban geothermal spring.

*Helang* geothermal spring is approachable through the Helang village, located on the left bank of the river Alaknanda near the Bangina village. The area is covered by gneisses and schist of Helang Formation of Central Crystallines.

*Langsi* geothermal spring situated to the south of the Helang and spreads over a stretch of 10 m on the left bank of Alaknanda river channel. The associated rocks are mainly of dolomite of Garhwal group.

*Ganoi* geothermal spring is located on the left bank of Patal Ganga (tributary of river Alaknanda). The surface lithology near this spring consists of slate and carbonaceous rocks of the Garhwal group.

*Birahi* geothermal spring is situated at the left bank of Birahi Ganga, (tributary of river Alaknanda) near which quartzite is exposed as a major lithology.

*Gaurikund* geothermal spring is situated on the left bank of river Mandakini on the starting point of Rudraprayag-Kedarnath route in the Alaknanda valley. This is just behind the Gaurikund temple, the main outlet of springs is known as Garamkund. The rocks exposed around springs are calc-gneisses and augen-gneisses with schists coming together along a fault.

**(B) BHAGIRATHI VALLEY**

There are several geothermal springs located in the Bhagirathi valley and their geological set up has been documented in details (Tewari, 1970; Ranga Rao, 1972; Aggarwal & Kumar, 1973). However brief descriptions of these springs are given below:

*Bukki* geothermal spring is located on the right bank of Bhagirathi River. Main rocks types are gneiss and schist with amphibolites of Central Crystallines. Water from this spring emerges along the joints and bedding planes close to the river bank.

*Jhaya* geothermal spring is located about 50 m above from the river bed on the right bank of Bhagirathi River where water emerges through the cultivated field/talus debris on the west slope, covered with vegetation.

*Gangnani* spring have geothermal activities which are noticed ~100 m above the river bed on the left bank of the Bhagirathi valley. Geothermal water seems to be coming out through sericite-biotite schist interbedded with

medium to fine grained gneiss and calc-silicate rock on the east slope of the river.

*Thirang* geothermal spring is located at the left bank of Bhagirathi River near the Thirang village. The spring occurs on the eastern slope of the valley and issues from gneissic rock covered with thick vegetation.

**(C) YAMUNA VALLEY**

There are six active geothermal springs present in this valley between Gangnani and Yamnotri. The rocks include the limestone-quartzite; basic volcanic sequence of the Garhwal Group which are exposed to the south and southwest of the valley. These are structurally overlain by gneiss and schist with a band of basic rock near the MCT. The details of geological setup were first reported by the Geological Survey of India (Gyanprakash & Raina, 1974-75). Thermal activities in form of geothermal springs are observed at Yamnotri, Janakichatti, Banas, Wozari, Kotimanep and Matli. Many of these springs emerge through the quartzite interbedded with the gneiss and schist of Central Crystallines except the two at Kotimanep and Wozari, where the geothermal water comes out through massive quartzite of Garhwal Group. A brief description of thermal springs of Yamuna valley is given below:

*Yamnotri* geothermal spring activity is noticed at the temple site (Suryakund) which is situated on the left bank of the Yamuna River. Several outlets of this geothermal spring emerge from quartzites. Out of these, the main outlet lies in the compound of the Yamnotri temple in which bubbling activity is seen with water at boiling temperatures.

*Janakichatti* geothermal spring is situated on the right flank of the river Yamuna near Janaki-Chatti village. Geothermal water issues at this place through the terrace deposit/talus debris of quartzite and have mild sulphurous odour.

*Kotimanep* geothermal spring is situated about 500 meter towards north of the Koti-Manep village on the right bank of Badiyar Gad, a tributary stream of Yamuna river.

*Banas* geothermal spring is situated on the right bank of river Rishi Ganga (a tributary of the river Yamuna) near Banas village where the geothermal spring emerges through the jointed quartzite with gneiss and overlain by garnet mica schist.

*Wozari* geothermal spring lies between the massive quartzite of Garhwal Group near the MCT on the right bank of river Yamuna at Wozari village.

*Matli* geothermal spring is situated near Matli village, south of the MCT, in the Yamuna Valley. The main lithology near this spring comprises Phylite and metasedimentary rocks of lesser Himalayan sequence.

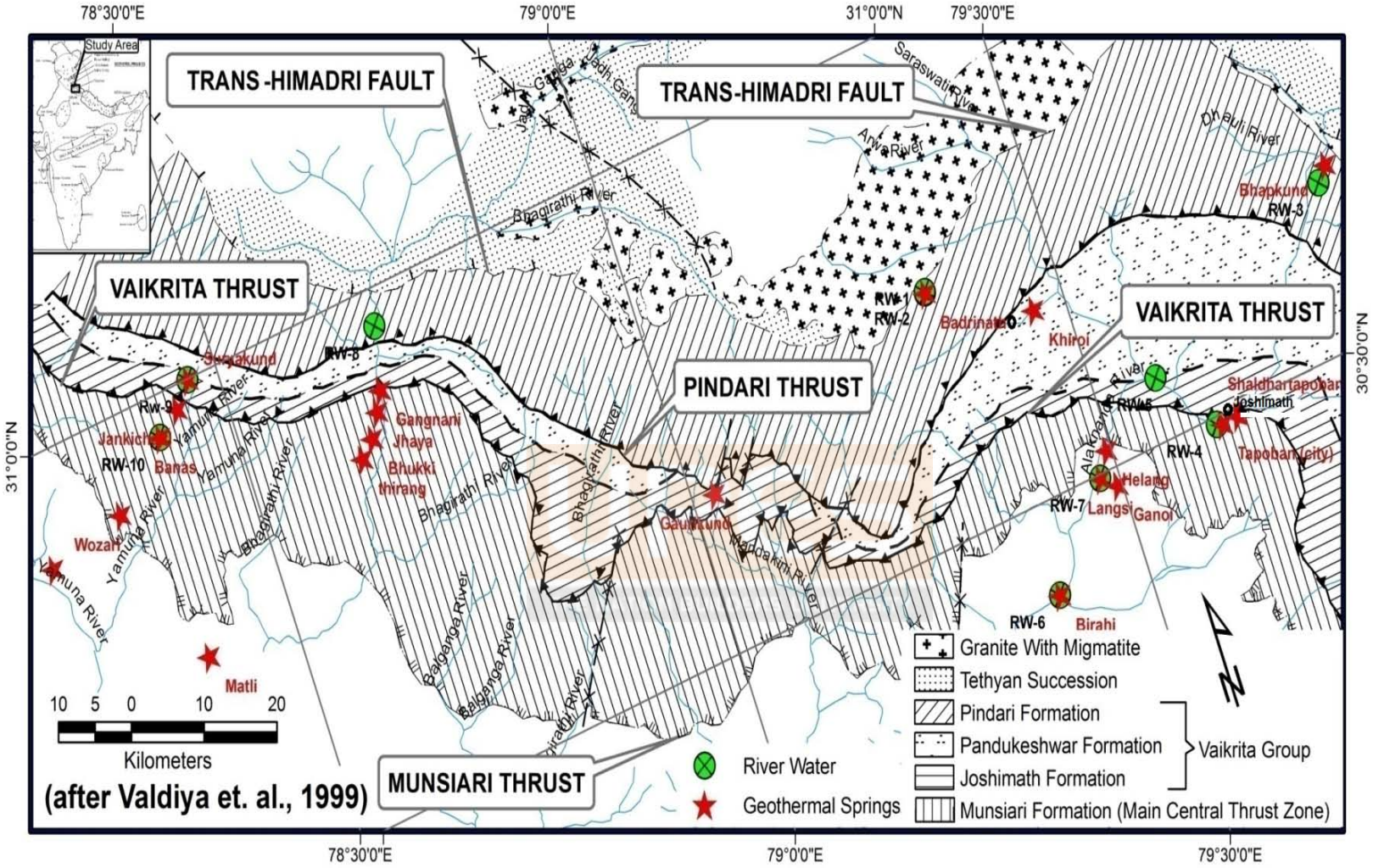


***Fig. 2.6:*** *Geological map of Garhwal Himalaya showing the location of geothermal springs base map from Valdiya, (1999).*

***Table 2.5:*** *Sampling and geographical distribution of geothermal springs and river waters of Garhwal region.*

| Sr. No | Sample No | Sites name | date of Sampling | Lat. | Long. | Elevation (m,asl) |
|---|---|---|---|---|---|---|
| 21 | HS-1 | *Taptkund-Badrinath* | 17-11-10 | 30˚ 44' 41" | 79˚ 20' 29" | 3089 |
| 22 | HS-2 | *Khiroi* | 18-11-10 | 30˚ 40' 48" | 79˚ 27' 35" | 2973 |
| 23 | HS-3 | *Bhapkund* | 19-11-10 | 30˚40' 05″ | 79˚ 50'0 5″ | 2680 |
| 24 | HS-4 | *Shaldhar, Tapoban* | 20-11-10 | 30˚29' 02″ | 79˚ 39' 02″ | 1953 |
| 25 | HS-5 | *Tapoban(city)* | 21-11-10 | 30˚29' 02″ | 79˚ 38' 01″ | 1890 |
| 26 | HS-6 | *Birahi* | 23-11-10 | 30˚ 24’ 31″ | 79˚ 23’ 19″ | 1190 |
| 27 | HS-7 | *Ganoi* | 24-11-10 | 30º 28' 58″ | 79˚ 29' 03″ | 1409 |
| 28 | HS-8 | *Langsi* | 24-11-10 | 30˚ 29' 47″ | 79˚ 28' 36″ | 1225 |
| 29 | HS-9 | *Helang* | 25-11-10 | 30˚ 31' 10″ | 79˚ 29' 38″ | 1210 |
| 30 | HS-10 | *Gaurikund* | 25-11-10 | $30^{o}$ 39' 26" | $79^{o}$ 01' 39" | 1930 |
| 31 | HS-11 | *Gangnani* | 27-11-10 | 30˚ 54' 11″ | 78˚ 40' 50″ | 1900 |
| 32 | HS-12 | *Jhaya* | 27-11-10 | 30˚ 53' 05″ | 78˚ 40' 10″ | 1808 |
| 33 | HS-13 | *Bhukki* | 27-11-10 | 30˚ 50' 00″ | 78˚ 39’ 05″ | 1730 |
| 34 | HS-14 | *Thirang* | 27-11-10 | 30˚ 50' 54″ | 78˚ 38' 08″ | 1640 |
| 35 | HS-15 | *Matli* | 28-11-10 | 30˚ 44' 16″ | 78˚ 23' 20″ | 1062 |
| 36 | HS-16 | *Koti-Manep* | 28-11-10 | 30˚ 53' 17″ | 78˚ 14' 25″ | 1429 |
| 37 | HS-17 | *Suryakund* | 29-11-10 | 30˚ 59' 58″ | 78˚ 27' 46″ | 3070 |
| 38 | HS-18 | *Jankichatti* | 29-11-10 | 30˚ 58' 39″ | 78˚ 26' 24″ | 2568 |
| 39 | HS-19 | *Banas* | 30-11-10 | 30˚ 57' 34″ | 78˚ 24' 38″ | 2210 |
| 40 | HS-20 | *Wozari* | 30-11-10 | 30˚ 54' 24″ | 78˚ 20' 14″ | 1630 |
| 41 | RW-1 | *Alaknanda upstream before HS-1* | 17-11-10 | 30˚ 44' 41" | 79˚ 20' 29" | 3089 |
| 42 | RW-2 | *Alaknanda upstream after HS-1* | 17-11-10 | 30˚ 44' 45" | 79˚ 20' 30" | 3089 |
| 43 | RW-3 | *Girithiganga upstream before HS-3* | 19-11-10 | 30˚ 40' 00″ | 79˚ 50' 00″ | 2681 |
| 44 | RW-4 | *Dhauliganga upstream before HS-4* | 21-11-10 | 30˚ 29' 34″ | 79˚ 37' 49″ | 1800 |
| 45 | RW-5 | *Alaknanda at Vishnuprayag* | 21-11-10 | 30˚ 33' 47″ | 79˚ 34' 35″ | 1468 |
| 46 | RW-6 | *Birahiganga downstream after HS-6* | 23-11-10 | $30^{0}$ 24’ 31″ | 79˚ 23' 19″ | 1190 |
| 47 | RW-7 | *Alaknanda upstream before HS-8* | 24-11-10 | 30˚ 29' 47″ | 79˚ 28' 36″ | 1225 |
| 48 | RW-8 | *Bhagirathi river at dabrani Village* | 27-11-10 | 30˚ 57' 49″ | 78˚ 41' 48″ | 2148 |
| 49 | RW-9 | *Yamuna river upstream at Yamnotri* | 29-11-10 | 30˚ 59’ 58″ | 78˚ 27' 46″ | 3070 |
| 50 | RW-10 | *Naradganga upstream before HS-19* | 30-11-10 | 30˚ 57' 34″ | $78^{0}$ 24' 38″ | 2210 |

***Table 2.6:*** *Places of occurrence of geothermal springs, Garhwal region.*

| Sites name | Discharge (L/min) | Places of Occurrence | Geological Settings |
|---|---|---|---|
| | | **Alaknanda Valley** | |
| Badrinath | 430 (G.S.I)*<br>400 | Situated on the over burden of moraine deposit at the right bank of Alaknanda river near the Badrinath Temple | Gneiss & Schist with bands of calc-silicate calc-Schist, marble &quartzites. |
| Khiroi | 200 | River bank (Benakuli village) ~35 km from Badrinath toward Tapoban | Gneiss and Schist of Pandukeshar quartzite formation. |
| Bhapkund | 100-150 | Situated at the right bank of Dhauliganga/Girithiganga river. | Gneiss & Schist with bands of calc-silicate rocks and quartzites |
| Tapoban | 50-60 | Emerge through quartzitic talus material on the bank of Dhauliganga. | Gneiss schist and quartzite with amphibolite &Calc silicate |
| Shaldhar (Joshimath) | 300 | Situated along the Dhauliganga river and the fault trending in NNW-SSE direction to the west of Ringi Village. | Granite-gneisses in contact with basic rocks. Gneiss schist, quartzite with calc rock of Central Crystalline. |
| Helang | 100 | Situated in the deep section of Alaknanda valley at river level. There are several seepages on both sides of river bed. | The rocks are mainly quartzite with intercalations of slate belonging to Helang Formation of Central Crystalline Group. |
| Langsi | 100 | Number of outlets occurred over a stretch of 10 m, in the river bed on the left bank of river Alaknanda. | Dolomite rocks of Garhwal Group |
| Ganoi | 50 | Situated in the shear zone and on the right bank of Patal Ganga. | Slate and carbonaceous types of rocks of the Garhwal group. |
| Birahi | 40 | This geothermal spring is situated at left bank of Birahi Ganga river. | The rocks are mainly quartzite with intercalations of slate |
| Gaurikund | 200 from many outlets. | Situated at the left bank of Mandakni river. Numbers of outlets are found inside the Temple. | Fault contact between calc-gneisses and augen-gneisses with schist's |
| | | **Bhagirathi Valley** | |
| Bhukki | 16, G.S.I*<br>25 | Emerges through gneiss and schist on the right bank of Bhagirathi river along bedding joint plane. | Gneiss & schist with amphibolite, comprising Central Crystallines, are the main rock types. |
| Jhaya | 30 | Situated on the right bank of Bhagirathi river. Just below the road about 50 m. above from the river bed | Gneiss and schist with amphibolite of central Crystallines are the main rock types in the area. |
| Gangnani | 100 | Eastern slope of the Alaknanda Valley about 100 m. above the river bed. | Sericite-biotite schist with gneiss & calc. silicate rocks. |
| Thirang | 60 | Spring emerges on the left bank of Bhagirathi River. | Sericite-biotite schist inter-bedded with gneiss &calc-silicates |
| | | **Yamuna Valley** | |
| Yamnotri (Suryakund) | 150-200 | The main geothermal springs occur within the premises of the Yamnotri temple in which bubbling activity is noticed. | The laminated quartzite inter-bedded with gneiss & schist of Central Crystalline. |
| Janakichatti (Kharsali) | 100 (GSI) *<br>70 | Located on the right flank of Yamuna valley at an altitude of 2568m and emerges through the terrace deposit. | Crystalline rocks comprising sericite biotite schist, gneiss, and quartzite& associated basic rocks. |
| Banas | 50 | On the right bank of Rishi Ganga, near the Banas. | Jointed quartzite, with gneiss & schist and overlain by garnet mica schist |
| Wozari | 30 | On the right bank of Yamuna with partially submerged in the river. | Massive and jointed quartzite of 'Garhwal Group' |
| Kotimanep | 80 | ~ 0.5 km. north of Kotimanep on the right bank of Badiyar Gad | Massive, jointed quartzite of the Garhwal Group |
| Matli | 30 | Near Matli village, south of the MCT in the Yamuna Valley. | Phlyite/ meta sedimentary of Lesser Himalaya Sequence. |

*Discharge measured by Geological Survey of India during (1975-80).

# CHAPTER 3

# METHOD AND ANALYTICAL TECHNIQUES

# CHAPTER 3:

# METHOD AND ANALYTICAL TECHNIQUES

## 3.1 OVERVIEW OF RESEARCH METHODOLOGY

The research problem is centered on the isotopic and geochemical studies of the geothermal springs. Towards this, surface temperature (˚C), water discharge (L/min), pH, total dissolved solids (mg/L), electric conductivity (μS/cm), and geographic locations of these geothermal springs were measured in-situ. A total number of fifty (50) samples were collected during the two field visits carried out during the years 2010 and 2011. These include water samples from forty geothermal springs covering Ladakh, Himachal and Garhwal region and ten river waters. A suit of analytical methods were adopted during the course of this study, which are given in this chapter and also presented in form of flow chart of analytical techniques (Fig. 3.1). A synopsis of the methods used in this work may be listed as follows.

*[1] Field work including structural and lithological survey to know the places of occurrence of the thermal springs.*

*[2] Sampling of thermal springs with field measurement of physical parameters like temperature, pH, electric conductivity and surface discharge of thermal springs.*

[3] *Geochemical analyses (major ion, alkalinity, trace element, and dissolved $SiO_2$) using Ion Chromatograph (IC), Auto-Titrator and Inductively Coupled Plasma Mass Spectrometer (ICPMS), respectively.*

[4] *Stable Isotopic analysis of geothermal springs using Gas Source Isotope Ratio Mass Spectrometer (IRMS).*

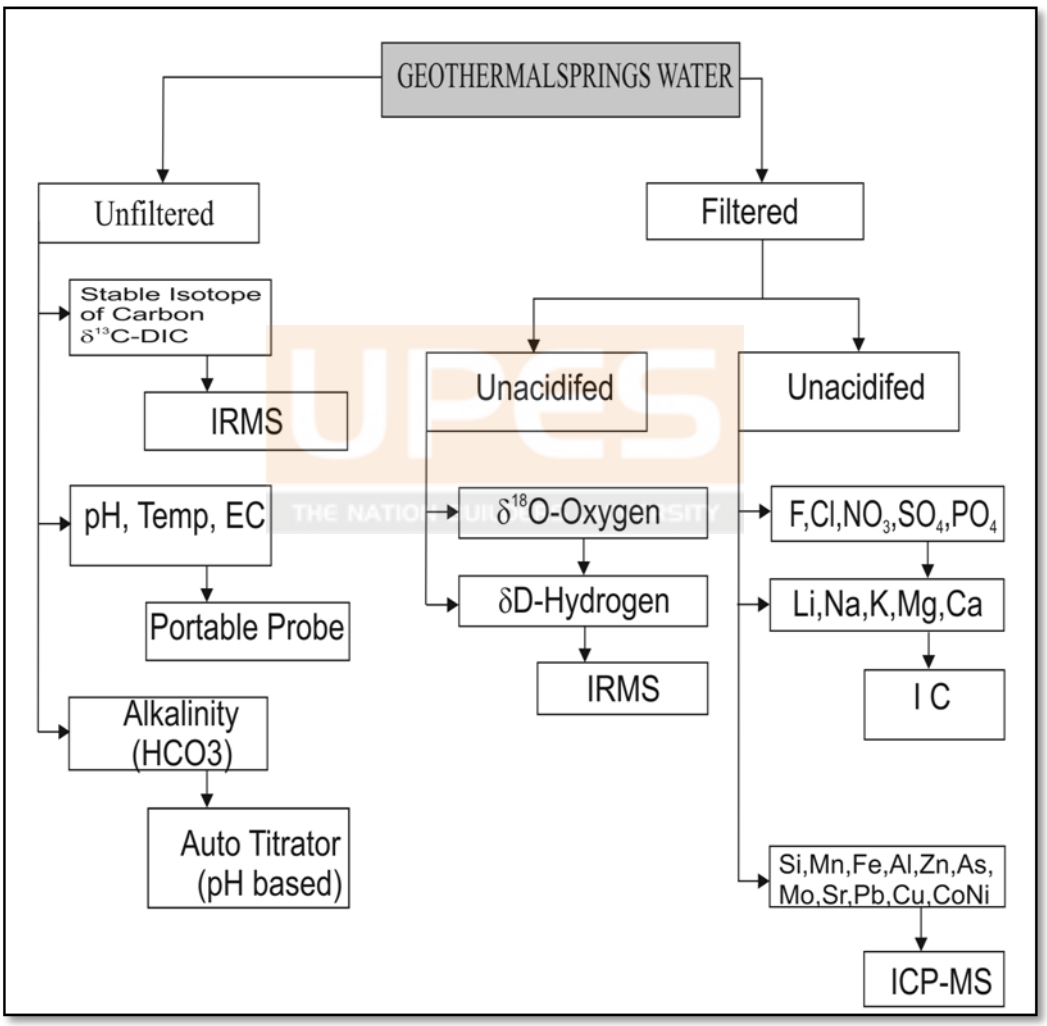


***Fig. 3.1:*** *Flow chart for different analytical techniques adopted for the study.*

## 3.2 FIELD WORK

Samples of geothermal springs and river waters were collected in the field and examined in the laboratory for their chemical properties. Details of covering all the measurements are given in the chapter as follows:

### 3.2.1 SAMPLE COLLECTION

Two field works were carried out during the November-December, 2010 and September-October, 2011 to collect samples of geothermal springs and river waters from Ladakh, Himachal, and Garhwal regions of northwest Himalaya. Water samples of these springs and rivers were collected near the source vent, and the mid-stream of river to avoid any local contamination. Samples were stored in pre-cleaned polyethylene bottles, which were properly rinsed with milli-Q (de-ionized) water and then with the sample water twice before sampling. About 125 ml of unfiltered water were stored in pre-cleaned polyethylene bottles for alkalinity and carbon stable isotope measurements. Another aliquot of 250 ml of water was filtered with 0.22µ milli-pore nylon membrane filter and kept in the amber color narrow mouth HDPE bottles for stable isotopes measurements. In addition, another aliquot of 250 ml of water was filtered with above said procedure and kept in to the pre-cleaned narrow mouth HDPE bottles for major and trace elements. All the samples splits were sealed onsite using Teflon tape and transported to the laboratory at Wadia Institute of Himalayan Geology, Dehradun for the measurements.

### 3.2.2 IN-SITU MEASUREMENTS

#### (A) GEOGRAPHICAL LOCATION AND ALTITUDE

Altitude and geographical coordinates (Latitude/Longitude) of these sampling sites were acquired using a hand-held Garmin Etrex Global Positioning System (GPS). It works with vertical and horizontal accuracies of±15 m, ±3.9 m (Ackerman et al., 2001) respectively. It is a useful substitute if no other source of Ground Control Point (GCP) is available at remote locations (Racoviteanu et al., 2007).

#### (B) pH, ELECTRIC CONDUCTIVITY (EC), DISCHARGE AND SURFACE TEMPERATURE

pH (negative logarithm of hydrogen ion concentration in aqueous solutions), temperature of the geothermal spring and river waters were measured on site using microprocessor based field pH meter (The LaMotte pH 6 Series meter which includes electrode and temperature probe. It can measure pH ranging from 0.01 to 14.00 with precision of ±0.01 (SD). Calibration of this instrument was done before measurements using buffer solutions (pH 4, 7 and 9.2 of Merck®) prepared in the field. Discharges of springs were measured using stop watch, measuring cylinder and a bucket with specific quantity. Electrical conductivity of the water samples were measured on site using LaMotte Con6 (Code-50038-02) with ranges from 1 to 20,000 µS/cm with a precision of ±1% (SD). Electric conductivity meter was calibrated before measuring the samples using standard solutions of 1413 µS/cm and 6668 µS/cm whereas the total

dissolved solids (TDS) of samples were measured using LaMotte Con6 (Code-50036-02) electrode.

## 3.3 GEOCHEMICAL ANALYSES

### 3.3.1 ALKALINITY MEASUREMENTS

Alkalinity ($HCO_3^-$) of geothermal springs and river waters were measured in unfiltered water samples (within 15 days of their collection) by adopting acid based titration with dilute HCL of known strength (0.01M) using an autotitrator (Metrohm-877, Titrino-plus) with glass electrode. These measurements were based on fixed end point method to achieve end point (best of three end points) within the higher and lower values of pH 8.3 and 4.3, for $CO_3^{2-}$ and total carbonate species ($HCO_3^-$ and $CO_3^{2-}$) following the earlier procedure (Dalai, 2001, unpublished Ph. D, Thesis).



### 3.3.2 MAJOR IONS ANALYSES

Major ion in these geothermal springs and river waters ($Cl^-$, $F^-$, $SO_4^{2-}$, $NO_3^-$, $Li^+$, $Na^+$, $K^+$, $Mg^{2+}$, $Ca^{2+}$) were analyzed by Ion Chromatograph (Dionex series ICS-5000). For these measurements, National Institute of Standard Technology (NIST) traceable primary standards [Dionex (six cation-II, standard product no.046070 & seven anion standard – II, product no. 057590)] were used for calibration of ICS-5000 before the sample measurements. Typical chromatograms for various ions are given in Figs. 3.2 & 3.3. Whereas

Fig.3.4 shows a good correlation ($r^2$=0.99) between the reported vs. measured values of elemental concentrations in these standards.

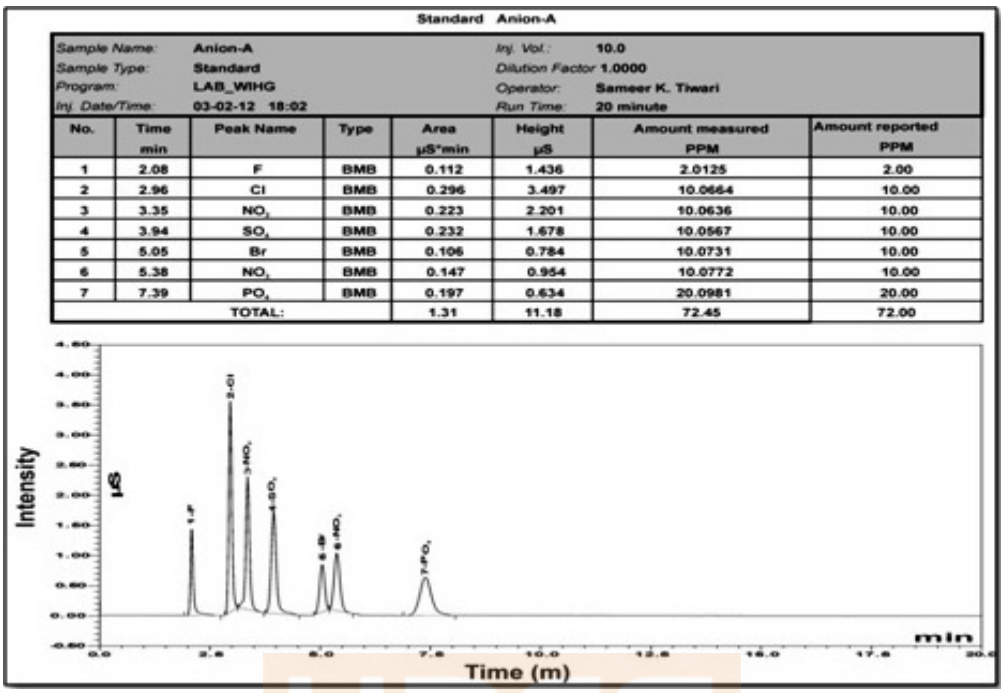

Standard Anion-A

| | | | |
|---|---|---|---|
| Sample Name: | Anion-A | Inj. Vol.: | 10.0 |
| Sample Type: | Standard | Dilution Factor | 1.0000 |
| Program: | LAB_WIHG | Operator: | Sameer K. Tiwari |
| Inj. Date/Time: | 03-02-12 18:02 | Run Time: | 20 minute |

| No. | Time min | Peak Name | Type | Area µS*min | Height µS | Amount measured PPM | Amount reported PPM |
|---|---|---|---|---|---|---|---|
| 1 | 2.08 | F | BMB | 0.112 | 1.436 | 2.0125 | 2.00 |
| 2 | 2.96 | Cl | BMB | 0.296 | 3.497 | 10.0664 | 10.00 |
| 3 | 3.35 | $NO_2$ | BMB | 0.223 | 2.201 | 10.0636 | 10.00 |
| 4 | 3.94 | $SO_4$ | BMB | 0.232 | 1.678 | 10.0567 | 10.00 |
| 5 | 5.05 | Br | BMB | 0.106 | 0.784 | 10.0731 | 10.00 |
| 6 | 5.38 | $NO_3$ | BMB | 0.147 | 0.954 | 10.0772 | 10.00 |
| 7 | 7.39 | $PO_4$ | BMB | 0.197 | 0.634 | 20.0981 | 20.00 |
| | | TOTAL: | | 1.31 | 11.18 | 72.45 | 72.00 |



***Fig.3.2:*** *Chromatograph of primary standard of Dionex, (seven anion standards-II, product no-057590) traceable to National Institute of Standard (NIST).*

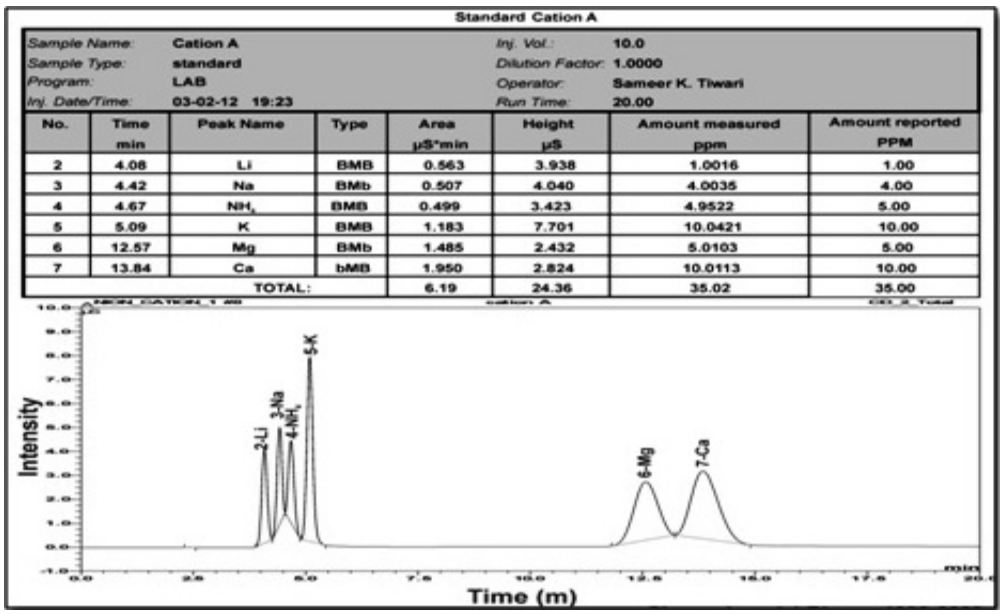

Standard Cation A

| | | | |
|---|---|---|---|
| Sample Name: | Cation A | Inj. Vol.: | 10.0 |
| Sample Type: | standard | Dilution Factor: | 1.0000 |
| Program: | LAB | Operator: | Sameer K. Tiwari |
| Inj. Date/Time: | 03-02-12 19:23 | Run Time: | 20.00 |

| No. | Time min | Peak Name | Type | Area µS*min | Height µS | Amount measured ppm | Amount reported PPM |
|---|---|---|---|---|---|---|---|
| 2 | 4.08 | Li | BMB | 0.563 | 3.938 | 1.0016 | 1.00 |
| 3 | 4.42 | Na | BMb | 0.507 | 4.040 | 4.0035 | 4.00 |
| 4 | 4.67 | $NH_4$ | BMB | 0.499 | 3.423 | 4.9522 | 5.00 |
| 5 | 5.09 | K | BMB | 1.183 | 7.701 | 10.0421 | 10.00 |
| 6 | 12.57 | Mg | BMb | 1.485 | 2.432 | 5.0103 | 5.00 |
| 7 | 13.84 | Ca | bMB | 1.950 | 2.824 | 10.0113 | 10.00 |
| | | TOTAL: | | 6.19 | 24.36 | 35.02 | 35.00 |



**Fig. 3.3:** *Chromatograph of primary standard of Dionex, (six cation – II standard, product no-046070), traceable to NIST.*

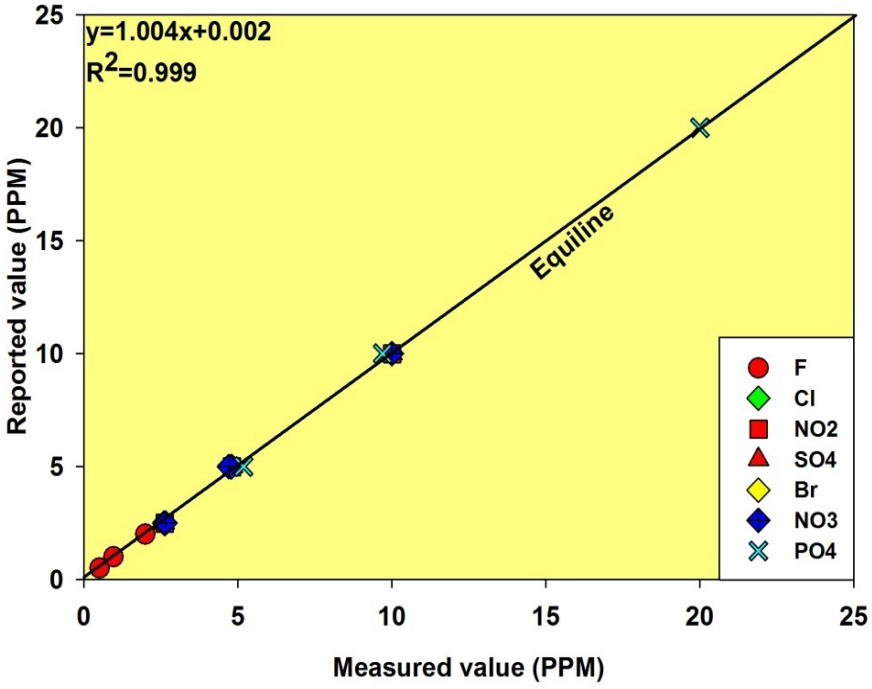


*(a)*

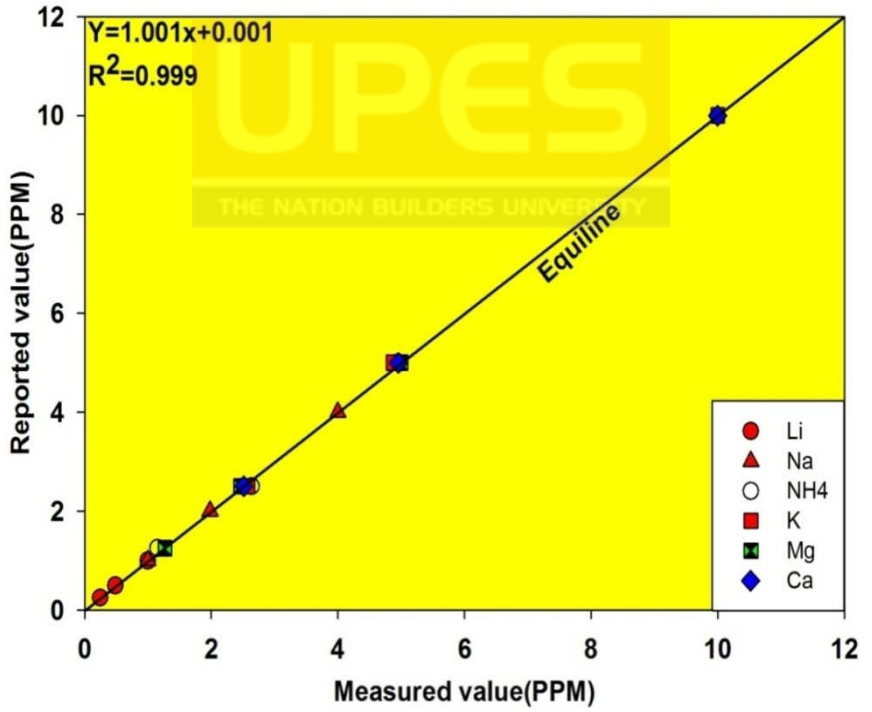


*(b)*

***Fig. 3.4:*** *Measured vs. reported elemental concentrations in reference material of National Institute of Standard Technology (NIST) traceable primary standards of Dionex (a) seven anion-II, Product no.057590; (b) seven Cation-II, Product no.046090 to check the accuracy of measurements.*

***Repeat measurements of major ions in geothermal springs***

The precision of major ions in the samples are important for the reliable measurements. These were assessed by repeat measurements in random samples of geothermal springs and are presented below in (Tables 3.1 & 3.2).

***Table 3.1:*** *Repeat analyses of major anions of random samples show the precision better than ± 5% (concentrations in mg/L, nd- not determined).*

| Sr. No | Sample Name | $F^-$ | $Cl^-$ | $SO_4^{2-}$ | $NO_3^-$ |
|---|---|---|---|---|---|
| 01 | HS-24 | 11.8 | 8.9 | 46.7 | nd |
| | HS-24_R | 11.2 | 8.4 | 43.9 | nd |
| 02 | HS-11 | 2.4 | 60.3 | 47.3 | nd |
| | HS-11_R | 2.4 | 59.4 | 45.6 | nd |
| 03 | HS-40 | 0.9 | 45.4 | 34.3 | nd |
| | HS-40_R | 0.7 | 45.1 | 34.1 | nd |

***Table 3.2:*** *Repeat analyses of major cations of random samples show the precision better than ± 5%, (concentrations in mg/L).*

| Sr. No. | Sample Name | $Li^+$ | $Na^+$ | $K^+$ | $Mg^{+2}$ | $Ca^{+2}$ |
|---|---|---|---|---|---|---|
| 01 | HS-24 | 0.3 | 79.8 | 5.0 | 4.2 | 1.1 |
| | HS-24_ REPEAT | 0.3 | 76.3 | 5.0 | 4.2 | 1.3 |
| 02 | HS-12 | nd | 90.1 | 4.6 | 0.8 | 7.2 |
| | HS-12_ REPEAT | nd | 87.4 | 4.2 | 0.9 | 9.1 |
| 03 | HS-40 | 5.7 | 36.5 | 13.9 | 11.7 | 13.9 |
| | HS-40_ REPEAT | 5.9 | 35.4 | 13.6 | 11.3 | 13.3 |

### 3.3.3 TRACE ELEMENTS ANALYSES

Trace elements and dissolved silica were measured in unacidified, filtered aliquot of these waters using a quadrupole Inductively Coupled Plasma-Mass Spectrometer (ICP-MS). It combines a high-temperature inductively coupled plasma source with a mass spectrometer which is used for elemental

determinations. It is useful for elements with lower abundances, particularly for the trace elements, due to its superior detection capabilities over other analytical techniques. The reproducibility of measurement in this study was better than ± 5% for trace elements and dissolved silica in water samples.

## 3.4 STABLE ISOTOPES ANALYSES

The stable isotopes ($\delta^{18}O$, and $\delta D$) were measured by standard equilibration method in which water samples were equilibrated with $CO_2$ and $H_2$, respectively. The equilibrated $CO_2$ and $H_2$ gases were then analyzed in Delta V plus Isotope Ratio Mass Spectrometer (IRMS) at Wadia Institute of Himalayan Geology (WIHG), Dehradun, India (Fig.3.5). Before the stable isotopes measurements ($\delta^{13}C$, $\delta^{18}O$ and $\delta D$), the reference gases [$CO_2$ (99.999 %) & $H_2$ (99.999 %)] were calibrated against the international standards; IAEA-NBS-18 and the (IAEA-GISP & VSMOW), respectively. Measured isotopic compositions are reported in terms of $\delta^{13}C_{DIC}$ and ($\delta^{18}O$ and $\delta D$) against (VPDB & VSMOW), respectively. $^{18}O/^{16}O$ and D/H ratios were used to compute $\delta^{18}O$ and $\delta D$ following the earlier procedure (Despande et al., 2010). The reproducibility of measurement was better than 0.1‰ (1SD) for $\delta^{18}O$ and 1‰ (1SD) for $\delta D$. In addition, inter laboratory standards (supplied by the National Institute of Hydrology, Roorkee, India) with varied range of isotopic compositions were also measured for their $\delta^{18}O$ and $\delta D$ to check the consistency of the results. Carbon isotope composition of dissolved inorganic carbon ($\delta^{13}C_{DIC}$) in water samples were measured on $CO_2$ released by acidification with pure $H_3PO_4$ (99%) in vacuum following the earlier

procedures (Galy & France-Lanord 1999; Evans et al. 2008). To check the accuracy and consistency of the results, a laboratory standard (Merck $CaCO_3$ calibrated against NBS-18) was run several times during the course of this study (table 3.3). Repeat measurements of the water samples show a precision better than 0.1‰ for $\delta^{13}C$ which are also presented in Table. 3.4.

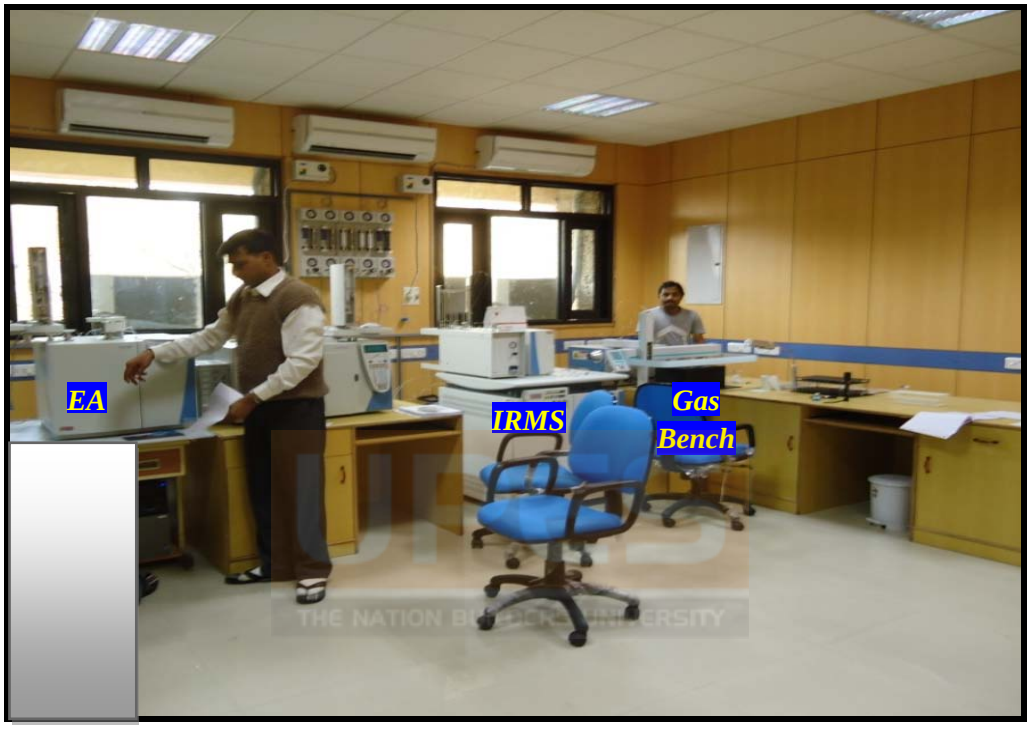


***Fig.3.5:*** *Stable Isotope Ratio Mass Spectrometer (IRMS) laboratory of Wadia Institute of Himalayan Geology (WIHG), Dehradun.*

**Carbon stable isotope ($\delta^{13}C_{DIC}$) measurement**

The ratio of stable isotopes of carbon is analysed against the international standards of International Atomic of Energy Agency (IAEA). The isotopic ratio ($^{13}C/^{12}C$) of the sample is expressed in term of notation as $\delta^{13}C$ with respect to the standard and the unit is expressed as parts per mill (‰). It is define as:

$$\delta^{13}C\ (‰) = \left[ \frac{\left(\frac{^{13}C}{^{12}C}\right)_{sample}}{\left(\frac{^{13}C}{^{12}C}\right)_{standard}} - 1 \right] x\ 1000$$

Dissolved inorganic carbon (DIC) is the sum of inorganic carbon species in the natural waters which include carbon dioxide, bicarbonate anion and Carbonate.

$DIC = (CO_2^*) + (HCO_3^-) + (CO_3^{2-})$

Where, DIC is the Dissolved inorganic carbon; $(CO_2^*)$ is the sum of carbon dioxide and carbonic acid concentrations $[(CO_2^*) = (CO_2) + (H_2CO_3)]$; $(HCO_3^-)$ is the bicarbonate concentration; $(CO_3^{2-})$ is the carbonate concentration.

Carbon isotopic composition ($\delta^{13}C_{DIC}$) of thermal waters were analyzed using a Finnigan Gasbench II (Fig. 3.5) and isotope ratio mass spectrometer (IRMS, Delta V-Plus) at stable isotope laboratory at Wadia Institute of Himalayan Geology (WIHG), Dehradun (India). For calibration of the instrument, National Bureau of Standard (NBS-18) procured from International Atomic Energy Agency (IAEA) was also measured. Further, an internal lab standard (MERCK $CaCO_3$) was prepared and measured several times against the NBS-18. This was taken as in-house standard (Merck pure GR-Grade, $CaCO_3$) and was run with every batch of analyses. It yielded an average value of –46.9 ±0.07‰ which is consistent with earlier values measured in the lab (table 3.3). In addition, to check whether the measurement procedure is reliable, several blanks were measured which did not give any signal.

**Analytical flowchart of ($\delta^{13}C_{DIC}$) for sample preparation procedure**

From sample preparation to their analyses was completed in four steps. The first step is to put 50 to 70 µl of the pure phosphoric acid (99%) into a clean vial of (12 ml) with cap and septa. Closed vials are then placed into the tray attached with Gas bench maintained at the temperature of $32^0$C. All the vials are treated with 99.999% pure Helium gas by passing through the flushing needle attached with PAL auto sampler of gas bench unit. This is required to flush the vials to remove all the atmospheric gases present already, and then inject ~700 µl of water samples into the vial via a disposable syringe.

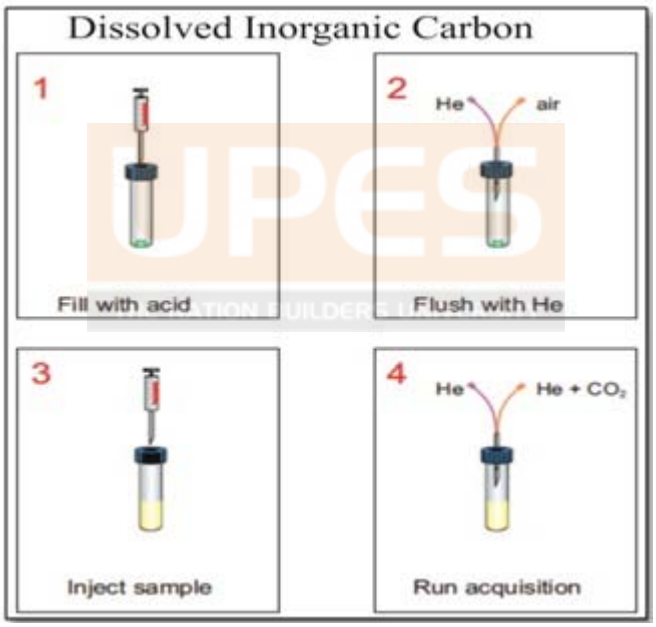


***Fig 3.6:*** *Four steps schematic diagram showing samples preparation for measurements using Finnigan Gasbench II of IRMS.*

After injecting the samples into the vials, it is allowed for a minimum time of 18 hours at $32^0$C to equilibrate with $CO_2$ (fig. 3.6) of known amount and composition. Finally the sample is ready to measure the $\delta^{13}C_{DIC}$ using continuous flow IRMS through analysis needle attached with gas bench.

Towards this, NBS-18 (IAEA, primary standard) have been analysed to calibrate the IRMS before the sample measurements. The material, NBS-18 is a carbonatite from Fen locality of Norway. It was collected by B. Taylor, University of California, Davis, USA, and crushed by H. Friedrichsen at University of Tubingen (Germany) to distribute it to different laboratories around the world. Its recommended $\delta^{13}C$ value (–5.014±0.03‰, $_{VPDB}$) was determined through an international calibration study. The measured value of NBS -18 for $\delta^{13}C$ (–5.2±0.1‰, $_{VPDB}$) in this study is consistent and given in the Table-3.3 & Fig. 3.7. Along with each batch of samples, several laboratory standards were analyzed to check the accuracy of measurements. The secondary lab standard of Merck $CaCO_3$ was calibrated against the primary standard of NBS-18. The measured value for $\delta^{13}C$ of Merck $CaCO_3$ is –46.99±0.05‰, $_{VPDB}$. Values of (Merck $CaCO_3$) are mentioned in the Table 3.3 & Fig.3.8. Based on repeat measurements of about seven samples of geothermal spring, the reproducibility was found to be better than ±0.1 (Table 3.4 & Fig. 3.9).

***Table 3.3:*** *$\delta^{13}C$ calibration of International Atomic Energy Agency (IAEA) primary standard (NBS-18) and secondary laboratory standard (Merck-$CaCO_3$).*

| **Sample name** | **Reported value of $\delta^{13}C$ ‰ by (IAEA)** | **Measured value of $\delta^{13}C$‰ at (WIHG)** | **Standard deviation** |
|---|---|---|---|
| NBS-18 | –5.01±0.03‰ | –5.21(n=20) | 0.1 |
| Merck ($CaCO_3$) | | –47.02 (n=20) | 0.02 |

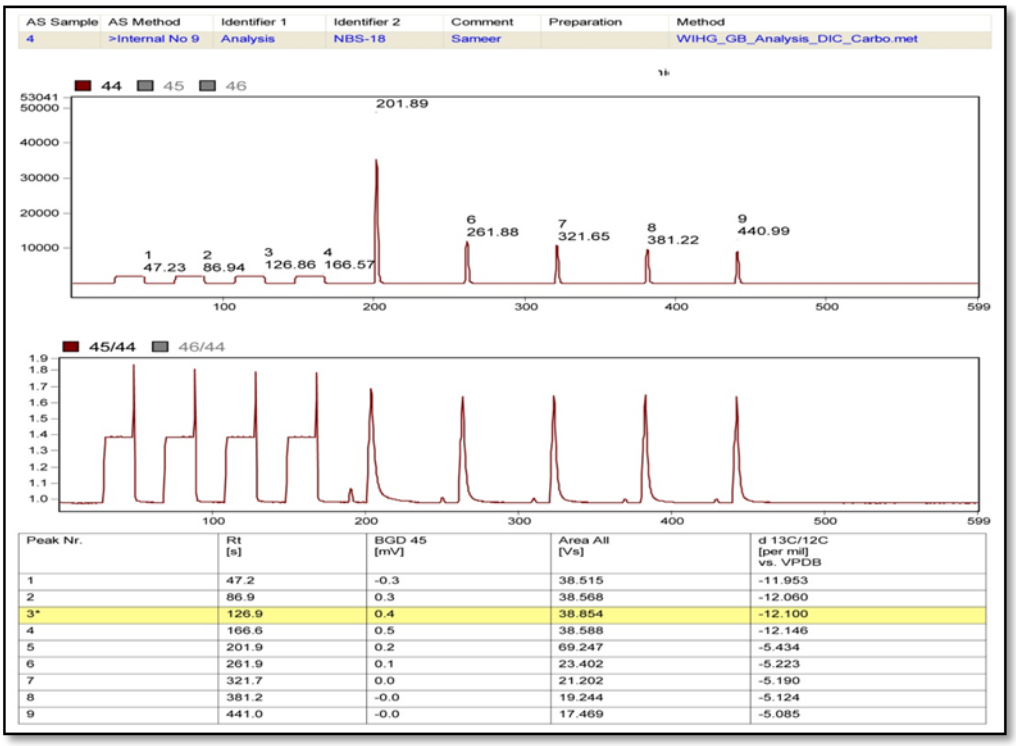


| Peak Nr. | Rt [s] | BGD 45 [mV] | Area All [Vs] | d 13C/12C [per mil] vs. VPDB |
|---|---|---|---|---|
| 1 | 47.2 | -0.3 | 38.515 | -11.953 |
| 2 | 86.9 | 0.3 | 38.568 | -12.060 |
| 3* | 126.9 | 0.4 | 38.854 | -12.100 |
| 4 | 166.6 | 0.5 | 38.588 | -12.146 |
| 5 | 201.9 | 0.2 | 69.247 | -5.434 |
| 6 | 261.9 | 0.1 | 23.402 | -5.223 |
| 7 | 321.7 | 0.0 | 21.202 | -5.190 |
| 8 | 381.2 | -0.0 | 19.244 | -5.124 |
| 9 | 441.0 | -0.0 | 17.469 | -5.085 |

***Fig 3.7:*** *Mass* spectrum *of reference material NBS-18, measured at WIHG lab for calibration of IRMS for* $\delta^{13}C$‰ *measurements.*

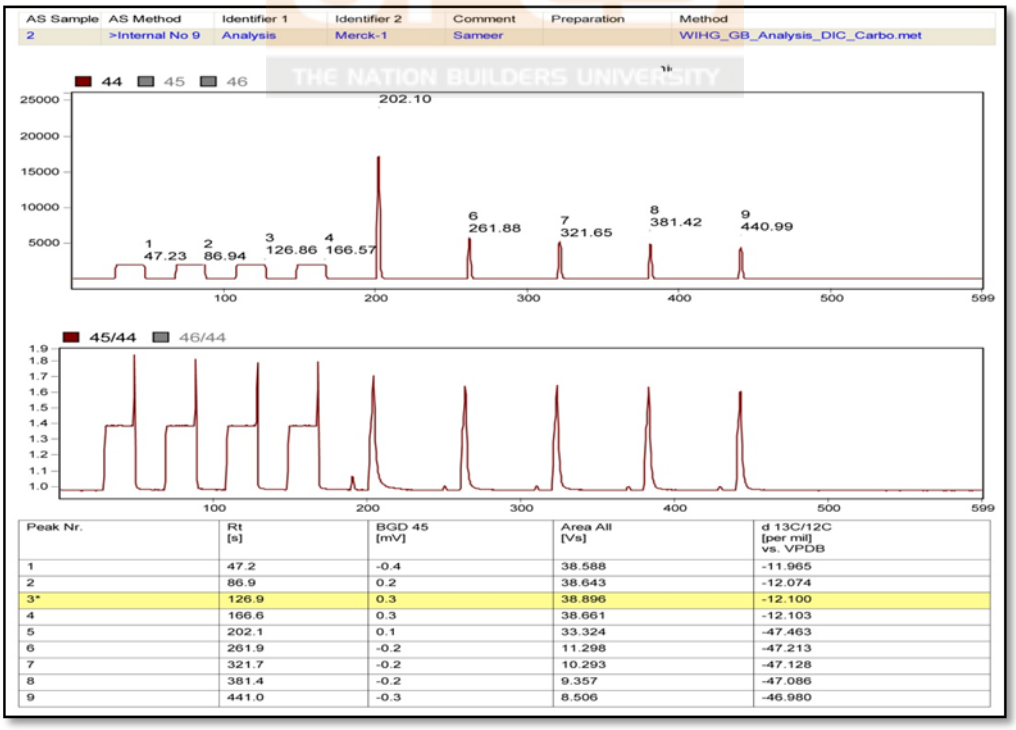


| Peak Nr. | Rt [s] | BGD 45 [mV] | Area All [Vs] | d 13C/12C [per mil] vs. VPDB |
|---|---|---|---|---|
| 1 | 47.2 | -0.4 | 38.588 | -11.965 |
| 2 | 86.9 | 0.2 | 38.643 | -12.074 |
| 3* | 126.9 | 0.3 | 38.896 | -12.100 |
| 4 | 166.6 | 0.3 | 38.661 | -12.103 |
| 5 | 202.1 | 0.1 | 33.324 | -47.463 |
| 6 | 261.9 | -0.2 | 11.298 | -47.213 |
| 7 | 321.7 | -0.2 | 10.293 | -47.128 |
| 8 | 381.4 | -0.2 | 9.357 | -47.086 |
| 9 | 441.0 | -0.3 | 8.506 | -46.980 |

***Fig. 3.8:*** *Mass spectrum of Merck (pure,* $CaCO_3$*) lab standard, measured against reference material of NBS-18 at WIHG lab for use as secondary standard.*

***Repeat measurements of geothermal springs***

***Table 3.4:*** *Results of repeat analyses of ($\delta^{13}C_{DIC}$) in geothermal springs.*

| Sr. No | Sample Name | Value of $\delta^{13}C_{DIC}$ (‰) | Standard Deviation |
|---|---|---|---|
| 1 | HS-1 | 0.9 | 0 |
| | HS-1 _REPEAT | 1 | 0.1 |
| 2 | HS-3 | –5.2 | 0.1 |
| | HS-3_REPEAT | –5.7 | 0 |
| 3 | HS-4 | 1.6 | 0.1 |
| | HS-4 _REPEAT | 1.4 | 0.1 |
| 4 | HS-5 | 4.1 | 0.1 |
| | HS-5_REPEAT | 4.2 | 0.1 |
| 5 | HS-25-2 | –3.8 | 0.1 |
| | HS-25-2 REPEAT | –3.8 | 0.04 |
| 6 | HS-33 | –3.8 | 0.1 |
| | HS-33 REPEAT | –3.8 | 0.1 |
| 7 | HS-40 | –5.5 | 0.05 |
| | HS-40 REPEAT | –5.6 | 0.1 |



The precision of $\delta^{13}C_{DIC}$ in the samples have been assessed by repeat measurements in random samples. It is found to be 0.1‰ which is presented in Table 3.4 & Fig. 3.9.

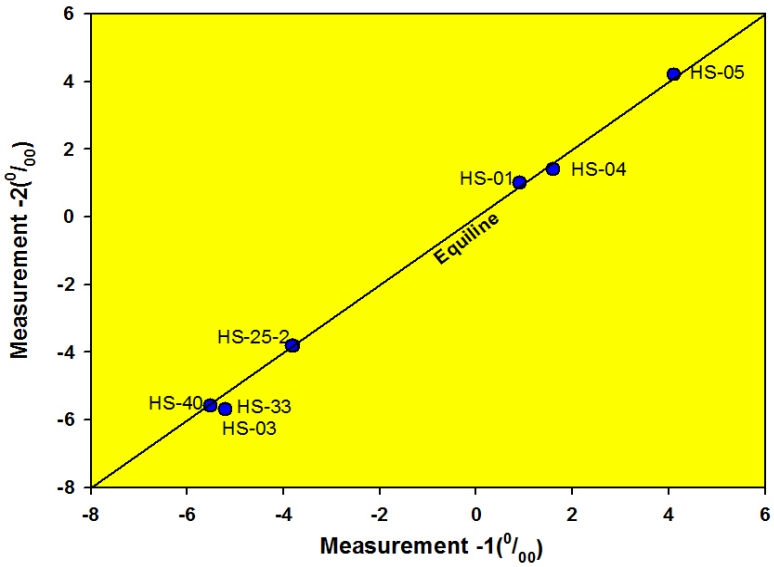


**Fig. 3.9:** *Repeat measurements of $\delta^{13}C_{DIC}$ in random samples of geothermal springs, showing good repeatability ($r^2$=0.99).*

**Stable isotope of oxygen ($\delta^{18}O$) measurement**

The $\delta^{18}O$ measurements are expressed in per mill (‰) and given as following:

$$\delta^{18}O\ (‰) = \left[\frac{\left(\frac{^{18}O}{^{16}O}\right)_{sample}}{\left(\frac{^{18}O}{^{16}O}\right)_{standard}} - 1\right] x\ 1000$$

The filtered water samples were analyzed using gas bench attachment at Stable Isotope Laboratory of WIHG against the international standards (VSMOW, GISP). All water samples (stored in amber colour narrow mouth bottles) were homogenised and shaken well before analyses. About 200 µl of water was kept into the clean Labco Exetainer vial (12 ml) by using an adjustable pipette with disposable tips. Screw capped vials were kept in a thermostatic sampling tray (preset at temperature ~32$^0$C) on gas bench peripheral (Fig. 3.10). Head space of every vial was flushed through He-$CO_2$ gas mixture (He+0.1% $CO_2$) for ~12 minutes to remove the atmospheric gases (Fig. 3.11). During the flush filling, the flow rates of flush gas were measured by a flow meter which is typically kept at 15 ml/minute. After the flushing is complete, the samples were left at least for 18 hours for equilibration with flushed gas headspace $CO_2$ gas at the constant temperature of 32$^0$C. The equilibrated gas was sampled from the head space of every vial by introducing pure 99.999%, helium (He, pressure 0.8 bar) with the help of automated analysis needle (Fig. 3.11). The gas mixture was then passed through online moisture removal traps (nafion tube) to remove moisture. After removal of moisture, it is passed through an isothermal gas-chromatographic column (set at 60$^0$C) to separate the gases. Now, pure $CO_2$ sample gas is introduced in to IRMS for measuring the isotope ratios.

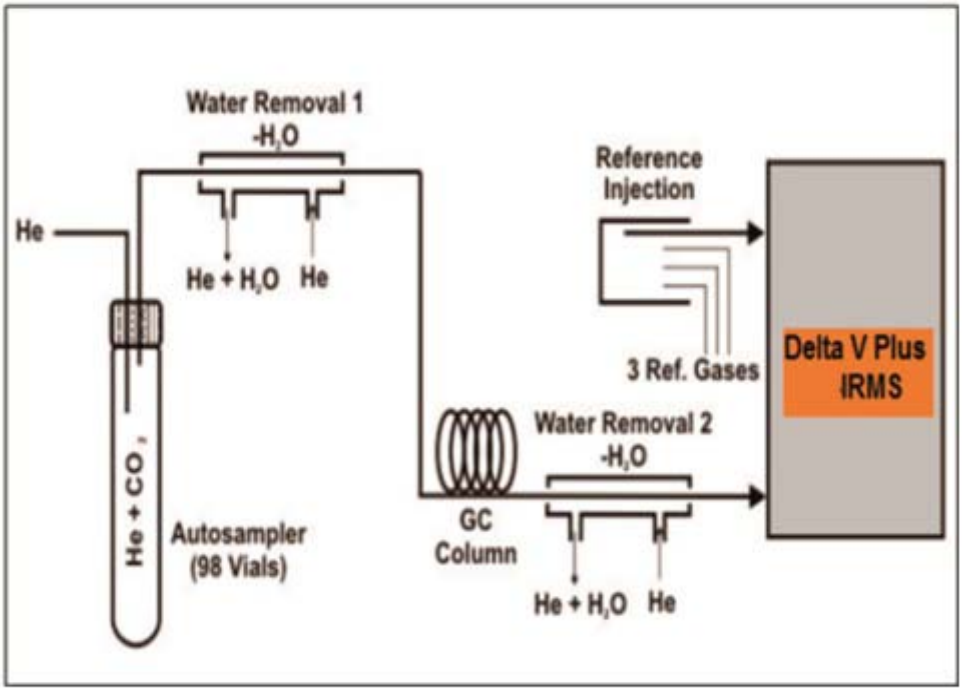


***Fig. 3.10:*** *Schematic diagram showing different functional part of Finnigan Gasbench II of IRMS.*

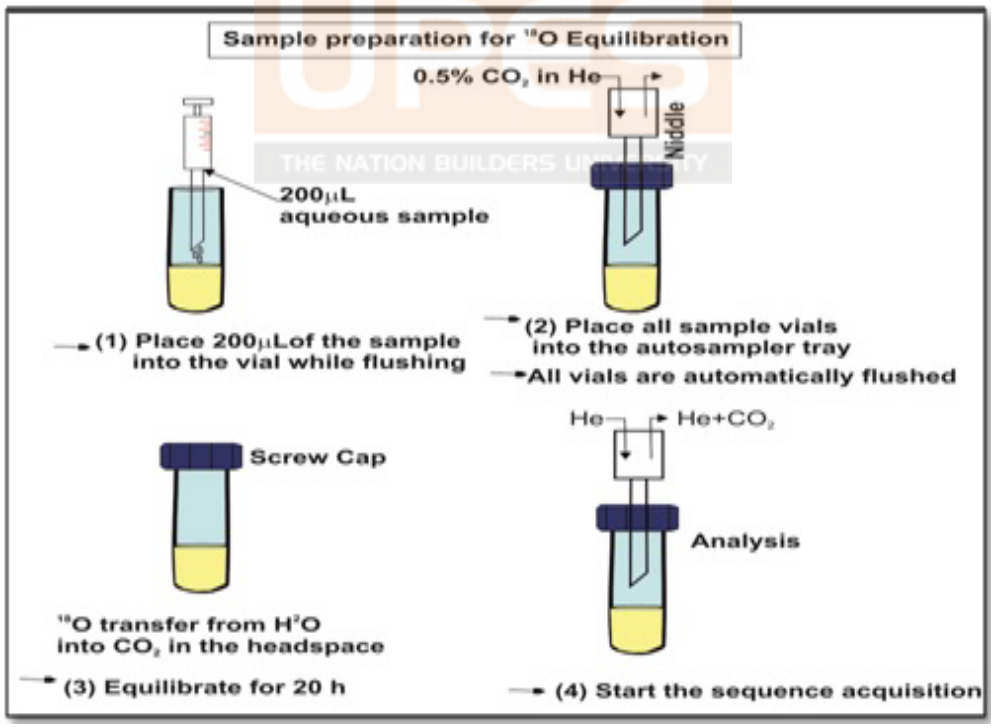


***Fig. 3.11:*** *Schematic diagram showing sample preparation procedure for $\delta^{18}O$ measurements using Finnigan Gasbench II of IRMS.*

During the course of this work, IRMS was calibrated with primary standards VSMOW (Vienna Standard Mean Ocean Water) and GISP (Greenland Ice Sheet Precipitation) and the results are consistent and presented in Tables 3.5 & 3.6. The primary standard (VSMOW-2) is an international standard for the measurement of stable isotopes of oxygen and hydrogen in water. This standard was prepared by water material at the IAEA isotope Hydrology Lab in the year 2006 which replaced the exhausted VSMOW standard. VSMOW-2 is a mixture of carefully calibrated distilled natural water samples in order to get a stable isotope composition as similar to VSMOW. The reported value of VSMOW-2 for oxygen isotope is 0±0.02‰ which is proved by IAEA with standard materials. GISP (Green Land Ice Sheet Precipitation) was prepared by W. Dansgaard at University of Copenhagen, from a snow sample of Greenland. The $\delta^{18}O$ values of GISP are based on VSMOW-SLAP scale. The reported value of GISP for oxygen isotope is –24.76±0.09‰ and is approved by IAEA with standard materials.

***Table 3.5:*** *$\delta^{18}O$ results of (VSMOW), primary standard of IAEA.*

| **Sr. No.** | **Sample Name** | **Reported value of $\delta^{18}O$‰ by( IAEA)** | **Measured value of $\delta^{18}O$‰ at (WIHG)** |
|---|---|---|---|
| **01** | Analysis_1 | 0±0.02‰ | 0.0 |
| **02** | Analysis_2 | | 0.1 |
| **03** | Analysis_3 | | 0.0 |
| **04** | Analysis_4 | | –0.1 |
| **05** | Analysis_5 | | 0.0 |
| **06** | Analysis_6 | | 0.0 |

***Table 3.6:*** *$\delta^{18}O$ results of (GISP), primary standards of IAEA.*

| Sr. No. | Sample Name | Reported value of $\delta^{18}O$‰ by (IAEA) | Measured value of $\delta^{18}O$‰ at (WIHG) |
|---|---|---|---|
| 01 | Analysis_1 | (–24.76±0.09‰) | –24.49 |
| 02 | Analysis_2 | | –24.40 |
| 03 | Analysis_3 | | –24.44 |

***Repeat measurements of oxygen ($\delta^{18}O$) in geothermal springs***

During the measurements of water samples in IRMS, several randomly selected samples were measured in duplicate for the checking precision and the results as presented in (Tables 3.7 & Fig. 3.12).

***Table 3.7:*** *Results of repeat analyses of $\delta^{18}O$ in geothermal springs.*

| Sr. No. | Sample ID | Average of $\delta^{18}O$‰ (VSMOW) |
|---|---|---|
| **1** | HS 03 | –11.48 |
| | HS 03 _ (REPEAT) | –11.48 |
| **2** | HS 06 | –8.32 |
| | HS 06 _(REPEAT) | –8.32 |
| **3** | HS-17 | –8.40 |
| | HS-17 _(REPEAT) | –8.39 |
| **4** | HS-19 | –8.92 |
| | HS-19 _(REPEAT) | –8.80 |
| **5** | RW-06 | –10.19 |
| | RW-06_(REPEAT) | –10.25 |
| **6** | HS 26 | –14.34 |
| | HS 26 _(REPEAT) | –14.34 |
| **7** | HS 33 | –6.28 |
| | HS 33 _(REPEAT) | –6.30 |
| **8** | HS 37 | –10.29 |
| | HS 37_(REPEAT) | –10.29 |
| **9** | HS 40 | –8.88 |
| | HS 40_ (REPEAT) | –8.82 |

Based on these measurements precision of the $\delta^{18}O$ analyses is better than 0.1‰. Therefore, it can be suggested that the procedure adopted for the stable isotope analyses are robust and reliable.

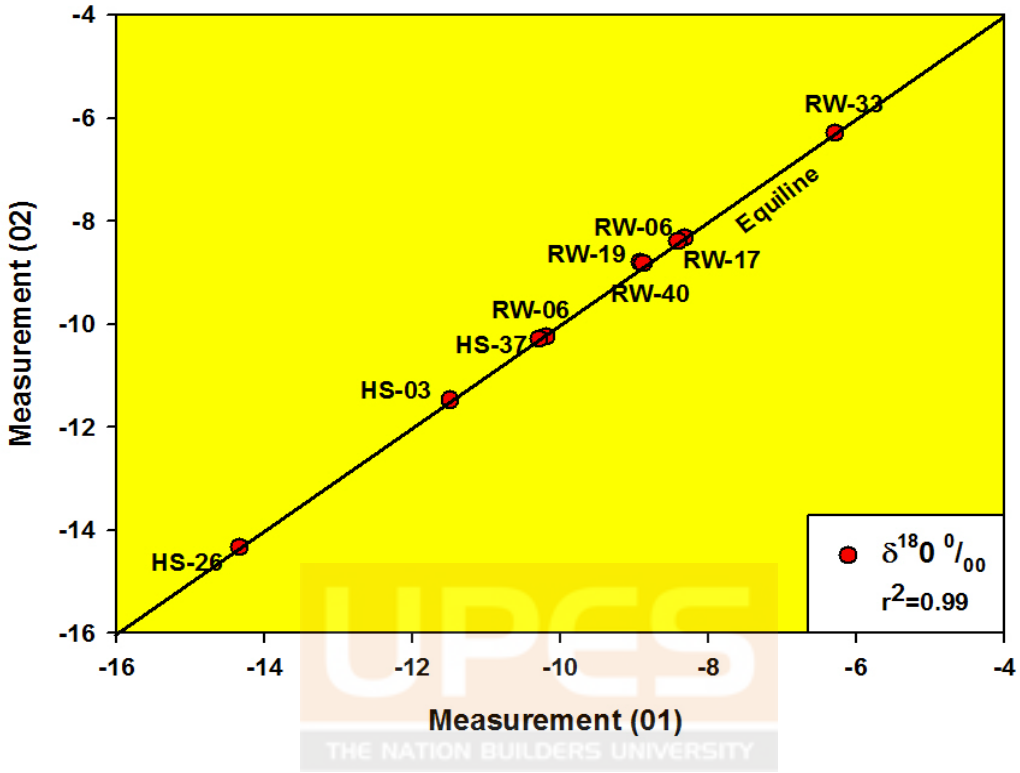


**Fig. 3.12:** *Repeat measurements of $\delta^{18}O$ in random samples of geothermal springs showing good repeatability ($r^2$=0.99).*

**Stable isotope of hydrogen (δD) measurement**

The analytical procedure for measurements of δD is almost similar to that of $\delta^{18}O$ by using IRMS delta V plus except the equilibration method where a platinum stick is kept into the vial before flush filling. The platinum acts as catalyst for reducing the time of equilibration to one hour. In this procedure, the mixture of He and 0.05% $H_2$ was used for equilibration (Fig. 3.13). The isotope ratio X (where X-unknown and T-tank) was measured with

respect to a reference $H_2$ gas from the tank. IRMS was also calibrated with primary standards of (GISP) and (VSMOW) supplied by IAEA (Tables 3.8 and 3.9) for δD measurements. The reported value of VSMOW-2 for $^{2}H$ isotope is 0±0.3‰ which is assigned by IAEA with standard materials. The reported value of GISP for $^{2}H$ (or D) isotope is –189.5±1.2‰. $^{18}O/^{16}O$ and D/H ratios were measured to compute $\delta^{18}O$ and δD following the standard procedure (Despande et al., 2010). The reproducibility of measurement was better than 1‰ (1SD) for δD. In addition, three laboratory standards (supplied by the National Institute of Hydrology, Roorkee, India) with varied range of isotopic compositions were also measured for their δD to check the consistency of the results (Table 3.10) on inter laboratory level.

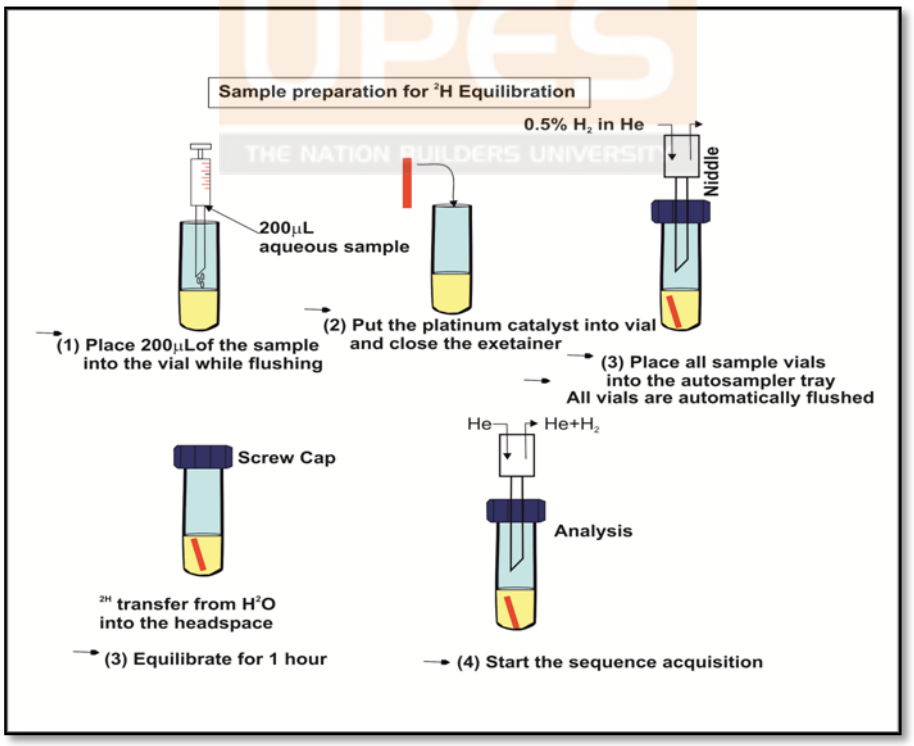


***Fig. 3.13:*** *Schematic diagram for sample preparation procedure for δD measurements.*

**Correction of $H_3^+$ factor**

The $H_3$ factor, K, is a parameter used in high precision mass spectrometric measurements of hydrogen $^2H$ isotopic ratios. $H_3^+$ factor corrections were executed during the measurement of $^2H$. When $H_2$ is required as the sample gas, $R^* = R - K_{i2}$, where $R^*$ is the true $HD/H_2$ ratio, and R is the observed (mass3)/(mass2) ion current ratio, and $i_2$ is the ion current at mass 2.

$H_3^+$ is formed during electron impact in the ion source by the following reaction (Friedman, 1953).

$$H_2^+ + H_2 \longrightarrow H_3^+ + H^+ \quad \text{.....Eqn. (3.1)}$$

Charge and mass of $H_3^+$ and HD is similar, $H_3^+$ contributes to mass-3 and thus affect the D/H ratio. Therefore a correction is required to reduce the contribution of $H_3$ from mass 3 which are described as $H_3^+$ correction. The abundance of $H2^+$ is proportional to the partial pressure of $^2H$, hence, the production of $H3^+$ is proportional to the second power of the partial pressure of $H_2$, $[i_{H3} = K(i_{H2})^2]$. Fig. 3.14 graphically represents the importance of $H_3^+$ correction. Experimental calculation of $H_3^+$ correction involved in following steps. The slope ($H^{3+}$ correction) in the Fig. 3.14 was estimated through the Isodat in built software in the IRMS by increasing the reference gas pressure and its simultaneous monitoring. The calculated $H_3^+$ factor for the measurements of forty geothermal samples was found to be *3.329*, which is also mentioned in the mass spectrum for VSMOW-2 measurement.

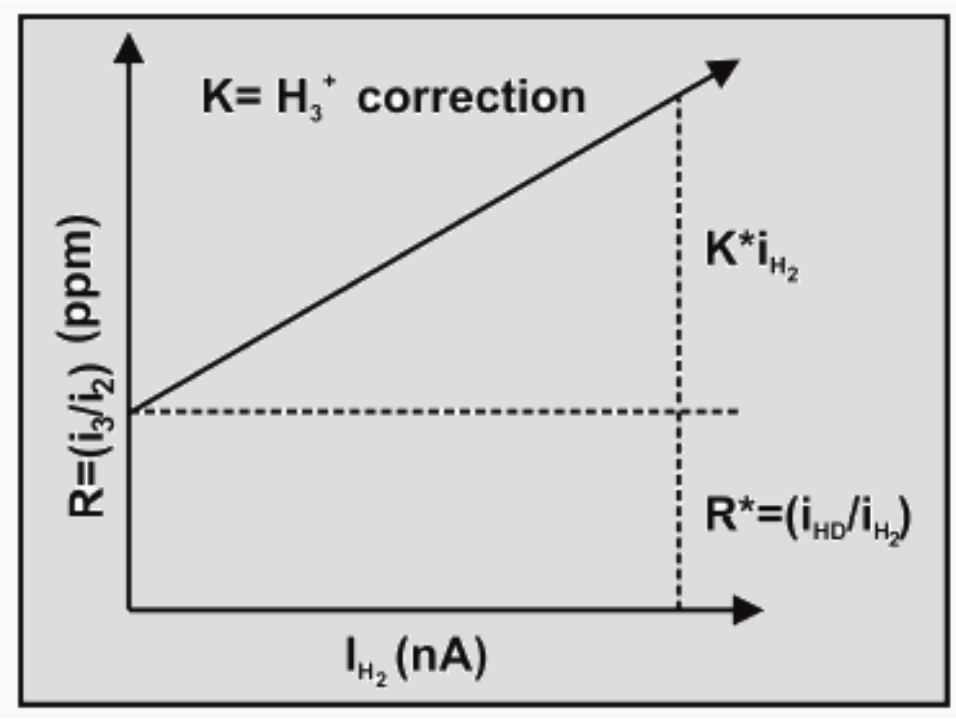


***Fig.3.14:*** *Schematic diagram for determination of $H_3^+$ factor for δD measurement.*

***Table 3.8:*** *δD results of (GISP) primary standards of IAEA.*

| **Sample Name** | **Reported value of δD‰** | **Measured value of δD‰** | **(STDEV) ‰** |
|---|---|---|---|
| **Analysis_1** | (–189.5±1.2‰) | –187.3±1.2 | 1 |
| **Analysis_2** | | –186.3±1.2 | |
| **Analysis_3** | | –188.4±1.5 | |

***Table 3.9:*** *δD results of (VSMOW) primary standards of IAEA.*

| **Sample ID** | **Reported value of δD‰** | **Measured value of δD‰** | **(STDEV) ‰** |
|---|---|---|---|
| Analysis_1 | 0±0.3‰ | –1.1±1 | 1 |
| Analysis_2 | | –1.3±1 | 1 |

***Inter Laboratory Comparison: Secondary standard measurements of National Institute of Hydrology***

***Table 3.10:*** *δD results of secondary standards of National Institute of Hydrology (NIH).*

| No of Measurements | Sample ID | NIH Reported | Measured at WIHG | Average measured |
|---|---|---|---|---|
| | | δD‰VSMOW | | |
| Analysis-1 | Sea water | 2.3 | 3.1 | 2.7 |
| Analysis-2 | | | 2.5 | |
| Analysis-3 | | | 2.5 | |
| Analysis-1 | Gangotri Water | -112.9 | –110.4 | -111.6 |
| Analysis-2 | | | –112.0 | |
| Analysis-3 | | | –111.5 | |
| Analysis-4 | | | –111.3 | |
| Analysis-5 | | | –112.6 | |
| Analysis-6 | | | –112.1 | |
| Analysis-1 | Bisleri water | -49.7 | –48.4 | -48.4 |
| Analysis-2 | | | –48.4 | |

***Repeat measurements of (δD) in the geothermal springs***

During the measurements of geothermal water samples through IRMS, several randomly selected samples were also measured as repeat analyses for checking precision as presented in Table 3.11 & Fig. 3.15. This shows that reproducibility of these measurements is good.

***Table 3.11:*** *Results of repeat analyses of δD of geothermal springs.*

| Sample Name | Measurement -01 ‰ | Standard deviation | Measurement -02 ‰ | Standard deviation |
|---|---|---|---|---|
| HS-23 | –119.18 | 0.78 | –117.39 | 0.78 |
| HS-28 | –71.75 | 0.91 | –72.47 | 0.39 |
| HS-37 | –68.48 | 0.58 | –68.04 | 0.56 |
| HS-40 | –55.88 | 0.49 | –56.63 | 0.77 |
| HS-01 | –95.38 | 1.19 | –94.61 | 0.67 |
| HS-11 | –63.48 | 0.75 | –62.54 | 0.86 |
| HS-18 | –64.55 | 1.21 | –64.37 | 0.62 |
| RW-01 | –97.64 | 1.06 | –97.63 | 0.54 |

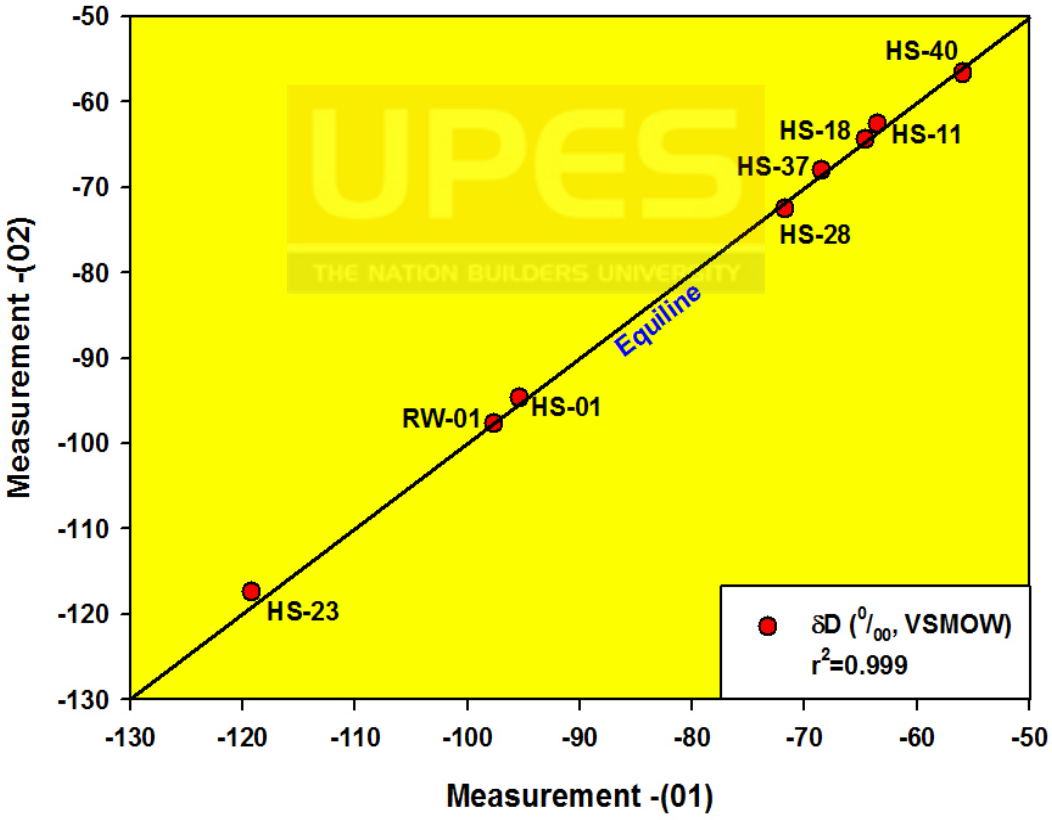


**Fig. 3.15:** *Comparisons of repeat measurements of δD in random samples of geothermal springs, showing the good repeatability ($r^2$=0.99).*

# CHAPTER 4

# GEOCHEMICAL CHARACTERTICS

# CHAPTER 4:

# GEOCHEMICAL CHARACTERTICS

## 4.1 INTRODUCTION

Geothermal systems are the manifestations of rock water interaction at moderate to high temperature with their discernable response on the Earth surface. These include the features like geothermal springs and geezers emanating volatiles and fluids from them. Water rock interactions are often imprinted in the chemical composition of springs and therefore, the chemical composition provide a valuable tool to study these geothermal systems. Such systems are found all over the world, with varying geological environments including zones of volcanism, mountain building, quaternary or recent volcanism activity, faulting, and junction of crustal plates.

This chapter presents the results and discussion on major and trace element chemistry of geothermal springs of Garhwal, Himachal Pradesh and Ladakh regions. Geochemical results of major and trace elements are interpreted to derive useful information on the compositions and source of major and trace elements in these springs situated along the Alaknanda, Bhagirathi, and Yamuna, valleys of Garhwal Himalaya; Sutlej, Parbati, Beas and Spiti valleys of Himachal Himalaya; Indus, Shyok and Nubra valleys of Ladakh Himalaya.

The details of geological setup, geographical distributions and places of occurrence of these springs are described in chapter-2. Major geothermal fields of northwest Himalaya are situated in different geological and tectonic settings. Therefore, each of them has their distinct characteristics which are likely to be reflected in their hydro-chemical composition. The characteristics of the fluid depend on its chemistry, temperature and discharge at the surface. In addition, it is also reflected by the reservoir temperature and the nature of source rock. The common criteria for the classification of geothermal resources are based on the enthalpy of the geothermal fluids carrying heat and volatiles from the depth to the surface.

The Most of the geothermal fields of northwest Himalaya are situated around the junction of Indian and Asian plates, especially in Ladakh region, where rapid uplift and erosion have moved hot rocks near the surface. The interaction of these hot rocks and part of meteoric water may give rise to these geothermal springs with elevated surface temperature up to as high as 95˚C in the Himalayan region. The geothermal activity can largely be seen along the major thrust zones or structural discontinuities (i.e., MCT, MBT, and ITSZ) in form of numerous geothermal springs in the deeply incised river valleys. Two types of geothermal systems exist which are termed as cyclic types and storage type. The Himalayan geothermal fields fall in the cyclic system category where the hot water is mostly believed to be of meteoric nature. It passes through a complex cycle of percolation up to deeper depth, heating and upwelling to the surface. In the storage system, water is stored in the rocks for relatively longer periods and warmed in situ (due to the heat accumulated from

the radioactive decay of uranium and thorium elements) before it reaches to surface via cracks and joints, developed in them. Geochemical analyses of geothermal water are extensively employed as an essential method in characterizing geothermal reservoirs and their evolution (Fournier, 1981; Nicholson, 1993). Ionic ratio and composition of geothermal waters may be useful to trace the rock water interaction during the flow to the surface (Edmunds et al., 2003; Han et al., 2010). Major cations (sodium, potassium, calcium, and magnesium), major anions (fluoride, chloride, nitrate, sulphate, bicarbonate) and trace elements (lithium, boron, manganese, rubidium, cesium, and iron) and some other important species (silica, ammonia, arsenic, and noble gases) are found in these waters as dissolved contents. These contents can be used to trace the origin of waters associated with these thermal systems. Mainly four types of water are reported in the geothermal systems which are (i) sodium chloride type, (ii) acid sulphate chloride type, (iii) acid sulphate type, and (iv) calcium bicarbonate type (Ellis & Mahon, 1977; Henley et al., 1985; Giggenbach, 1988). However, these water types may mix with each other giving rise to hybrid types.



## 4.2 RESULT AND DISCUSSION

The details of studied geothermal spring locations (latitude, longitude, and altitude), place of occurrences and geological setup are elaborated in the chapter-2. The data of field measurements i.e. (pH), temperature (˚C), Electric Conductivity (EC), Total Dissolved Solids (TDS) and laboratory analyses of major ion and trace element of these springs are presented in the (Tables: 4.1, 4.2 & 4.3), respectively.

***Table 4.1:*** *Physical parameters and major ions concentration (in µE) of geothermal springs and river waters of Garhwal region.*

| Sample No | Sites Name | Temp ($^0$C) | pH | TDS (mg/L) | Conductivity (µS/cm) | $F^-$ | $Cl^-$ | $NO_3^-$ | $SO_4^{2-}$ | $HCO_3^-$ | $SiO_2$ | $Na^+$ | $K^+$ | $Mg^{2+}$ | $Ca^{2+}$ | *NICB |
|---|---|---|---|---|---|---|---|---|---|---|---|---|---|---|---|---|
| **HS-1** | *Taptkund* | 55.6 | 7.3 | 1910 | 2690 | 151 | 3469 | 12 | 605 | 21553 | 1358 | 25909 | 1151 | 1081 | 3171 | 19.3 |
| **HS-2** | *Khiroi* | 57.8 | 8.5 | 241 | 340 | 85 | 221 | 7 | 901 | 1697 | 1526 | 2720 | 117 | 0 | 257 | 6.1 |
| **HS-3** | *Bhapkund* | 44.7 | 8.1 | 255 | 359 | 59 | 152 | 3 | 376 | 3009 | 1334 | 2916 | 89 | 118 | 445 | -0.9 |
| **HS-4** | *Shaldhar* | 93 | 7.3 | 572 | 805 | 40 | 198 | 7 | 616 | 3979 | 1385 | 769 | 226 | 1989 | 4362 | 41.1 |
| **HS-5** | *Tapoban* | 45.6 | 6.2 | 261 | 368 | nd | 95 | 32 | 424 | 3278 | 1368 | 436 | 132 | 999 | 1951 | -8.5 |
| **HS-6** | *Birahi* | 64.6 | 6.2 | 845 | 1190 | 176 | 3509 | nd | 474 | 14749 | 1541 | 16825 | 883 | 721 | 896 | 2.2 |
| **HS-7** | *Ganoi* | 25.6 | 6.5 | 930 | 1310 | 86 | 328 | 7 | 983 | 10249 | 1541 | 881 | 1017 | 7178 | 5217 | 20.3 |
| **HS-8** | *Langsi* | 53 | 6.7 | 715 | 1007 | 69 | 650 | nd | 1016 | 8161 | 941 | 2660 | 819 | 4644 | 1611 | -1.7 |
| **HS-9** | *Helang* | 60.8 | 6.2 | 536 | 755 | 72 | 260 | 10 | 665 | 4538 | 1123 | 941 | 191 | 1979 | 1915 | -9.8 |
| **HS-10** | *Gaurikund* | 47.3 | 6.6 | 731 | 1029 | 40 | 540 | 89 | 234 | 5224 | 1908 | 2056 | 309 | 1886 | 6454 | 54.4 |
| **HS-11** | *Gangnani* | 61 | 6.7 | 933 | 1314 | 128 | 1702 | nd | 987 | 8651 | 1956 | 9168 | 498 | 703 | 2683 | 12.9 |
| **HS-12** | *Jhaya* | 44.1 | 8.6 | 373 | 525 | 204 | 1076 | 38 | 736 | 2622 | 1567 | 3938 | 119 | 69 | 361 | -4.1 |
| **HS-13** | *Bukki* | 52 | 6.5 | 1243 | 1751 | 173 | 3752 | nd | 452 | 13561 | 382 | 16841 | 512 | 218 | 1577 | 6.5 |
| **HS-14** | *Thirang* | 52.2 | 6.4 | 1051 | 1480 | 33 | 2029 | nd | 368 | 11842 | 1709 | 12536 | 515 | 238 | 664 | -2.3 |
| **HS-15** | *Matli* | 29.4 | 7.2 | 974 | 1372 | 39 | 5492 | 38 | 1442 | 4222 | 497 | 6829 | 534 | 1849 | 3726 | 14.1 |
| **HS-16** | *Kotimanep* | 35 | 5.9 | 1162 | 1637 | 60 | 10516 | nd | 1388 | 3542 | 2004 | 10859 | 885 | 1191 | 1870 | -4.6 |
| **HS-17** | *Suryakund* | 84.3 | 7.1 | 753 | 1060 | 97 | 4226 | nd | 752 | 4315 | 1495 | 6246 | 579 | 528 | 1841 | -2.1 |
| **HS-18** | *Jankichatti* | 28.8 | 6.6 | 3515 | 4950 | 43 | 21986 | nd | 1694 | 8136 | 2040 | 19829 | 2330 | 8543 | 22851 | 50.8 |
| **HS-19** | *Banas-HS* | 70 | 6.1 | 312 | 440 | 52 | 617 | nd | 1154 | 2181 | 1495 | 1139 | 160 | 472 | 1938 | -7.6 |
| **HS-20** | *Wozari* | 54.8 | 6.1 | 1441 | 2030 | 208 | 4674 | nd | 908 | 14149 | 814 | 16887 | 984 | 1166 | 1384 | 2.4 |
| **RW-1** | *RW-1* | 4.5 | 7.3 | 55 | 78 | 14 | 12 | 18 | 216 | 229 | 221 | 75 | 22 | 48 | 366 | 4.4 |
| **RW-2** | *RW-2* | 4.5 | 7.3 | 51 | 71 | 14 | 14 | 23 | 218 | 261 | 226 | 94 | 23 | 54 | 428 | 12.2 |
| **RW-4** | *RW-4* | 6.2 | 7.5 | 176 | 248 | 4 | 13 | 28 | 1055 | 1260 | 212 | 146 | 47 | 381 | 622 | -65.5 |
| **RW-5** | *RW-5* | 9.8 | 7.6 | 42 | 59 | 2 | 7 | 34 | 68 | 339 | 207 | 74 | 33 | 44 | 346 | 9.9 |
| **RW-6** | *RW-6* | 15 | 8.2 | 192 | 271 | 10 | 23 | 19 | 380 | 2766 | 255 | 133 | 77 | 1228 | 1366 | -13.1 |
| **RW-8** | *RW-8* | 5.3 | 8.2 | 124 | 174 | 5 | 40 | 37 | 748 | 400 | 159 | 228 | 82 | 705 | 794 | 38.1 |
| **RW-9** | *RW-9* | 1.8 | 8 | 58 | 81 | 3 | 30 | 28 | 244 | 289 | 164 | 90 | 42 | 73 | 448 | 9.5 |
| **RW-10** | *RW-10* | 8.1 | 7.6 | 103 | 146 | 16 | 22 | 35 | 271 | 948 | 197 | 88 | 56 | 285 | 927 | 4.8 |

*Normalized Inorganic Charge Balance (*NICB) [200*($\mu E^+ - \mu E^-$)/ ($\mu E^+ + \mu E^-$)].(nd- not determined)*

***Table 4.2:*** *Physical parameters and major ions concentration (in µE) of geothermal springs of Himachal and Ladakh region.*

| Sample No | Sites Name | Temp ($^0$C) | pH | EC (µS/cm) | TDS (mg/L) | $F^-$ | $Cl^-$ | $SO_4^{2-}$ | $NO_3^-$ | $HCO_3^-$ | $Li^+$ | $Na^+$ | $K^+$ | $Mg^{2+}$ | $Ca^{2+}$ | $SiO_2$ | B | *NICB |
|---|---|---|---|---|---|---|---|---|---|---|---|---|---|---|---|---|---|---|
| **HS-21** | *Changlung* | 74 | 7 | 2650 | 1855 | 740 | 2433 | 2448 | 15 | 9840 | 91 | 13920 | 1141 | 321 | 12 | 3733 | 1972 | 11 |
| **HS-22** | *Pulthang* | 29 | 7 | 672 | 470 | 301 | 183 | 853 | 17 | 4520 | nd | 4405 | 234 | 601 | 359 | 1667 | 444 | 3 |
| **HS-23** | *Panamic* | 73 | 8 | 755 | 529 | 478 | 174 | 1281 | 40 | 4320 | 47 | 5246 | 177 | 320 | 93 | 3347 | 472 | 1 |
| **HS-24** | *Gaik* | 55 | 9 | 415 | 291 | 620 | 254 | 972 | 0 | 3400 | 48 | 3485 | 129 | 342 | 53 | 2067 | 944 | -5 |
| **HS-25_1** | *Chumathang* | 87 | 9 | 1620 | 1134 | 530 | 9404 | 13684 | 28 | 7340 | 3550 | 13918 | 1422 | 235 | 193 | 3680 | 10361 | -4 |
| **HS-25_2** | *Chumathang* | 87 | 9 | 1580 | 1106 | 429 | 2273 | 13684 | 0 | 6900 | 1139 | 9887 | 641 | 308 | 103 | 3740 | 10944 | -1 |
| **HS-26** | *Puga* | 84 | 8 | 2790 | 1953 | 583 | 10843 | 13808 | 30 | 13400 | 654 | 14385 | 1511 | 717 | 412 | 3660 | 30194 | 19 |
| **HS-27** | *Sumdo* | 61 | 8 | 5240 | 3668 | 163 | 22438 | 20756 | 34 | 9650 | 2337 | 15453 | 1898 | 5153 | 4313 | 1620 | 30167 | 11 |
| **HS-28** | *Thopan* | 46 | 8 | 428 | 300 | 536 | 421 | 2907 | 478 | 2680 | 55 | 4771 | 109 | 164 | 1706 | 1513 | 611 | 5 |
| **HS-29** | *Tapri* | 44 | 8 | 328 | 230 | 121 | 94 | 3262 | 17 | 1300 | 35 | 1232 | 197 | 190 | 2643 | 613 | 111 | -9 |
| **HS-29B** | *TapriHandpump* | 47 | 7 | 571 | 400 | 81 | 591 | 807 | 41 | 2680 | nd | 2719 | 283 | 49 | 658 | 1500 | 361 | -3 |
| **HS-30** | *Naptha* | 57 | 7 | 1300 | 910 | 357 | 5134 | 277 | 15 | 5080 | 922 | 7667 | 447 | 244 | 164 | 2767 | 2639 | 10 |
| **HS-31** | *Jeori* | 56 | 7 | 5130 | 3591 | 193 | 12060 | 17320 | 48 | 3400 | 1127 | 20703 | 911 | 1939 | 2019 | 1600 | 4556 | -6 |
| **HS-32** | *Jhakri* | 43 | 8 | 354 | 248 | 60 | 1164 | 490 | 32 | 1400 | nd | 1873 | 158 | 1008 | 148 | 760 | 306 | 10 |
| **HS-33/34** | *Jharar* | 21 | 7 | 589 | 412 | 30 | 2138 | 1987 | 162 | 3940 | nd | 2606 | 234 | 1534 | 3739 | 553 | 83 | -1 |
| **HS-35** | *Bashist* | 53 | 7 | 1080 | 756 | 400 | 3509 | 1202 | 12 | 4080 | 876 | 7136 | 451 | 115 | 65 | 2073 | 694 | 1 |
| **HS-36** | *KhiralBihal* | 41 | 6 | 1650 | 1155 | 177 | 7748 | 273 | 16 | 6920 | 1706 | 9735 | 792 | 113 | 215 | 2113 | 1250 | -10 |
| **HS-37** | *Kalath* | 42 | 6 | 2400 | 1680 | 174 | 12024 | 321 | 20 | 9740 | 2321 | 12347 | 949 | 352 | 2462 | 2267 | 1500 | -12 |
| **HS-38** | *Ramshila Kullu* | 35 | 6 | 6780 | 4746 | 82 | 5412 | 19064 | 31 | 10800 | 2612 | 19835 | 1990 | 4212 | 1603 | 1547 | 2639 | -8 |
| **HS-39** | *Manikaran* | 95 | 7 | 812 | 568 | 64 | 3682 | 501 | 12 | 2880 | 455 | 4242 | 692 | 427 | 630 | 2227 | 944 | 3 |
| **HS-40** | *Kasol* | 69 | 7 | 555 | 389 | 45 | 1296 | 715 | 0 | 2760 | 832 | 1593 | 356 | 966 | 697 | 1553 | 444 | 1 |

*Normalized Inorganic Charge Balance (*NICB) [200*($\mu E^+ - \mu E^-$)/($\mu E^+ + \mu E^-$)].(nd- not determined)*

### 4.2.1 GENERAL OBSERVATIONS AND PHYSICAL PARAMETERS

Details of methodology of field measurements and geochemical analyses are discussed in details in Chapter 3. The physical parameters (temperature, pH, EC) and major ion concentrations of these springs are presented in (Tables 4.1 & 4.2), respectively whereas the variation of physical parameters of these springs is described below:

**pH**

pH values of these samples vary from 5.9 to 9, which are slightly acidic to alkaline by nature in Garhwal, Himachal, and Ladakh regions (Fig. 4.1).

**EC (Electric Conductivity)**

Electric conductivity of these samples vary from 328 to 6780 µS/cm (Fig 4.1), with peak value of (6780) at Kullu-Ramshila (HS-38).



**Temperature**

Surface temperature of these samples vary from 21to 95˚C (Fig. 4.1), with the highest temperature (95˚C) at Manikaran (HS-39).

**Total Dissolved Solids (TDS)**

Total dissolved solids in these samples vary from 230 to 4746 mg/L with peak value of (4746) indicates that some of these are highly mineralized. This is likely that more interaction time for fluid with host rock causing dissolution of material giving rise to TDS (Fig.4.1).

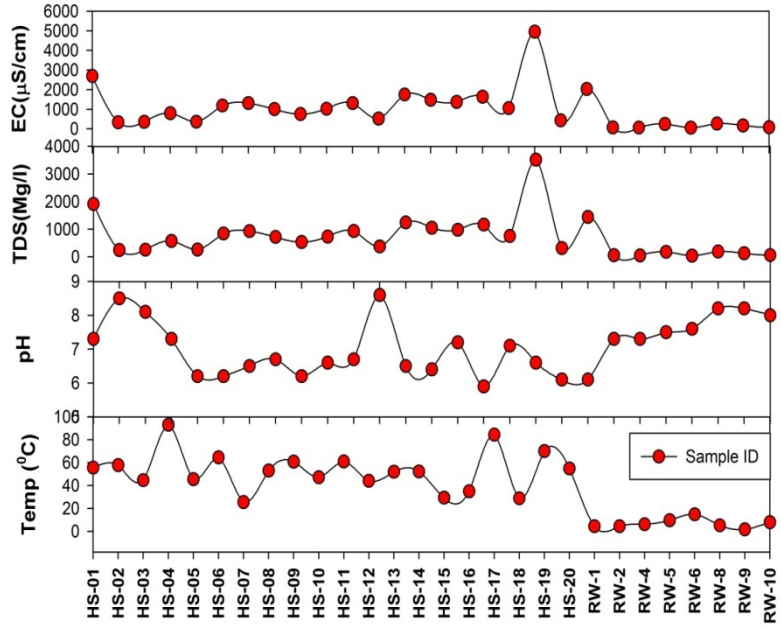


**(a)**

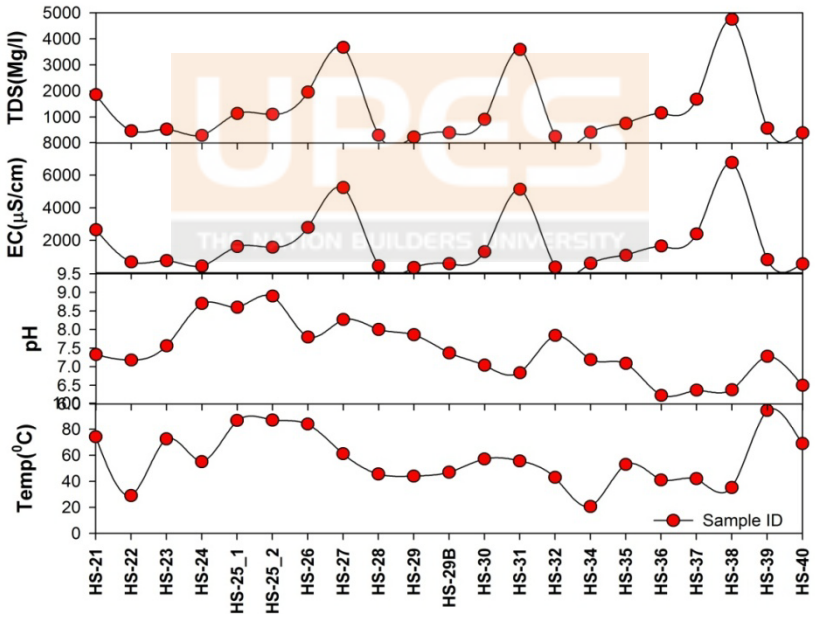


**(b)**

***Fig 4.1:*** *Spline curve line and scatter plots of physical parameters concentration. (a) Garhwal region, and (b) Himachal and Ladakh regions.*

### 4.2.2 MAJOR ION CHEMISTRY

**Major anions and their variation**

Fluoride ($F^-$), chloride ($Cl^-$), sulphate ($SO_4^{2-}$), and bicarbonate ($HCO_3^-$) are the major anions present in these springs. The details of major ion are presented in the Tables 4.1 & 4.2, respectively. The variations of major ions of these springs are given below:

**Fluoride ($F^-$)**

Fluoride varies from 1 to 208 µE in the Garhwal and 301 to 740 µE in the Himachal and Ladakh regions (Fig. 4.2).

**Chloride ($Cl^-$)**

Chloride varies from 95 to 21986 µE and 174 to 10843 µE in the Garhwal and Himachal & Ladakh regions respectively. It is a common and conservative element in geothermal waters and hence making it an important solute in the interpretation of their water chemistry (Fig. 4.2).

**Sulphate ($SO_4^{2-}$) and Bicarbonate ($HCO_3^-$)**

$SO_4^{-2}$ abundance is generally found towards the lower side in these springs. It varies from 233to1694 µE, in Garhwal and 853 to13808 µE and 273 to 20756 µE in Himachal and Ladakh regions, respectively (Fig. 4.2). High sulphate could come from the oxidative weathering of pyritiferous shales or dissolution of gypsum as major halite. $HCO_3^-$, a major anion in these springs, varies from 1697 to 21553 µE in Garhwal and 3400 to 13400 µE in Ladakh region (Puga and Shyok valley) and it varies from 1300 to 10800 µE in different valleys of Himachal region (Fig. 4.2).

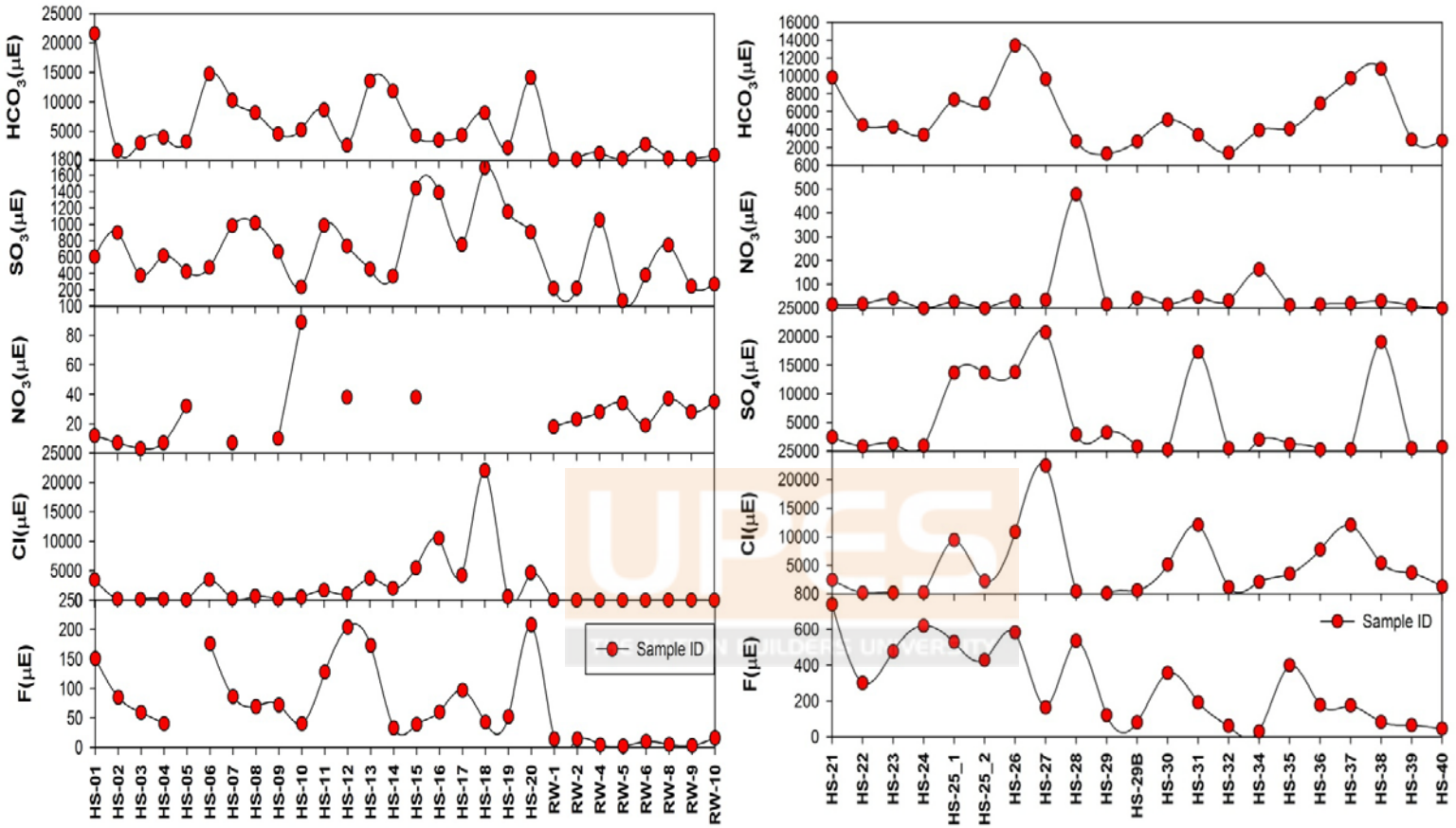


***(a)*** ***(b)***

***Fig 4.2:*** *Spline curve line and scatter plots of major anions concentration. (a) Garhwal region and, (b) Himachal and Ladakh regions.*

**Major cations and their variation**

Sodium ($Na^+$), potassium ($K^+$), magnesium ($Mg^{+2}$), and calcium ($Ca^{+2}$) are the major cations found in these waters. However, at few places, trace elements are also found in significant concentrations comparable to major elements.

**Sodium ($Na^+$)**

Sodium concentration in the geothermal water varies from 436 to 25908 µE in Garhwal and 3330 to14385 µE, 1232 to 20703 µE in Ladakh and Himachal regions, respectively. The geothermal springs situated near the MCT and ITSZ, show higher $Na^+$ concentrations which seem to indicate about the process of high temperature silicate weathering (Fig.4.3) in these thermal systems.

**Potassium ($K^+$)**

It varies from 89 to 2330 µE in Garhwal and 128 to1511 µE, 109 to1990 µE in the Ladakh and Himachal regions, respectively (Fig. 4.3).

**Magnesium ($Mg^{2+}$)**

$Mg^{2+}$ varies from 235 to 717 µE and 49 to 5153 µE in the geothermal water of Himachal and Ladakh regions, respectively. It is relatively higher in Garhwal area which is found to be 8543 µE (Fig. 4.3).

**Calcium ($Ca^{2+}$)**

Calcium abundances vary by 3 orders of magnitude from 257 to 22851 µE in Garhwal region however its range of variation is less in the Ladakh (12 to 412 µE) and in Himachal regions (65 to 4313 µE). This is also shown in Fig.4.3.

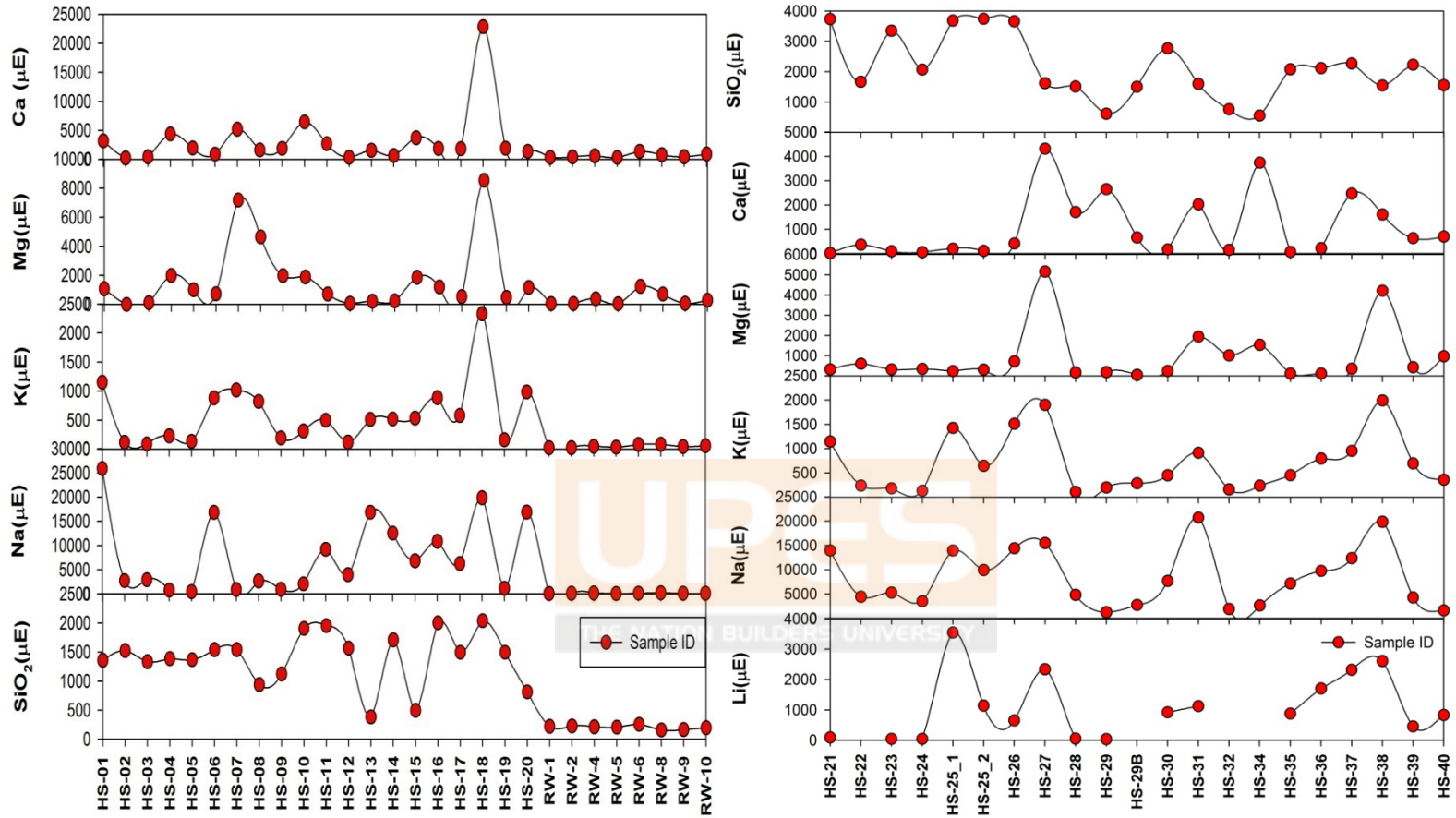


***(a)*** ***(b)***

***Fig 4.3:*** *Simple spline curve line and scatter plots of major cations and dissolved silica concentration. (a) Garhwal region, and (b) Himachal and Ladakh regions.*

### 4.2.3 TRACE ELEMENT CHEMISTRY

The concentrations of trace elements of the geothermal springs are given in the Table 4.3 & Fig. 4.4. These elements in the thermal waters, such as iron (Fe), boron (B), lithium (Li), zinc (Zn), strontium (Sr), manganese **(**Mn), aluminium (Al), molybdenum (Mo), and arsenic (As) are mainly driven by rock-water interaction and high temperature weathering processes. Abundances of iron (Fe) and aluminium (Al) vary from (5 to 118 and 61to 1892 µg/L) in Ladakh and (5 to 96 and 1 to 23 µg/L) in the Himachal region. The concentration of boron (B) in the geothermal springs is relatively high and varies from 444 to 30194 µE in the Puga, Shyok, Sutlej, and 83 to 4556 µE in the Himachal.

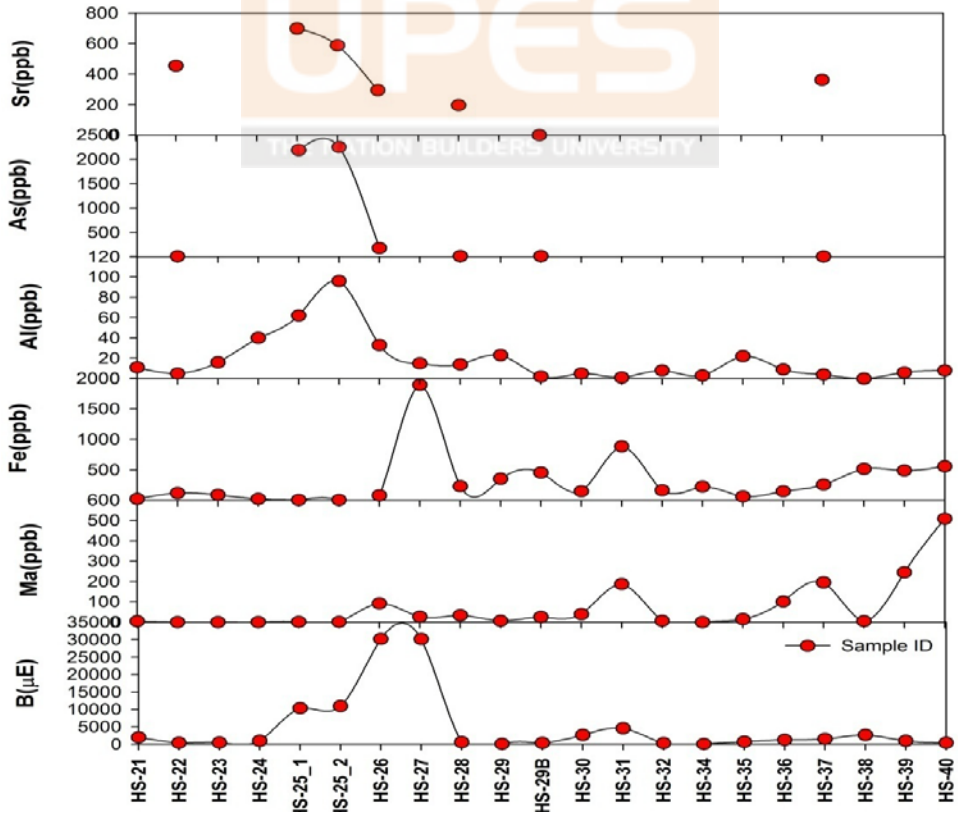


***Fig. 4.4:*** *Simple spline curve line and scatter plot of trace elements concentration of the geothermal springs of Himachal and Ladakh regions.*

***Table 4.3:*** *Trace elements concentration (in ppb) of thermal springs of Himachal and Ladakh regions. (nd-not determined)*

| Sample No | Sites Name | Mn | Fe | Al | Zn | As | Mo | Sr | Pb | Cu | Co | Ni |
|---|---|---|---|---|---|---|---|---|---|---|---|---|
| **HS-21** | *Changlung* | 4 | 21 | 11 | nd | nd | nd | nd | nd | nd | nd | nd |
| **HS-22** | *Pulthang* | 0 | 118 | 5 | 2 | 11 | 18 | 454 | 0 | 2 | <1 | 0 |
| **HS-23** | *Panamic* | 0 | 88 | 16 | nd | nd | nd | nd | nd | nd | nd | nd |
| **HS-24** | *Gaik* | 0 | 21 | 40 | nd | nd | nd | nd | nd | nd | nd | nd |
| **HS-25_1** | *Chumathang* | 1 | 5 | 62 | 6 | 2186 | 6 | 698 | 0 | 5 | <1 | <1 |
| **HS-25_2** | *Chumathang* | 1 | 5 | 96 | 6 | 2246 | 6 | 588 | 0 | 5 | <1 | <1 |
| **HS-26** | *Puga* | 92 | 80 | 33 | 2 | 181 | 1 | 294 | 0 | 8 | 0 | <1 |
| **HS-27** | *Sumdo* | 26 | 1892 | 15 | nd | nd | nd | nd | nd | nd | nd | nd |
| **HS-28** | *Thopan* | 33 | 230 | 14 | 1 | 13 | 7 | 196 | 0 | 1 | 0 | <1 |
| **HS-29** | *Tapri* | 6 | 355 | 23 | nd | nd | nd | nd | nd | nd | nd | nd |
| **HS-29B** | *Tapri (Handpump)* | 25 | 454 | 2 | 32 | 13 | 51 | 0 | 1 | <1 | 1 | nd |
| **HS-30** | *Naptha* | 39 | 147 | 5 | nd | nd | nd | nd | nd | nd | nd | nd |
| **HS-31** | *Jeori* | 187 | 883 | 1 | nd | nd | nd | nd | nd | nd | nd | nd |
| **HS-32** | *Jhakri* | 6 | 164 | 8 | nd | nd | nd | nd | nd | nd | nd | nd |
| **HS-33/34** | *Jharar* | 0 | 224 | 3 | nd | nd | nd | nd | nd | nd | nd | nd |
| **HS-35** | *Bashist* | 14 | 61 | 22 | nd | nd | nd | nd | nd | nd | nd | nd |
| **HS-36** | *Khiral Bihal* | 101 | 147 | 9 | nd | nd | nd | nd | nd | nd | nd | nd |
| **HS-37** | *Kalath* | 195 | 255 | 4 | 1 | 6 | 1 | 362 | 0 | 7 | <1 | <1 |
| **HS-38** | *Ramshila Kullu* | 5 | 514 | 0 | nd | nd | nd | nd | nd | nd | nd | nd |
| **HS-39** | *Manikaran* | 244 | 488 | 6 | nd | nd | nd | nd | nd | nd | nd | nd |
| **HS-40** | *Kasol* | 508 | 558 | 8 | nd | nd | nd | nd | nd | nd | nd | nd |

### 4.2.4 DISSOLVED SILICA ($SiO_2$)

Silica is an important constituent of all the geothermal fluids. Its concentration in water is controlled by the solubility of different silica polymorphs (amorphous silica, opal, quartz, cristobolite and chalcedony) and other silicate minerals. The concentration of silica on geothermal springs of Garhwal, Himachal and Ladakh regions is given in the Tables 4.1 & 4.2. Its abundance varies from 380 to 2040 µE in the Garhwal region and from 553 to 3740 µE in the Himachal (Sutlej-Spiti, Parbati, and Beas, rivers valleys) and Ladakh regions including Puga, Shyok, and Nubra, valleys (Fig. 4.3). A general discussion on the silica based thermometry is presented in chapter-7.

## 4.3 SOURCE OF MAJOR ION IN GARHWAL REGION

***ANIONS*:** Fluoride is a key anion in these geothermal springs which varies from 1 to as high as 208 µE. Among these springs, sample from the Bhagirathi valley and Yamuna valley (Gangnani-HS-11, Jhaya-HS-12, Bhukki-HS-13, and Wozari-HS-20) show elevated concentration of 128 to 208 µE probably due to the occurrence of fluoride bearing minerals (i.e. fluorite, tourmaline, etc) in its catchment. Fluoride enrichment in thermal springs depends upon the solubility of mineral fluorite ($CaF_2$) during water-rock interactions (Mahon, 1964). In certain cases, the high concentration of deep fluids (with high $pCO_2$) may also remove available Ca during calcite deposition leaving excess fluoride in remnant thermal waters (Nicholson, 1993). Chloride is a common and conservative element in geothermal waters, making it an important solute in these waters. Generally, it is incompatible in almost all natural water-rock

interaction at different temperature and it does not enter into the lattice of common rock forming mineral by adsorption on the mineral surface (Ellis, 1970; Arnorsson & Andresdottir, 1995). Its concentration in these springs varies from 95 to 21986 µE displaying characteristics of Cl:Na type water (Nicholson, 1993). Jankichatti (HS-18, with a value of 21986 µE) contains exceptionally high chloride concentration with elevated level of major ions and dissolved inorganic carbon (DIC). High chloride concentrations in spring waters suggest a link to the deeper reservoir with minimal mixing effects during ascend of fluid to the subsurface. Therefore, the chemistry of geothermal fluids can be employed to define and tracing the origin of geothermal waters. In addition, it is helpful in evaluating the mixing between geothermal water and ground water in the up flow zones of the geothermal systems (Truesdell et al., 1989; Janik et al., 1991).

$SO_4^{-2}$ concentrations in these springs are relatively low (varying from 233 to1694 µE) indicating an affinity with deeper fluids. Lower concentrations of sulphate (<50 mg/L) is observed generally in deep geothermal fluids which increases with increasing oxidation of hydrogen sulphide (Nicholson, 1993). However condensation of volatiles into near surface waters may also lead to elevated concentrations of sulphate (Nicholson 1993). These springs exhibit high concentration of $HCO_3^-$ ranges from 1697 to 21553 µE in these springs with the highest value in Taptkund (HS-1).

Giggenbach (1991) proposed a triangular diagram of major anions ($Cl^-$: $SO_4^{2-}$ :$HCO_3^-$) to classify waters from different origins. These include meteoric waters coming from precipitation, mature waters having deeper origin with relatively direct pathway to the surface and peripheral waters with a possibility

of mixing with cold water or magmatic volatiles like $CO_2$, $SO_2$, and steam, etc. It helps differentiate among different water masses and their mixing relationships in varying geological setups. Based on the triangular Fig.4.5 and piper diagrams Fig.4.6 for these waters from different valleys of Garhwal Himalaya can be classified in to three major groups as follows.

*Group 1:* Most of the geothermal springs show the affinity toward peripheral types of waters (Figs. 4.5 & 4.6) and hence indicating the mixing of deep thermal fluids with the meteoric water at the different depth.

*Group 2:* Springs from the Yamuna valley (Matli-HS-15, Kotimanep-HS-16, Suryakund-HS-17, and Jankichatti-HS-18) show their affinity towards mature types of water with relatively undisturbed pathway to surface from depths. Therefore these springs could be explored for further energy resources.

*Group 3:* Geothermal springs (Khiroi-HS-2, Banas-HS-19, and Jhaya-HS-12) show the signature of meteoric types of waters. Since these geothermal springs are situated very close to the river or local water channels and therefore the possibility of mixing with groundwater may be a likely scenario. However, other proxies including stable isotopes ($\delta^{13}C_{DIC}$, $\delta^{18}O_{H2O}$ and $\delta D_{H2O}$), can better constrain towards their origin and mixing which are discussed with the stable isotopes data in fifth and sixth chapters respectively.

***CATIONS*:** Geothermal springs in the MCT zone are associated mostly in the areas dominated by silicate rocks. It influences $Na^+$ and $K^+$ abundances in them which contribute to their cation budget. The high concentration of $Na^+$ in

the geothermal fluids on the surface suggests high temperature silicate weathering, which is also evident from the elevated cations. The major cation data (Table 4.1 & Fig. 4.3) reveals that sodium concentration in the spring varies from 436 to 25908 µE. $K^+$ is the other major ion which is sourced mainly from silicate weathering in the Garhwal springs and it ranges from 89 to 2330 µE. Excluding three of them, Badrinath-HS-1,Ganoi-HS-7, and Janaki Chatti-HS-18, all the springs have their $K^+$ abundances below 1000 µE. Na/K ratio of a group of the springs close to MCT zone in the Alaknanda valley (Shaldhar, HS-4; Tapoban, HS-5; Birahi, HS-6; Ganoi, HS-7; Langsi, HS-8; Helang, HS-9) show a value of <10. Such a scenario is possible with high permeability rocks which are likely to be present in the MCT zone. However, geothermal springs that are far from MCT (i.e., Badrinath- HS-1, Khiroi- HS-2, and Bhapkund-HS-3) display higher Na/K (>20) ratios in them. Calcium abundances in these thermal springs vary from 257 to 22851 µE which could also be influenced by the higher solubility of minerals such as calcite, fluorite, and Ca rich alumino-silicates. It is also shown in Figs. 4.5 & 4.6. High temperature geothermal fluids generally have very low levels of magnesium (0.01-0.1mg/L) and it is incorporated into secondary minerals like chlorite. Present study shows that the higher concentration of Ca are associated with geothermal springs having relatively lower temperature (<50°C) which include Jankichatti (HS-18, T=29°C &Ca =22851 µE); Ganoi (HS-7, T=26°C & Ca =5217 µE), and Gaurikund (HS-10, T=47°C&Ca =6454 µE). However, in certain springs like Jhaya (HS-12, T=44°C &Ca=361 µE), it may exhibit lower concentration under the influence of other factors like the precipitation of Ca bearing minerals brought by $CO_2$ degassing.

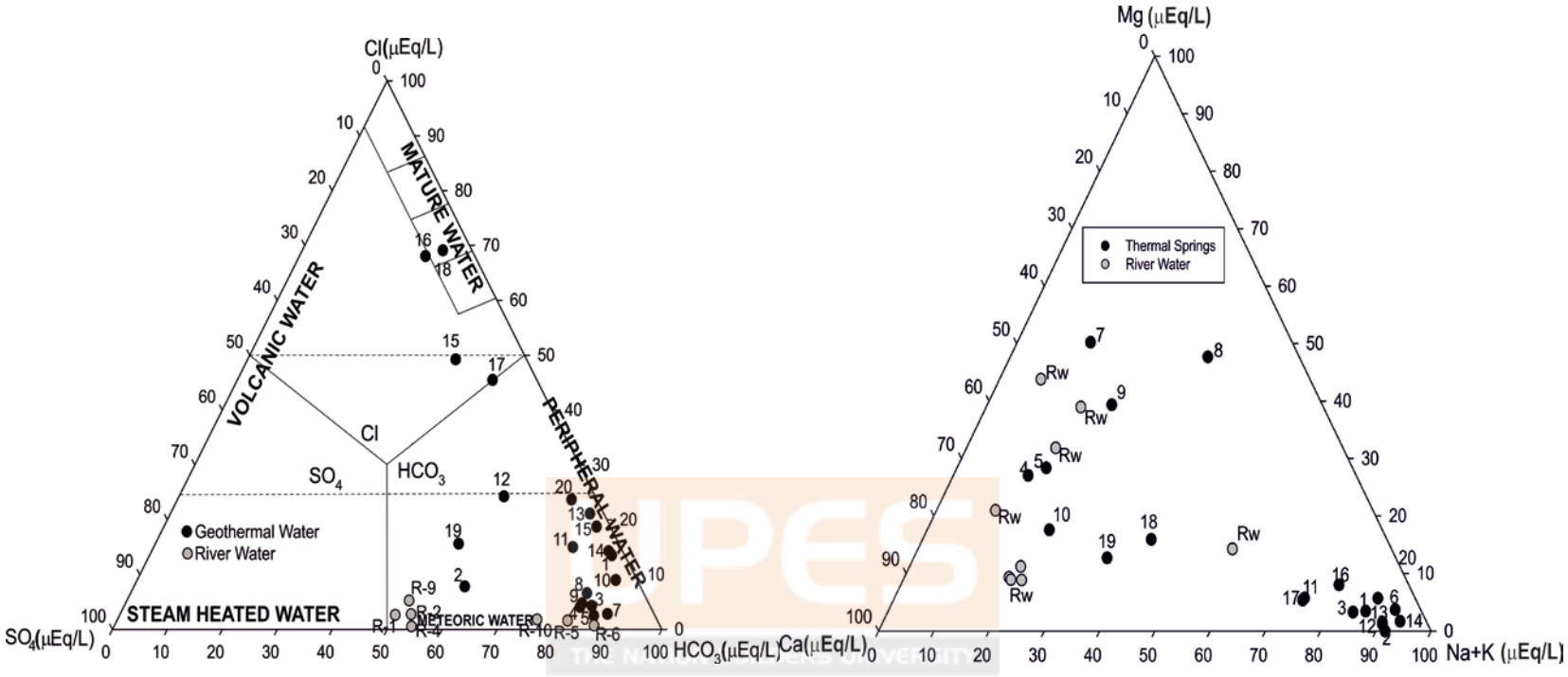


***Fig. 4.5:*** *Ternary plots for geothermal springs of Garhwal region. Anions ($Cl^-$:$HCO_3^-$:$SO_4^{2-}$) show different sources of origin, majority of these springs bear signature of peripheral water. Cations ($Na^+$+$K^+$:$Mg^{2+}$:$Ca^{2+}$) show the dominance of ($Na^+$+$K^+$), indicating the high temperature silicate weathering.*

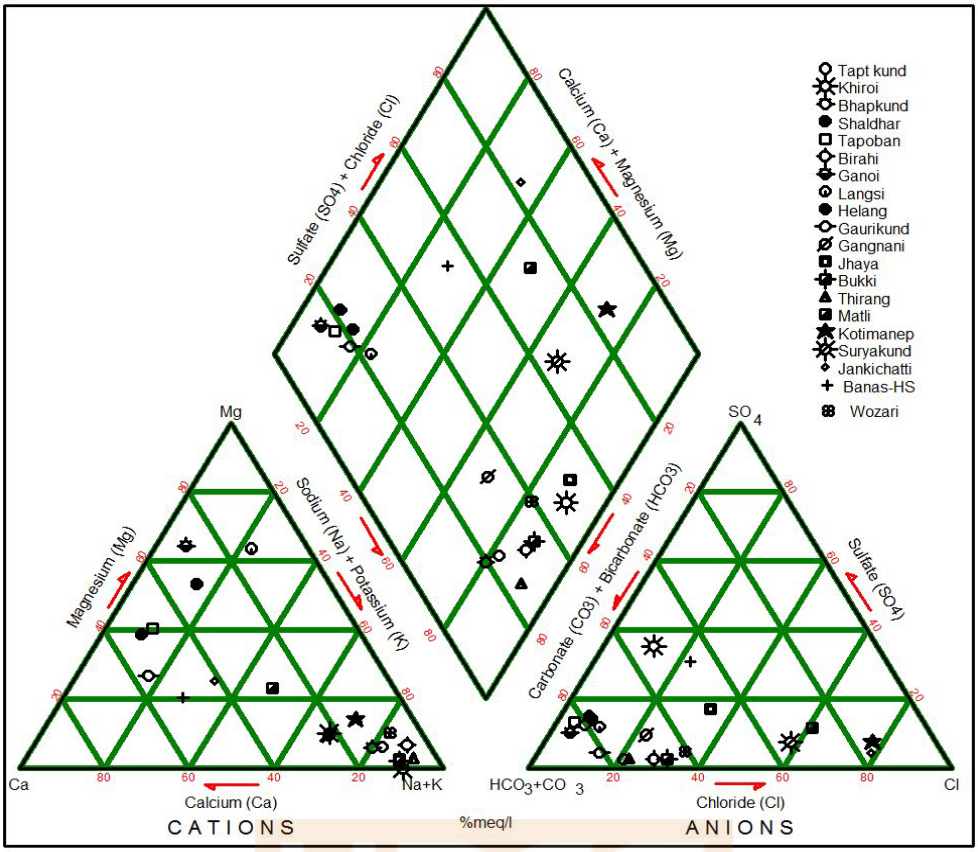


***Fig. 4.6:*** *Piper diagram for the geothermal springs of the Garhwal region showing that they bear $Cl^-$:$HCO_3$ characteristics.*

## 4.4 SOURCE OF MAJOR ION IN HIMACHAL AND LADAKH REGIONS

***ANIONS*:** Major ions and dissolved silica of these springs are given in the Table 4.2, Fig. 4.2. It indicates that the abundance of $F^-$ varies from 301 to 740 µE with the elevated concentration in the Chumathang (HS-21), and Gaik (HS-24) of Puga valley, Ladakh. Whereas $F^-$ ranges from 22 to 536 µE in Himachal with high concentration in the Sutlej valley (Thopan, HS-28) and minimum in (Kasol, HS-40) of Parbati valley (Fig. 4.2). The occurrence of fluoride in these springs may be due to the dissolution of fluoride bearing

minerals such as $CaF_2$ and tourmaline in the host lithology. However, higher concentrations of $F^-$ in the geothermal waters may also be encountered when volcanic gases are condensed into meteoric water with elevated level of Cl and $SO_4$. $Cl^-$ abundance in the geothermal springs of the Puga and Shyok valley varies from 174 to 10843 µE whereas it ranges from 92 to 22438 µE in the Himachal region. This indicates that these springs are of Cl:Na type (Nicholson, 1993). Some of these springs Puga (HS-26), Chumathang (HS-25-1) and Sumdo (HS-27, Sutlej valley) contain elevated high chloride, $HCO_3^-$, and high temperature (86˚C) which suggests a deeper source of fluids with minimum mixing effect may be prevalent in them. Concentration of $SO_4^{2-}$ in these springs varies from 273 to 20756 µE, and 853 to 13808 µE, respectively (Fig.4.2). Plotting the data on triangular (Fig. 4.7) and piper diagrams (Fig.4.8), these waters from different regions can be classified mainly in four groups as follows



*Group 1:* The group of springs consisting of Changlung (HS-21), Pulthang (HS-22), Panamic (HS-23), Gaik (HS-24), Jharar (HS-34), and Kasol (HS-40). These show that the characteristics of peripheral types of waters indicating the mixing of deep thermal fluids with meteoric water during their movement towards the surface.

*Group 2:* Constitute the assemblage of Naptha (HS-30), Jhakri (HS-32), Bashist (HS-35), Khiral Bahal (HS-36), Kalath (HS-37), and Manikaran (HS-39) springs are exhibiting the affinity towards mature water masses.

*Group 3:* Major geothermal activities along the ITSZ include the Chumathang (HS-25), Puga (HS-26), and Sumdo (HS-27) display that these

water masses are of volcanic types. This is further supported by the fact that the sulphur condensates are present as on old fumarolic activity around these springs.

*Group 4:* Four springs, namely Thopan (HS-28), Tapri (HS-29), and Ramshila Kullu (HS-38) display the steam heated water characteristics on the surface.

***CATIONS*:** Geothermal springs of this area occur mostly in the higher Himalaya where the host lithology includes the garnetiferous mica-schist, quartzite, paragneisses, and coarse grained garnet-kyanite gneisses with pegmatite lenticels. Higher $Na^+$, and $K^+$ abundance in the geothermal springs suggest that their sources could be silicate rocks which may give rise to elevated $Na^+$& $K^+$ as a result of high temperature silicate weathering in the major thrust zones (ITSZ, MCT).

Data were plotting on triangular and piper diagrams (Fig. 4.7 & 4.8), indicate the high abundance of $Na^+$+$K^+$ in the geothermal fluids affinity towards the silicate weathering. However, two thermal springs from Tapri (HS-29), and Jharar (HS-34) in Himachal region, display a Ca rich combination due to the presence of calc-micaschist and marble in the vicinity of the springs.

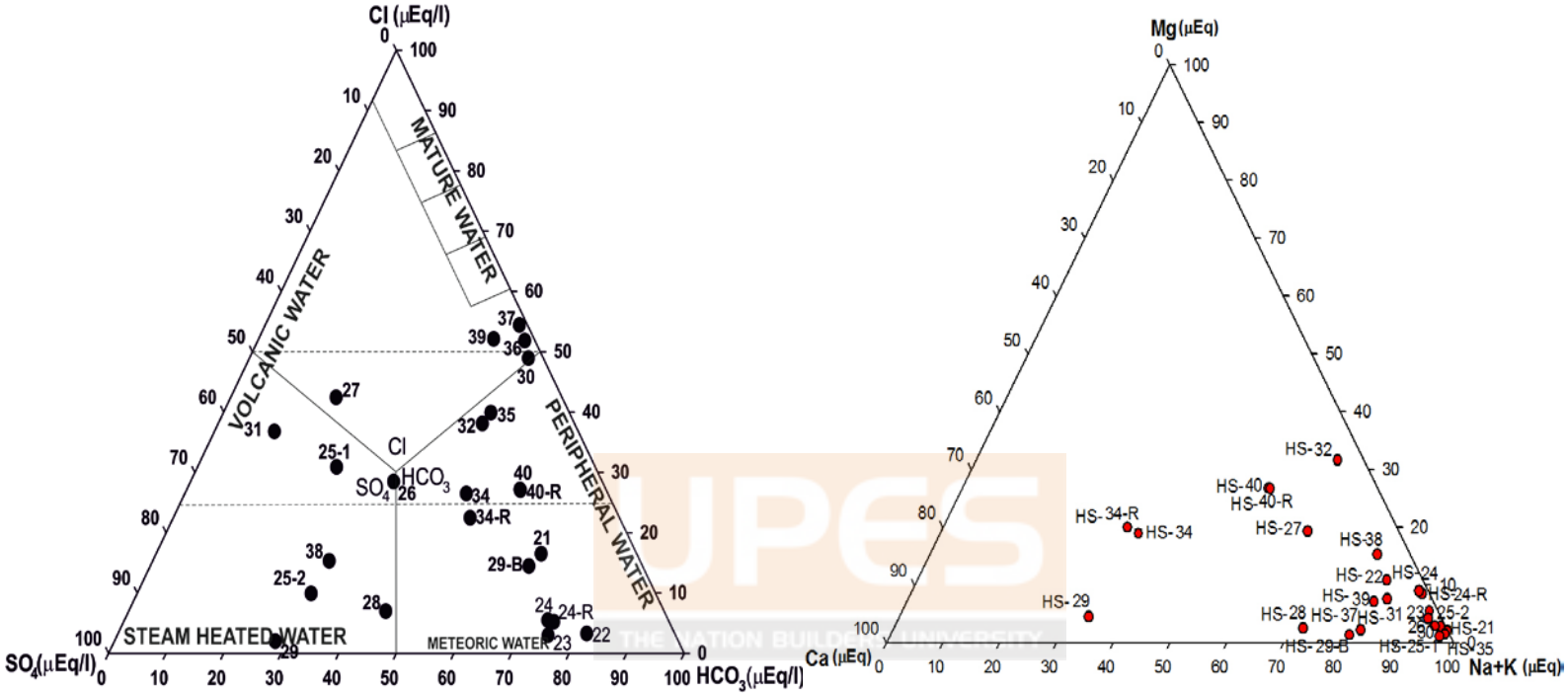


***Fig. 4.7:*** *Ternary plots for geothermal springs of Himachal and Ladakh regions. Anions ($Cl^-$:$HCO_3^-$:$SO_4^{2-}$) show different sources of origin, majority of these springs bear signature of peripheral, steam heated, mature and volcanic types of water. Cations (Na+K: Mg: Ca) show the dominance of (Na+K), indicating the high temperature silicate weathering.*

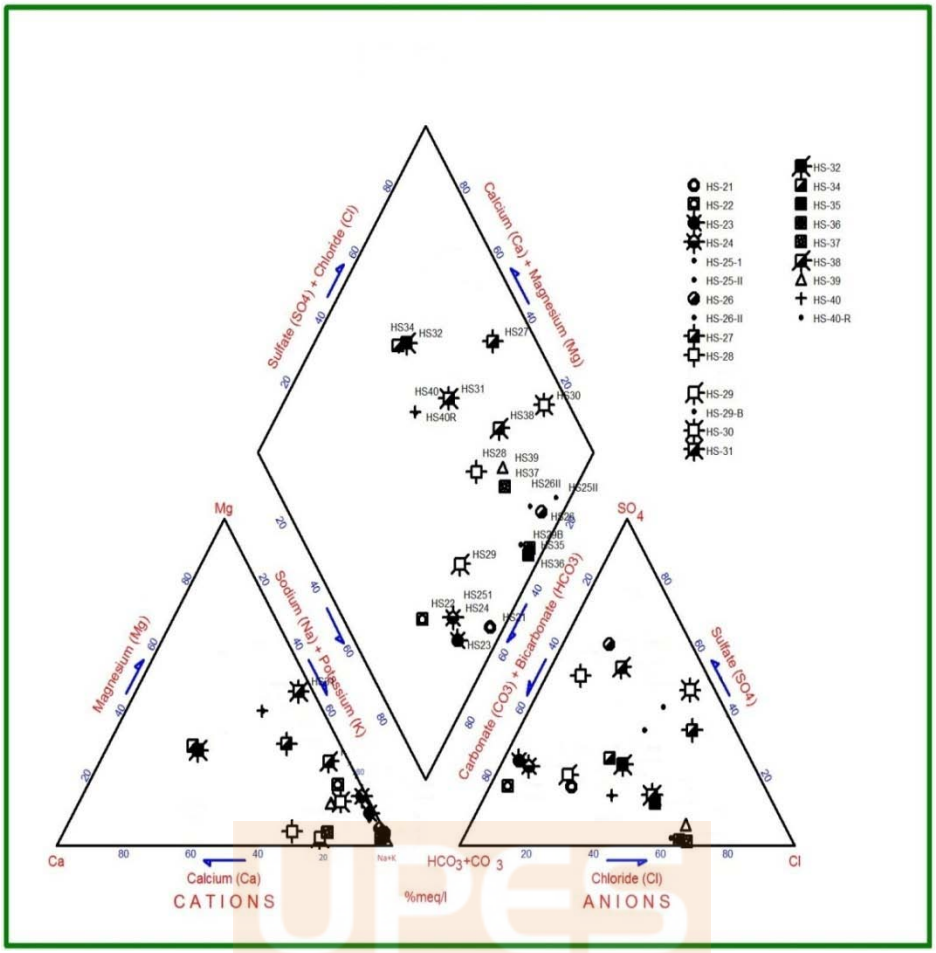


***Fig.4.8:*** *Piper diagram for the geothermal springs of Himachal and Ladakh regions showing that they bear different source of fluids.*

## 4.5 SOURCE OF TRACE ELEMENTS

The trace elements abundance in these geothermal fluids is presented in Table 4.3, which indicate that these waters have leaching of these elements from the host rock during their upward circulation. The high concentration of boron in these geothermal springs indicate that its source may be volcanic or magmatic (Bhattarai et al., 1980). The notable observations are the higher concentration of arsenic (As) in the thermal fluids which vary from 11 to 2246 µg/L and 6 to 13µg/L in the Ladakh and Himachal region respectively. This Higher concentration of As in Ladakh region may indicate their association with

arsenopyrites which may be found in the reducing environment such as purple shale (common in Indus basin). Results show that elevated abundances of arsenic (As) are present in the region, especially in Chumathang. This shows that it is a soluble component in deeper high-temperature fluids and hence indicating towards its association with deeper source. However it is depleted in the Himachal region probably due to destabilization of sulphide solution complex on the surface, where $H_2S$ is removed by boiling (Naboko & Karpov, 1977; Ewers & Keays, 1977). High concentrations of elements like boron, lithium, and strontium are present in these geothermal waters which could be the residual fluid of a crystallizing rock melt. The origin of magmatic type water in the geothermal fluids has been invoked by earlier workers in different parts of the world, Allen & Day (1935). Among the trace elements, relatively high concentrations of (Mn) and (Mo) suggest their higher solubility in high salinity and low pH environments.



## 4.6 CONCLUSIONS

Analytical data retrieved from these samples for their major ions and trace elements enable us to determine their acceptable source of origin. The region wise inferences drawn from these may be given as follows

I. Geothermal springs of Himachal and Garhwal regions Manikaran (HS-39) and Shaldhar (HS-4) show the highest temperatures (95˚C & 93˚C) on the surface, respectively.

II. Geothermal springs of Garhwal can be classified as ($Cl^-$: $SO_4^{2-}$: $HCO_3^-$) types on the basis of triangular and piper diagrams, which suggest that the geothermal Springs from Yamuna valley has the characteristics of mature

water type and those from the Bhagirathi valley exhibit the characteristics of peripheral waters. However, the Alaknanda valley contains geothermal springs which may have the meteoric affinity.

III. Geothermal springs of Himachal and Ladakh regions fall into four groups, which include the peripheral, mature, volcanic and steam heated types of characteristics of these waters.

IV. The suitable mechanism for the origin of geothermal springs of the northwest Himalaya may include a scenario in which water percolates downwards through faults and fractures, and is heated up by a steeper geothermal gradient before it rises to the surface through the permeable zones.

V. Ternary plots of (Na+K:Mg:Ca) major cations reveals that these springs show a strong influence of silicate weathering with elevated $Na^+$ and $K^+$ making up most of the cation budget. Further, the river waters of the region are relatively enriched in Ca and Mg indicating that they could be induced by carbonate weathering.

VI. High abundance of trace elements in these waters indicates high temperature deep fluid mixing may be a prevalent process in the region. Elevated concentrations of arsenic (As) in Ladakh region show a deep sourced mixing. Some of these trace elements like boron (B) and lithium (Li) indicate towards the past fumarolic characteristics in the Puga and Chumathang geothermal fields. Though the exact source of high ‘Boron’ is yet to be revealed, it seems to be sourced from magmatic activities.

# CHAPTER 5

# STABLE ISOTOPES OF OXYGEN ($\delta^{18}O$) AND HYDROGEN ($\delta D$)

# CHAPTER 5:

# STABLE ISOTOPES OF OXYGEN ($\delta^{18}O$) AND HYDROGEN ($\delta D$)

## 5.1 INTRODUCTION

Isotopes are the species of an atom having equal atomic number with varying mass. Oxygen and hydrogen elements form the water molecule and therefore their stable isotopic compositions are used to derive valuable information on the origin and sources of moisture in different water bodies, including the geothermal springs. These isotopic studies are important as they act as conservative hydro-chemical tracers. Stable isotope ratios ($\delta^{18}O$ & $\delta D$) in the geothermal waters and ground waters are affected by water-rock interaction such as mixing of deep fluids and evaporation (Clark & Fritz, 1997; Guay & Eastoe, 2006). A suit of isotopes Table 5.1 are used to determine different sources of water and to identify the altitudes of their precipitation and climatic conditions at the time of their recharge in certain reservoirs (Mazor, 1997; Ewen et al., 2004; Plummer et al., 2004; Sharp, 2007). These isotopes are presented in Table 5.1, which shows that ~0.2 % of all the oxygen atoms are $^{18}O$, and 0.016% of hydrogen atoms are $^{2}H$ (or D; deuterium). These isotopes are expressed by thee isotopic abundance ratios, i.e. $^{2}H/^{1}H$, or $^{18}O/^{16}O$ etc. The isotopic compositions are generally presented in $\delta$ a notation (in the units of

permil, ‰) which is the relative deviation of isotopic ratios in the sample with respect to the standard. A detailed discussion on this is given in the chapter 3. The accepted standard for the stable isotopes in water is VSMOW (Vienna standard Mean Oceanic Water) which is close to the original standard of SMOW as defined by Craig (1963).

***Table 5.1:*** *Stable isotopes of some useful light elements.*

| Element | Z | N | A | Abundance (%) | Symbol |
|---|---|---|---|---|---|
| **Hydrogen** | 1 | 0 | 1 | 99.985 | $^{1}$**H** |
| | 1 | 1 | 2 | 0.0155 | **D** |
| **Carbon** | 6 | 6 | 12 | 98.892 | $^{12}$**C** |
| | 6 | 7 | 13 | 1.108 | $^{13}$**C** |
| **Nitrogen** | 7 | 7 | 14 | 99.635 | $^{14}$**N** |
| | 7 | 8 | 15 | 0.365 | $^{15}$**N** |
| **Oxygen** | 8 | 8 | 16 | 99.759 | $^{16}$**O** |
| | 8 | 9 | 17 | 0.037 | $^{17}$**O** |
| | 8 | 10 | 18 | 0.204 | $^{18}$**O** |

Stable isotope ($\delta^{18}O$ & $\delta D$) of thermal springs can be used to trace the origin and movement direction of water masses and their migration in the geothermal systems. These are affected due to several processes including evaporation and mixing with shallow aquifers and isotopic exchange with minerals (Kharaka & Mariner 2005; Truesdell et al., 1977). Therefore, the intensity and nature of fluid-rock interaction can be assessed during fluid flow in the zones of high permeable rocks. In the context of the present study, geothermal water can be regarded as a “mixed average precipitation” during the period of time during which meteoric water percolates through the rocks and accumulate in the underground reservoir. Despite the fact, that isotope ratio in precipitation are controlled by the local latitude, altitude, temperature, humidity, and seasons (Yao, 2000), they are distinguishable in terms of magmatic and juvenile water. In this respect the Global Meteoric Water Line (GMWL) serves as a method to

represent the stable isotope variations in surface waters. This chapter presents results and discussion on stable isotopes of hydrogen and oxygen data of the geothermal springs of Garhwal, Himachal, and Ladakh regions of Himalaya.

### 5.1.1 GLOBAL METEORIC WATER LINE

The variations in the $\delta^{18}O$ and $\delta D$ compositions in meteoric water are shown to be correlated on global scale (Friedman, 1953; Craig, 1961a; Dansgaard, 1964, and Rozanski, 1993). Craig (1961a) observed that in spite of the great complexity in different compounds of the hydrological cycle, $\delta^{18}O$ and $\delta D$ in fresh surface waters (representing precipitation) correlate on a global scale. The regression line between $\delta^{18}O$ and $\delta D$ is referred to as GMWL and defined as:

$$\delta D = 8 * \delta^{18}O + 10 \text{ ---------- Eqn. (5.1)}$$

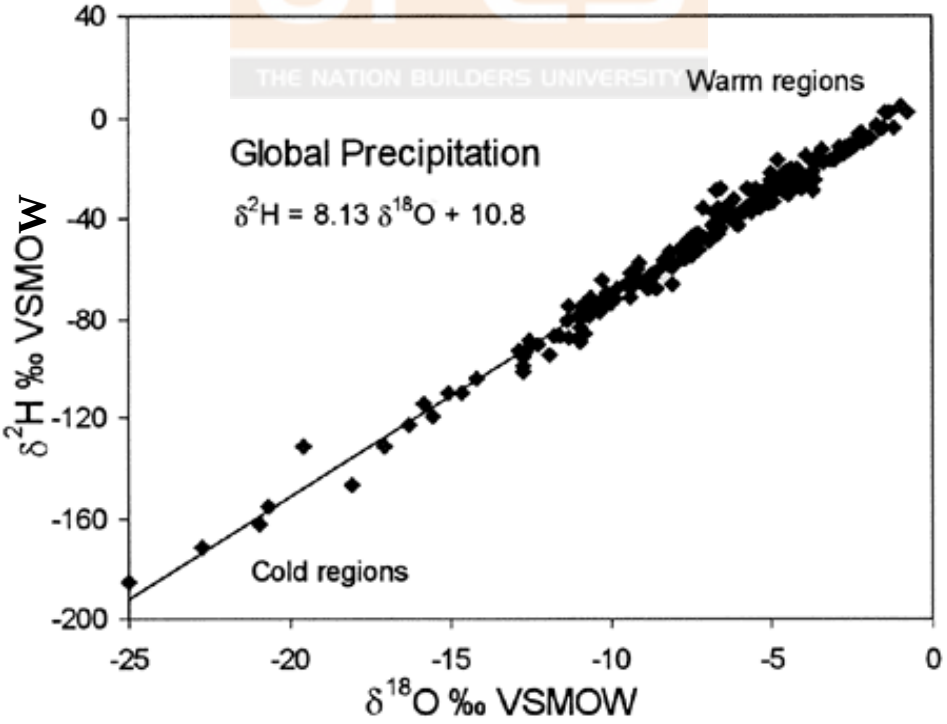


***Fig. 5.1:*** *Global Meteoric Water Line compiled by (Clark & Fritz, 1997).*

Towards improving the representativeness of the Craig's GMWL, Rozanski et al., (1993) compiled the isotopic data of actual precipitation from 219 stations of IAEA under global network for isotopes in precipitation (Eqn 5.2). This refined relationship between $\delta^{18}O$ and $\delta D$ yielded a better regression given as;

$$\delta D = 8.17(\pm 0.07) * \delta^{18}O + 11.27(\pm 0.65) \text{---------Eqn. (5.2)}$$

Further, Clark & Fritz (1997) refined the GMWL which shows that despite a minor variation the overall trend defining the relation remains unchanged from that observed by Craig (1961a).

### 5.1.2 ORIGIN OF GEOTHERMAL WATER (METEORIC Vs. DEEP SOURCE)

Geothermal fluids may incorporate waters from different sources which could be determined by the use of stable isotopes. Friedman (1970) was the first to report the dominance of meteoric component in these fluids by observing the $\delta D$ values of geothermal springs very close to local meteoric waters. However a better understanding about the origin of the water components of these fluids came through the combined measurements of oxygen and hydrogen (Craig, 1963). It demonstrated that the $\delta D$ values of geothermal springs are identical and very close to the local meteoric. However, the $\delta^{18}O$ values were slightly shifted ($\delta^{18}O$-shift) towards more enriched values. This led to conclude that geothermal spring waters, all over the world, were regulated by local meteoric waters. Although most of the geothermal fluids display their meteoric origin, chemical compositions and variations in isotopic ratios indicate towards the possibility of a small (5-10%) but significant mixing of magmatic or deeper component (Nicholson, 1993; Barbier, 2002). This shift in the $\delta^{18}O$ (but not in

δD) suggests that the composition of meteoric water could be understood in terms of hydrothermal interaction at depths. Geothermal systems and volcanic terrenes are characterized by cracks and fissures through which water from the precipitation enters into the ground and descends to a certain depth before it interacts with hot rocks and gets back to the surface. As results of rock-water interactions, isotopes are exchanged and the chemical constituents are incorporated into solution and transported to the surface. During this movement, oxygen from the meteoric water under goes exchange reactions with source rocks (Crystalline igneous/ carbonates) where hot fluids come to the surface in artesian conditions. Source rocks (mostly igneous) may have enriched values of $\delta^{18}O$ in comparison with meteoric waters and therefore, at high temperature, it would give rise to the $\delta^{18}O$ values of the waters and lowers the $\delta^{18}O$ in the rock. However, this process would keep the δD composition very similar to those waters in local precipitation. This observation is consisted with the fact that there is very little hydrogen present in igneous and carbonate rocks which is reflected in terms of a little change in the δD during exchanging the water. Therefore, the $\delta^{18}O$ and δD relationship of thermal waters may be used to study the altitude effects in precipitation, moisture source, and origin of geothermal waters in terms of Meteoric vs. Magmatic sources. This chapter presents $\delta^{18}O$ and δD systematics of the geothermal springs from Garhwal, Himachal, and Ladakh regions of northwest Himalaya.

### 5.1.3 SIGNATURE OF $\delta^{18}O$ AND $\delta D$ IN HYDROLOGICAL STUDIES

Generally, groundwater is recharged by local precipitation or remotely precipitated water followed by its subsequent movement from distant outcrop regions. However, some recharge contribution may also occur from the nearby surface water bodies. In many hydrological investigations, it is important to estimate the amount and source of recharge. This can be achieved by using the information on the variations in stable isotopes with following applications.

1) The seasonal dissimilarity in $\delta D$ and $\delta^{18}O$ of the precipitation could be employed to estimate the ground water recharge.
2) To identify the source of recharge to a ground water system and altitude effect in precipitation.
3) Although, the surface waters, such as rivers and lakes, have $\delta D$ and $\delta^{18}O$ contents significantly different from the local precipitation, recharge of surface water bodies to ground water system could be identified.
4) Recharge source of geothermal systems could be identified with the help of $\delta D$ and $\delta^{18}O$ systematics in terms of meteoric Vs magmatic origin.
5) Mechanism of salination to a groundwater body due to leaching and dissolution of salts from soils or aquifer material, sea water intrusion could be traced by using stable isotopes of $\delta D$ and $\delta^{18}O$.

## 5.2 RESULT AND DISCUSSION

The $\delta^{18}O$ and $\delta D$ composition of the geothermal springs and associated river waters from the study area is presented in the Table 5.2. The $\delta^{18}O_{\text{VSMOW and}}$

***Table 5.2:*** *Stable isotopic ratios and altitude (m,asl) of thermal springs of Garhwal region.*

| Sample no. | Sites name | Sample ID | δ $^{18}$O‰ (VSMOW) | δD‰ (VSMOW) | Altitude (m, asl) |
|---|---|---|---|---|---|
| **HS-1** | Taptkund | 1 | –13.1 | –95.4 | 3089 |
| **HS-2** | Khiroi | 2 | –12.6 | –86.7 | 2973 |
| **HS-3** | Bhapkund | 3 | –11.5 | –78.9 | 2680 |
| **HS-4** | Shaldhar | 4 | –10.5 | –74.3 | 1953 |
| **HS-5** | Tapoban | 5 | –10.1 | –68.1 | 1890 |
| **HS-6** | Birahi | 6 | –8.3 | –59.5 | 1190 |
| **HS-7** | Ganoi | 7 | –8.3 | –57.1 | 1409 |
| **HS-8** | Langsi | 8 | –8.8 | –59.6 | 1225 |
| **HS-9** | Helang | 9 | –7.4 | –59.2 | 1210 |
| **HS-10** | Gaurikund | 10 | –9.2 | –60.1 | 1930 |
| **HS-11** | Gangnani | 11 | –9.3 | –63.5 | 1900 |
| **HS-12** | Jhaya | 12 | –9.3 | –62.6 | 1808 |
| **HS-13** | Bukki | 13 | –9.0 | –61.5 | 1730 |
| **HS-14** | Thirang | 14 | –8.8 | –59.4 | 1640 |
| **HS-15** | Matli | 15 | –7.5 | –47.2 | 1062 |
| **HS-16** | Kotimanep | 16 | –8.6 | –56.0 | 1429 |
| **HS-17** | Suryakund | 17 | –8.4 | –65.6 | 3070 |
| **HS-18** | Jankichatti | 18 | –9.5 | –64.5 | 2568 |
| **HS-19** | Banas | 19 | –8.8 | –60.4 | 2210 |
| **HS-20** | Wozari | 20 | –9.7 | –65.4 | 1630 |
| **RW-1** | RW-1 | R-1 | –14.3 | –97.6 | 3089 |
| **RW-2** | RW-2 | R-2 | –14.2 | –97.4 | 3089 |
| **RW-4** | RW-4 | R-4 | –13 | –88.6 | 1800 |
| **RW-5** | RW-5 | R-5 | –12.8 | –76.3 | 1468 |
| **RW-6** | RW-6 | R-6 | –11.6 | –70.0 | 1190 |
| **RW-8** | RW-8 | R-8 | –10.4 | –69.0 | 2148 |
| **RW-9** | RW-9 | R-9 | –12.3 | nd | 3070 |
| **RW-10** | RW-10 | R-10 | –10.7 | nd | 2210 |
| **HS-21** | Changlung | 21 | –16 | –124 | 3410 |
| **HS-22** | Pulthang | 22 | –16 | –117 | 3175 |
| **HS-23** | Panamic | 23 | –16 | –119 | 3225 |
| **HS-24** | Gaik | 24 | –15 | –116 | 3770 |
| **HS-25_1** | Chumathang | 25-1 | –11 | –119 | 4029 |
| **HS-25_2** | Chumathang | 25-2 | –15 | –118 | 4029 |
| **HS-26** | Puga | 26 | –14 | –122 | 4410 |
| **HS-27** | Sumdo | 27 | –11 | –100 | 3270 |
| **HS-28** | Thopan | 28 | –11 | –72 | 2180 |
| **HS-29** | Tapri | 29 | –13 | –80 | 1702 |
| **HS-29B** | Tapri_Handpump | 29B | –10 | –69 | 1762 |
| **HS-30** | Naptha | 30 | –9 | –63 | 1793 |
| **HS-31** | Jeori | 31 | –9 | –59 | 1793 |
| **HS-32** | Jhakri | 32 | –8 | –53 | 1130 |
| **HS-33/34** | Jharar | 33/34 | –7 | –45 | 1033 |
| **HS-35** | Bashist | 35 | –12 | –78 | 2110 |
| **HS-36** | Khiral Bihal | 36 | –10 | –62 | 1750 |
| **HS-37** | Kalath | 37 | –10 | –68 | 1730 |
| **HS-38** | Ramshila Kullu | 38 | –8 | –53 | 1228 |
| **HS-39** | Manikaran | 39 | –9 | –57 | 1662 |
| **HS-40** | Kasol | 40 | –9 | –56 | 1600 |

δD composition of these thermal springs vary from –7 ‰ to –16 ‰ and –45 ‰ to –124 ‰, respectively. These variations are also associated with an altitude covering a range from of 1033 to 4410 (m, asl) in the study area.

Results indicate that the stable isotopic ratios in the geothermal waters are more depleted towards the higher altitude which is the characteristics of precipitation. Especially the springs of Ladakh region shows the depleted values of $\delta^{18}O$ and δD as compared to Himachal and Garhwal regions. This may be due to the altitude effect, where more depleted values are expected with higher altitudes. However, the possibility of moisture source dependent variation in terms of westerly vs. south west monsoon is not ruled out.

## 5.3 THE TWO ISOTOPE ($\delta^{18}O$, δD) PLOT AND CORRELATIONS

The relation between $\delta^{18}O$ and δD compositions in natural waters is described by equilibrium fractionations (Craig, 1961a; Dansgaard, 1964; and Rozanski, 1993). These studies have established a relation (GMWL) between $\delta^{18}O$ and δD ($\delta D = 8 * \delta^{18}O + 10$) in precipitations from the various part of the world which has a slope of 8 with intercept 10 which is a variable. A more general relation, may be expressed as $\delta D = S * \delta^{18}O + d$ with the slope S=8; which is explained by the ratio between the equilibrium isotope fractionation of oxygen and hydrogen for the condensation process of the rain or precipitation and d is the deuterium excess (d-excess) which is the intercept with the δD axis. This intercept may very as a function of locality, season and occurrences of extreme events which causes a departure from the intercept of 10. It also

varies with relative humidity and temperature conditions in the evaporation region.

The isotopic composition of water vapour (δD & $\delta^{18}O$) over seawater is 0‰ against Standard Mean Oceanic Water (SMOW). It is some what lighter than world's average precipitation. However, from the observed composition of vapour before and after the precipitation remain in isotopic equilibrium as it occur from saturated vapour (i.e. vapour in physical equilibrium with water). Therefore variation in δD and $\delta^{18}O$ values take place in such a way that both move along the meteoric water line. The δD and $\delta^{18}O$ relationship for rain or precipitation at any place, however, differs from the global equation and can be represented by local precipitation. This is defined by the Local Meteoric Water Line (LMWL) and is a manifestation of local meteorological conditions.



### 5.3.1 GARHWAL REGION

Isotopic compositions ($\delta^{18}O$ & δD) of the geothermal springs are presented in table 5.2. The slope and intercept of these springs are given in table 5.3. Results show that the oxygen and hydrogen isotopes of these springs fall closely on the meteoric water line (Fig.5.2), indicating their origin from meteoric water. Geothermal springs from high altitudes in Garhwal Himalaya exhibit depleted composition because of the dominant mixing of new water by precipitation associated with altitude effect. In geothermal springs, old water interacts with rock under hydrothermal conditions which causes change towards heavier $\delta^{18}O$ composition while still retaining its deuterium signature.

This happens as the hydrogen bearing minerals are less available to interact with meteoric water in hydrothermal conditions. Therefore in such a scenario, it forces the waters to plot to the right of LMWL (Witcher et al., 2004). The $\delta^{18}O$ and $\delta D$ isotopes data of the geothermal springs of this study are shown in the plot (Fig. 5.2a). These fall on the GMWL and therefore are in good agreement with the previous studies (Shivanna et al., 2008) based on rain water samples in this region. This indicates that the geothermal springs of the Garhwal region are recharged with local groundwater and meteoric water which are mixed with the old groundwater characterized with significant rock-water interaction. However in certain cases, a clear difference is seen where some geothermal springs [HS-17, Suryakund (Yamnotri); and HS-9 Helang (Alaknanda)] fall away from GMWL which indicate a deeper magmatic source that causes to the shift in the $\delta^{18}O$. To address this point, we have also used $\delta^{13}C_{DIC}$ which provides an independent check of revealing the deeper affinity (with enriched $\delta^{13}C_{DIC}$) of these waters and are given in the chapter 6. Stable isotope data of geothermal springs hint that samples falling off the GMWL [HS-17 and HS-9] exhibit enriched $\delta^{13}C_{DIC}$ ratios (1.4 to 3.7‰), which are characteristic of magmatic and deeper source. Therefore, it suggests that the meteoric waters are mixing in significant amount with deep fluids at depth and hence changing the composition noticed in spring waters.

To understand the relationship between $\delta^{18}O$ and $\delta D$ in the geothermal springs (under fair possibility for their meteoric origin) a regression line was drawn in a $\delta^{18}O$-$\delta D$ space along with meteoric water lines (GMWL and LMWL). This provides useful information about their dominant meteoric recharge source.

Regression analyses of the isotopic data (Williamson, 1968) for these samples yielded linear relationships which are represented as follows.

$\delta D_{(TS)} = (7.00 \pm 0.52) * \delta^{18}O + (0.81 \pm 4.9)$ $(n=20, r=0.95, p<0.005)$.....Eqn(5.3)

$\delta D_{(RW)} = (8.23 \pm 1.60) * \delta^{18}O + (21.0 \pm 20.0)$ $(n=6, r=0.95, p<0.005)$.....Eqn (5.4)

Where *n* is the number of samples; r is the correlation coefficient and p is the level of significance; *TS* and *RW* stand for geothermal springs and river waters, respectively.

The slope of the regression line for the geothermal waters (7.00±0.52; Eqn 5.3) overlaps with the river waters (LMWL; Eqn 5.4) which are marginally lower than GMWL (Craig, 1961a) and hence indicating a meteoric origin. However, two spring sample from Alaknanda and Yamuna valleys (Helang, HS-9, and Suryakund, HS-17) fall off the GMWL and hence invoke a deep fluid mixing with meteoric water. This inference is also well reflected in their enriched $\delta^{13}C_{DIC}$ and shift in the $\delta^{18}O$ however the slope of the best fit line of the River waters (monsoon season) from same region is marginally lower than LMWL (Shivanna et al., 2008) and GMWL (Craig, 1961). The $\delta^{18}O$-$\delta D$ plots of river waters show the scattered nature with the slope of 8.23 and intercept of 21 which is indicative of Local meteoric conditions. The $\delta^{18}O$-$\delta D$ relationship of thermal waters are compared with earlier studies (Shivanna et al., 2008; Dalai, 2002a; Bartarya et. al., 1995; and Ramesh & Sarin, 1992) from the headwaters of the Ganga and Yamuna systems along with the rain water from the Garhwal Himalaya and are presented in table 5.3. Similarities on the slopes and intercepts for thermal springs with those from the

precipitation of Garhwal Himalayan region suggest about their meteoric origin. Therefore, in principle, the geothermal waters may be representative of rains accumulated over a time period which may be regard as the residential time. In this way this study highlights the importance of using thermal springs samples for estimating the average characteristics of moisture integrated over their residence time.

### 5.3.2 LADAKH AND HIMACHAL REGIONS

Geothermal springs of Ladakh and Himachal regions receive moistures from diverse sources (local, westerly & Indian summer monsoon) and therefore their isotopic compositions ($\delta^{18}O$ and $\delta D$) may be highly variable and are given in the Table 5.2 whereas, the slope and intercept of the springs are given in table 5.3. The $\delta^{18}O$ and $\delta D$ for the geothermal springs of Ladakh and Himachal Pradesh fall on the meteoric water line and are consistent with their height (Fig 5.2b). They seem to indicate that more depleted isotopic composition ($\delta^{18}O$ and $\delta D$) are due to their higher altitude. However, it shows a shift in the $\delta^{18}O$ from some geothermal springs (Chumathang, HS-25; Puga, HS-26; Sumdo, HS-27) which plot away from the meteoric water line. Such departure from LMWL is indicative of their origin from additional source than meteoric. Generally areas showing little oxygen shift could be old systems of water through which the isotopic composition of the rocks had adjusted to equilibrium with recharge water (magmatic water or meteoric water) that percolated to great depths at elevated temperature (Craig, 1963). To establish a

relationship between δD and $\delta^{18}O$ in these springs, regression line was drawn along with the global precipitation.

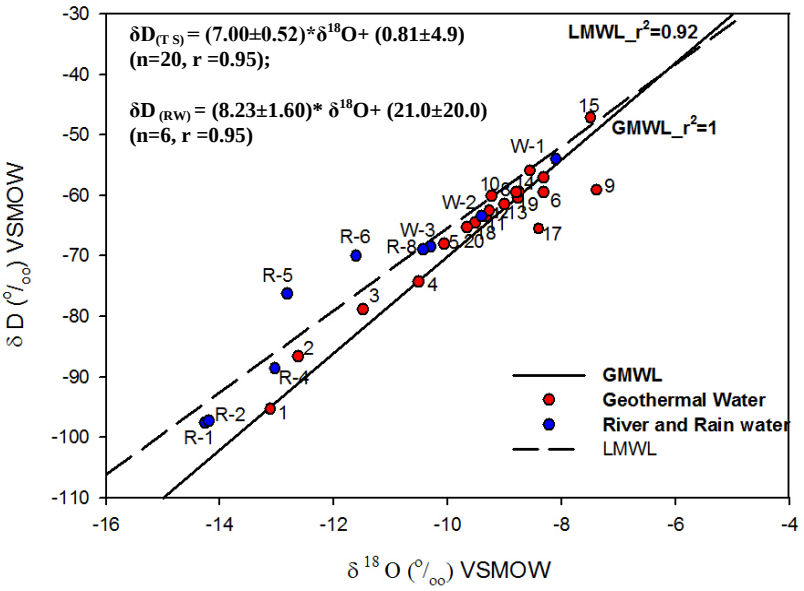


***(a)***

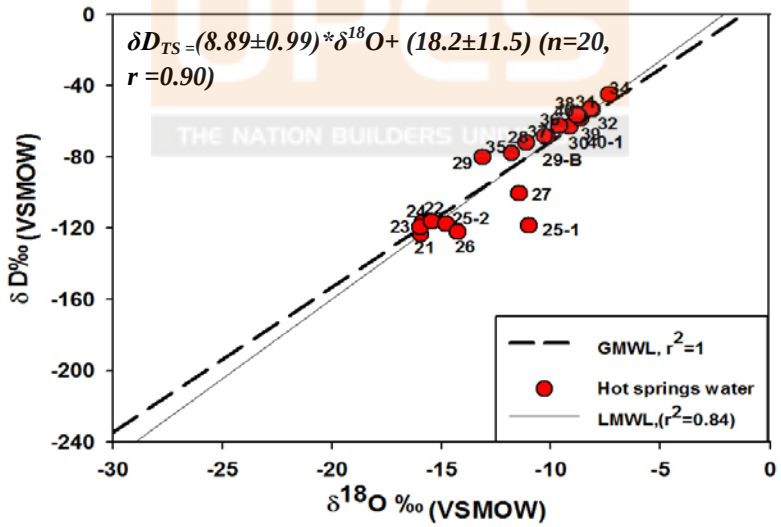


***(b)***

***Fig. 5.2:*** Scatter plots of *$\delta^{18}O$ and δD correlation geothermal springs, river waters and precipitation with respect to Global Meteoric Water Line (Rozanski et al., 1993), (a) Garhwal region, (b) Himachal and Ladakh regions. Data of rain waters (W-1, 2 and 3) are taken from Shivanna et al. (2008). Number of samples and regression equation [calculated using Williamson (1968) is also given. The errors are ±1σ) for both plots.*

Comparison of $\delta^{18}O$ and δD among the geothermal springs, GMWL, LMWL, surface and groundwater of the same region provides first-hand information about their recharge source. Regression analyses (Williamson, 1968) and d-Excess of the isotopic results of the geothermal springs, surface, and groundwater are given in the Table 5.3. The slope of the regression line of these spring waters is computed to be 8.89±0.99 and given by the equation (5.5).

$$\delta D_{TS} = (8.89 \pm 0.99) * \delta^{18}O + (18.2 \pm 11.5)\ (n=20,\ r=0.90,\ p<0.005) \quad \text{.....Eqn (5.5)}$$

Where *n* is the number of samples; r is the correlation coefficient and p is the level of significance; *TS* is geothermal spring. The slope of the regression line of the geothermal springs overlaps with the surface, ground, and river waters of the NW-Himalayan region (Shivanna et al., 2008; Dalai et al., 2002a; Ramesh & Sarin, 1992; Bartarya et al., 1995; Pande et al., 2000). Therefore it seems that meteoric water is the dominant mechanism for the recharge of thermal springs in this region.



## 5.4 DEUTERIUM EXCESS

The *'deuterium excess'* in precipitation defined as'd' is basically the intercept of the GMWL. It provides a measure of non-equilibrium effects (Dansgaard, 1964) in terms of their differences between measured δD and expected equilibrium value of δD which is derived from the measured $\delta^{18}O$. Its variability is an indicator of environmental conditions during phase changes under non-equilibrium conditions. The magnitude of'd' is determined by the

conditions of the vapour source (e.g. relative humidity, temperature and wind speed over the evaporating surface) and moisture recycling in the area of precipitation (Rozanski et al., 1993). Low humidity condition at the source region enhances kinetic evaporation, resulting in a lower slope of the δD – $\delta^{18}O$ regression line and higher deuterium excess in the resultant precipitation (Clark & Fritz, 1997). On the other hand, precipitation resulting from a source at high humidity defines a δD–$\delta^{18}O$ regression line close to GMWL (slope of 8) with 'd' values close to 10. It varies from region to region, owing to various origins and formation conditions of the vapour. For example, the vapour escaping from the open tropical ocean will give rise to condensation process with d-excess of about to 10 which, by and large, may be the representative of ocean precipitation. The shift in the deuterium excess occurs possibly as a result of evaporation occurring on a high continental air with lower humidity compared to the ocean. As'd' is generally correlated to the average relative humidity over the area of production, ($d_{excess}$=10 for relative humidity of 75), it represents a climate indicator for describing global paleo climate changes and identify paleo-precipitation. However, in some region, the linear correlation between $\delta^{18}O$ and δD of precipitation sample does not have a slope of 8 but lies between 4 and 6. This feature of *d-excess* has also been documented for surface waters such as lakes and close reservoirs, which suffer from extreme evaporation. These surface waters becomes enriched in $\delta^{18}O$ and δD during the evaporation and this enrichment continues as the evaporation progress up to a constant value termed as isotopic stationary state, even though the reaming fraction of liquid continues to decrease. This process operates due to the exchange of surface water with the atmospheric vapour. The enriched

values of $\delta^{18}O$ and $\delta D$ produced by evaporation have a complex relationship. This is a function of temperature, relative atmospheric humidity, and the speed of evaporation and the differential diffusion of isotopic molecules in air. In addition, the increase in the heavy isotopic composition varies in evaporating systems due to the above factors changing with the local climate.

### 5.4.1 GARHWAL REGION

Deuterium excess in geothermal springs in the region ranges from -0.05 to 14.2 with a mean of 10.2 (Table 5.3). This shows a relatively large range of characteristics due to the mixing of fluids in varying proportion. Two of the samples (Helang, HS-9 and Suryakund, HS-17) have the magmatic/deeper source and therefore the *d*-excess of HS-9 and HS-17 are also lower than the surface/rainwater characteristics. The $\delta D$ and $\delta^{18}O$ in geothermal springs of the region shows a strong relationship with local precipitation except those (Helang, HS-9, Suryakund, and HS-17) which exhibit deeper source and therefore could be the possible objects for future exploration for geothermal energy. The *d*- excess of geothermal water of the Garhwal region is similar to the Himalayan rivers and precipitation in its catchment (Shivanna et al., 2008; Dalai et al., 2002a; Ramesh & Sarin, 1992; Bartarya et al., 1995). Their inter comparison are presented in table 5.3. These results show that geothermal springs of Garhwal region act as good indicator of LMWL representing average precipitation integrated over their residence time (i.e. time elapsed from their precipitation, transport and their subsequent storage in deeper reservoirs). The $\delta D$ and $\delta^{18}O$ characteristics of the geothermal springs of this

region compare well with those from surface water and therefore it indicates that precipitation is the main recharge source for geothermal springs in the Garhwal Himalaya. However it seems that the meteoric source that mixes with the deeply sourced geothermal waters (with enriched $\delta^{13}C$ and $\delta D$ and $\delta^{18}O$ signals of deeper waters) look masked with the dominance of meteoric water. Further, for the conclusive inferences, other isotopes (such as B, Si) and geochemical proxies (Si/Ge) would be helpful in asserting the exact source of mixing present in geothermal waters.

### 5.4.2 LADAKH AND HIMACHAL REGIONS

Geothermal springs of the Ladakh & Himachal region show a slope of 8.89±0.99 with deuterium excess ranging from 3.9 to 10.2 (Table 5.3). However three of them (Chumathang, HS-25, Puga, HS-26, and Sumdo-27) indicate their affinity towards magmatic waters. This is also evident from their lower deuterium excess of -8.5. The geothermal spring of Himachal region shows a relatively higher d-excess ranging from 10.4 to 24.8; average 14.3±3.5 points their association with meteoric origin (Table 5.3). The slope and d-excess of Chumathang, Puga and Sumdo are suggestive of magmatic intrusion in the meteoric water. This could be the plausible scenario which hints that these regions consist of very high thermal anomalies which have also been suggested by the geophysical studies. A general comparison of *d*-excess of these thermal springs shows a value close to rivers and precipitation of the Garhwal Himalayan region (Shivanna et al., 2008; Dalai et al., 2002a; Ramesh & Sarin, 1992; Bartarya et al., 1995). This suggests that precipitation and ground water are dominating source of recharge for most of the

geothermal springs and some of them have significant input of magmatic waters. Individual proxy of $\delta^{13}C$ (discussed in chapter 6) also suggest about the mixing of deeper fluids with meteoric water in these springs. The δD & $\delta^{18}O$ relations and d-excess of geothermal springs of the Ladakh and Himachal region are presented in Table 5.3.

Geochemical characteristics lead to conclude that some geothermal springs from Garhwal region (Helang, HS-9; Suryakund, HS-17) and Ladakh and Himachal regions (Puga, HS-25, Chumathang, HS-26, Sumdo, HS-27) have their water mixed with deeper/magmatic source and hence could be suitable sites for energy exploration.

***Table 5.3:*** *δD and $\delta^{18}O$ relation and d-excess of thermal springs of the Garhwal, Himachal, and Ladakh regions and the contemporary other studies.*

| **Sites name** | **Month and Year** | **No. of Sample** | **Slope** | **Intercept** | **r** | **(deuterium excess)** | |
|---|---|---|---|---|---|---|---|
| | | | | | | **Range** | **Mean** |
| ***Thermal Springs** ***(****Garhwal Himalaya****)*** | Nov-10 | 20 | 7.00±0.52 | 0.81±4.9 | 0.95 | -0.05 –14.2 | 10.2±3.6 |
| ***Thermal springs** *(Ladakh & Himachal)* | Sep-11 | 20 | 8.89±0.99 | 18.2±11.5 | 0.9 | Ladakh (-8.5 to 10.2) Himachal (10.4 to 24.8) | 5.4±7.4 14.3±3.5 |
| ***River Water** | Nov-10 | 6 | 8.23±1.6 | 21±20 | 0.95 | 14.5 – 26.2 | 18.6±4.7 |
| **[a]Rain Water** | Sep-Dec,2004 | 6 | 6.8 | 0.3 | 0.99 | 10 – 12.45 | 11.25±1.3 |
| **Garhwal Himalaya** | | | | | | | |
| **[a]Cold springs** | Sep-04 | 4 | 5.2 | -17.6 | 0.96 | 1.5 – 9.1 | 6.1±2.6 |
| **[b] YRS** | Sep-99 | 14 | 7.71±0.27 | 7.1±2.3 | 0.98 | 5.3 – 12.8 | 9.6±2.2 |
| **[b]YRS** | Jun-99 | 28 | 5.61±0.26 | -9.5±2.1 | 0.92 | 5.2 – 17.3 | 9.9±3.1 |
| **[b]YRS** | Oct-98 | 31 | 6.34±0.24 | -1.8±2.1 | 0.98 | 7.7 – 16.2 | 12.7±2.0 |
| **[c]Ganga** | Apr-90 | 23 | 7.45±0.23 | 8.0±2.0 | 0.98 | 6.2 – 21.0 | 13.7±3.1 |
| **[d]Gaula** | Feb – Oct 1983,84,85 | 20 | 8.36±0.59 | 10.7±5.2 | 0.86 | 2.2 – 21.6 | 9.6±4.8 |
| **[e]Indus** | Aug-99 | 19 | 9.12±0.29 | 31.1±4.2 | 0.98 | 7.8 – 18.4 | 14.7±3.1 |

* Slopes and intercepts calculation based on Williamson (1968), Error are ±1σ, r is correlation coefficient of present study. Deuterium excess values, range, mean and one standard deviation. [a]Shivanna et al.,(2008); [b]Dalai et al.,(2002); [c]Ramesh and Sarin (1992) ; [d]Bartarya et al.,(1995); [e]Pande et al. (2000).

## 5.5 ALTITUDE EFFECT

In general terms, the altitude effects of stable isotopes are the observed decreasing trends in the δD and $\delta^{18}O$ compositions with increase in altitude from oceans to continents. However, its intensity also depends on the local climate and topography. This attribute is used as one of the important applications in stable isotopes hydrology which include the identification of the altitude at which groundwater recharge takes place. The reason for such altitude dependent variation in stable isotope composition is due to the progressive precipitation of the heavier isotopes during orographic ascent of the moisturized air masses (which occurs in the windward side in the mountainous region). For more negative values of the isotopic composition with increasing altitude is closely related to decrease in temperature. Therefore, isotopic compositions may be used for finger printing of rains with different moisture sources (Fig. 5.3).

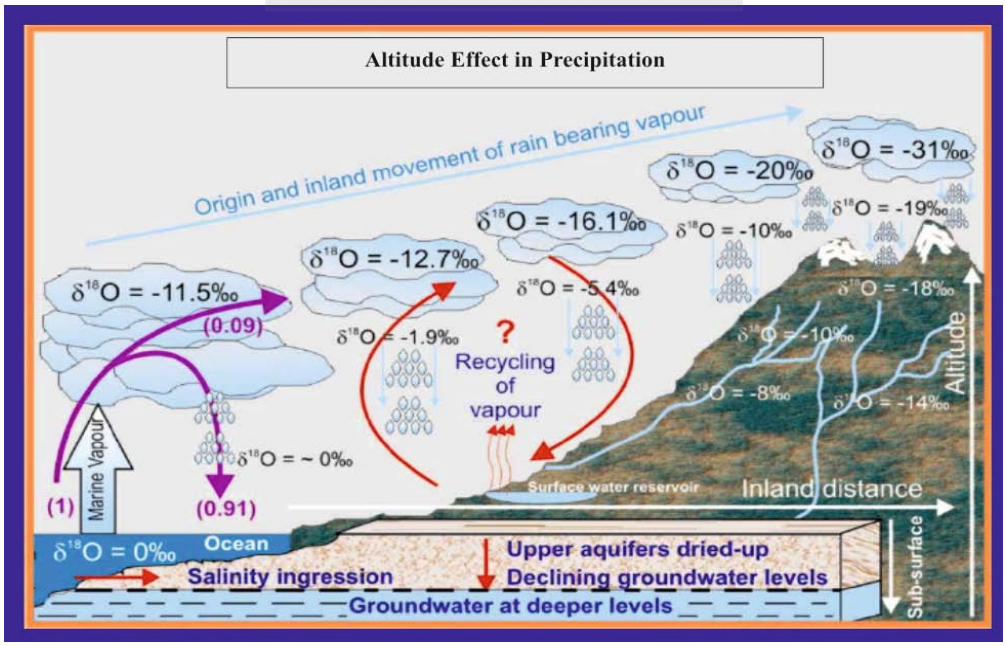


**Fig. 5.3:** *Isotope finger printing in water cycle and altitude effect in precipitation.*

The altitude effect in $\delta^{18}O$ in mid-latitude precipitation usually varies from 0.15 to 0.3‰ for every 100 m of altitude gained (Schotterer et al., 1997). Combined effects of continental and altitude are the manifestations of the Rayleigh distillation in which continental effect is in operation on a large spatial scale due to the cloud movement. In such a scenario, the altitude effect operates in a specific area due to continuous removal of water from the rising cloud as a function of decreasing temperature and increase in elevation. Earlier studies (Bhattacharya et al., 1985; Krishnamurthy & Bhattacharya, 1991) have modeled the continental effect in the north Indian precipitation to identify the sources of water vapor of the cloud system. These studies have shown that the precipitation is the main sources of water in the rivers, streams (particularly in the monsoon period) and therefore reflect in their isotopic composition. However, stream water at any given place represents a mixture of waters drained from higher elevation to the site. Therefore, the isotopic composition of the given site is lighter than the local precipitation at that site. Further, the studies from Ganga head waters (Ramesh & Sarin, 1992) and from Gaula river catchments (Bartarya et al., 1995) observed a decreasing trend in the isotopic composition of waters with increasing elevation of sampling sites. Studies carried out by Garzione et al., (2000 a, b) in the Seti River and Kali Gandaki watershed (Nepal Himalaya) has also reported a similar altitude effect in $\delta^{18}O$ in the stream waters. Such recharge source has also been studied for a geothermal system at mount Meager, a quaternary volcano in coast range of western British Columbia. This is based on the precipitation sites located between 250 m to 3250 m which have yielded an altitude effects of -0.25‰ per 100 m . In a similar study conducted in the Jura mountains of northern

Switzerland (Siegenthaler et al., 1983) has also estimated the altitude effect of -0.2 ‰ per 100 m rise.

### 5.5.1 GARHWAL REGION

Geothermal waters were collected from this region cover a total height difference of 1160 to 3089 meters. In the study, we have calculated a gradient of altitude effect in terms of $\delta^{18}O$ using geothermal springs which varies from -7.5‰ to -13.1‰. The regression equations (5.6 and 5.7) for the altitude effect of geothermal springs and river waters are drawn as follows:

$$\delta^{18}O_{(TS)} = (-0.236\pm0.025)*10^{-2}(\text{altitude m}) - 5.16\pm0.48 \quad (r=-0.92,\ P>0.01,\ n=20) \quad \text{.....Eqn. (5.6)}$$

$$\delta^{18}O_{(RW)} = (-0.16\pm0.003)*10^{-2}(\text{altitude m}) - 9.32\pm0.72 \quad (r=-0.96,\ P>0.01,\ n=6) \quad \text{....Eqn. (5.7)}$$

Where *n* is the number of samples. *TS* and *RW* are the geothermal springs and River Waters.



These equations indicate that altitude effect is 0.24‰ per 100 meters for the thermal springs and 0.16‰ per 100 meters for river waters. These lie within the values reported in earlier studies (Shivanna et al., 2008; Pande et al., 2002, Dalai et al., 2002; Ramesh & Sarin, 1992; Bartarya et al., 1995) from the Garhwal region (Fig.5.4 & Table 5.4). One of the advantages of this study is the estimation of altitude effect on geothermal springs which represents an average precipitation integrated over the residence time of these waters. Therefore, such estimates of altitude effect are more of a representative of the regional climate than those estimated from flash rain samples.

### 5.5.2 LADAKH AND HIMACHAL REGIONS

As mentioned earlier for Garhwal Himalaya, a similar exercise for the altitude effects of $\delta^{18}O$ were also computed for Ladakh and Himachal regions covering altitude difference from 4410 to 1033 meters which corresponds to the values of $\delta^{18}O$ from -7to -16‰. The regression equation (5.8) for the geothermal springs and river waters are drawn as follows.

$$\delta^{18}O_{(TS)} = (-0.25\pm0.027)*10^{-2}\,(\text{altitude m}) - 5.4\pm0.70 \quad (r=-0.89,\ P>0.01,\ n=20) \ldots \text{Eqn(5.8)}$$

Where n is the number of samples and TS is Geothermal Springs.

***Table 5.4:*** *Altitude effects of the geothermal springs and relative studies in the northwest Himalaya.*

| Sites name | Month | No. of Samples | Altitude effect | Intercept | r |
|---|---|---|---|---|---|
| *TS (Ladakh &Himachal) | Sep-11 | *20 | -0.25±0.027 | -5.4±0.70 | -0.89 |
| *TS (Garhwal Himalaya) | Nov-10 | *18 | -0.24±0.025 | -5.16±0.48 | -0.92 |
| *RW(Garhwal Himalaya) | Nov-10 | 6 | -0.16±0.03 | -9.32±0.72 | -0.96 |
| [a]RW(Garhwal Himalaya) | Sept-Dec,2004 | 6 | -0.55 | | |
| Yamuna[b] | June | 10 | -0.09±0.01 | -7.4±0.1 | -0.84 |
| Yamuna[b] | Oct-98 | 6 | -0.11±0.01 | -7.7±0.1 | -0.86 |
| Yamuna[b] | June, Oct-1999 | 16 | -0.11±0.01 | -7.3±0.1 | -0.85 |
| Ganga[c] | Apr-90 | 5 | -0.19±0.01 | -8.4±0.2 | -0.98 |
| Gaula[d] | Feb., June.,Oct.,1983-84-85 | 30 | -0.14±0.01 | -63±0.2 | -0.69 |
| Indus[e] | Aug-99 | 6 | -0.09±0.01 | -12.1±0.4 | -0.58 |
| Seti[f] | March/Apr 1999 | 12 | -0.29±0.03 | -5.9±0.2 | -0.96 |
| Kali- Gandaki[f] | Sept., Oct -1999 | 38 | -0.29±0.01 | -6.8±0.3 | -0.96 |

** $\delta^{18}O$ ‰ per 100 m, calculated based on Williamson (1968). The errors are ±1σ.[A] Shivanna et al., (2008), [b]Dalai et al., (2002), [c]Ramesh &Sarin (1992), [d]Bartarya et al.,(1995), [e]Pande et al.,(2000), [f]Garzione et al., (2000a,b), TS used for Geothermal Springs and RW for River Waters.*

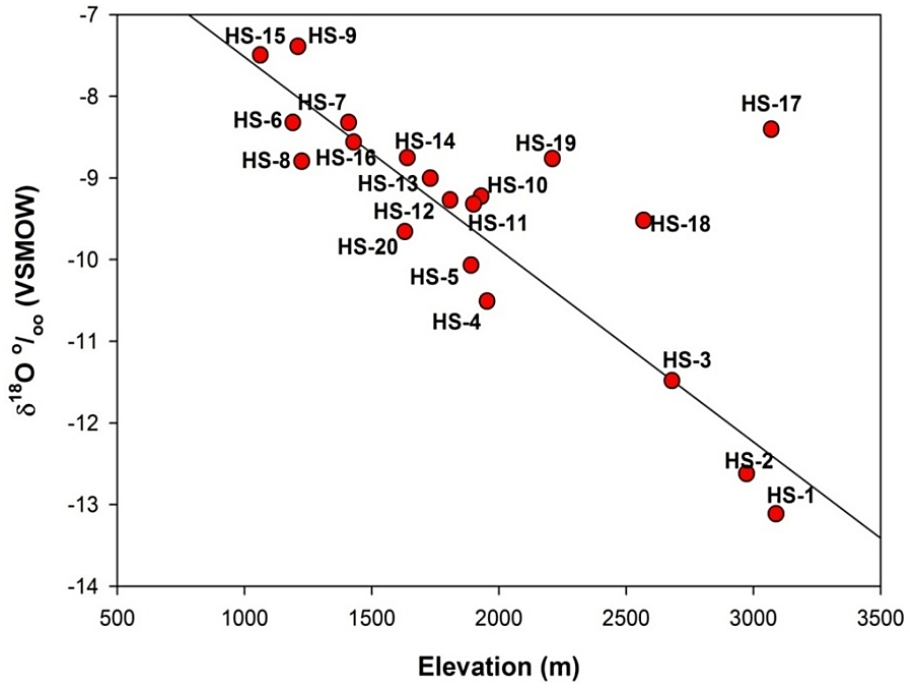


**(a)**

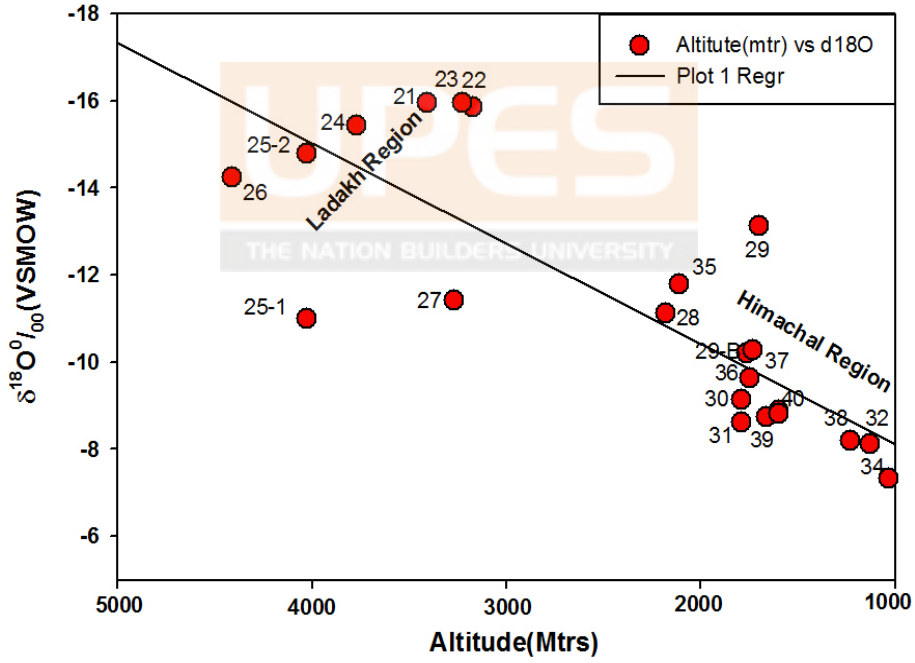


**(b)**

***Fig.5.4:*** Scatter plots of *altitude effect of* $\delta^{18}O$ *in geothermal springs. (a) Garhwal region, and (b) Ladakh and Himachal regions. The slope and regression line is a measure for altitude effect. (See equations 5.6, 5.8 in the text and Table 5.4).*

Equation 5.6 indicates that the altitude effect from the thermal springs is 0.24 ‰ per 100 meters (Table 5.4 and Fig. 5.4b) which falls within the limits of those reported from the Garhwal Himalaya and the Ladakh and Himachal regions.

## 5.6 CONCLUSIONS

The $\delta^{18}O$ and δD measurements of Garhwal, Himachal and Ladakh thermal springs have led to draw the following observations and conclusions:

1. The δD values range from -45‰ to -124‰ and $\delta^{18}O$ from -7.0‰ to -16 ‰, respectively which correspond to the altitude range from ~1033 to ~ 4410 m.

2. The isotopic ratios of $\delta^{18}O$ and δD in the geothermal waters are more depleted toward the higher altitude which is characteristics of precipitation. Geothermal springs of Ladakh region show the affinity towards depleted values of $\delta^{18}O$ and δD with respect to Himachal and Garhwal region due to the altitude effect.

3. Most of the waters appear meteoric in nature however, the δD and $\delta^{18}O$ relation for the geothermal springs of Garhwal region yield a slope of 7.00±0.52 and deuterium excess of 10.2±3.6. Towards this the geothermal springs of Himachal and Ladakh regions yield a slope of 8.89±0.99 and deuterium excess (Ladakh 5.4±7.4, Himachal 14.3±3.5) quite similar for the surface and river waters of the regions.

4. The recharge source of the geothermal springs of the Garhwal, Himachal, and Ladakh regions is mainly derived from the surface waters, ground waters and perceptions excepting few of the geothermal springs, which have the magmatic inputs.

5. The "altitude effect" in the geothermal springs of Garhwal and Himachal & Ladakh regions is derived for the first time which is found to be -0.25±0.027‰ and -0.24±0.025‰ per 100 m rise in altitude respectively. It covers the altitude range from ~1033 to ~ 4410 m.

6. Geochemical characteristics suggest that the springs (Helang, HS-9; Suryakund, HS-17) form Garhwal region and (Puga, HS-25, Chumathang, HS-26, Sumdo, HS-27) from Ladakh and Himachal regions have their water mixed with deeper/magmatic source and hence could be suitable sites for energy exploration.

# CHAPTER 6

# CARBON ISOTOPES ($\delta^{13}C_{DIC}$) AND DEGASSING OF METAMORPHIC $CO_2$

# CHAPTER 6:

# CARBON ISOTOPES ($\delta^{13}C_{DIC}$) AND DEGASSING OF METAMORPHIC $CO_2$

## 6.1 INTRODUCTION

This chapter presents the results and discussions on isotopic composition of carbon ($\delta^{13}C$) in dissolved inorganic carbon of geothermal springs from Garhwal, Himachal and Ladakh regions of Himalaya. This has led to derive valuable information regarding the origin of geothermal fluids and degassing of metamorphic $CO_2$ through these springs. It is a well-established that the atmospheric $CO_2$ has presumably moderated the earth's climate since water was first established on the surface of the earth. Atmospheric $CO_2$ creates a small reservoir and its size is controlled by the difference between the large fluxes involved in the cycle carbon on geological time scales. Nevertheless their significance, the relative importance and inter dependence of the various geological controls on the $CO_2$ fluxes to the atmosphere are uncertain. The key control on atmospheric $CO_2$ is considered by the inorganic carbon cycle in which it is consumed by weathering of Ca and Mg silicates on the earth surface followed by their deposition as calcium carbonate ($CaCO_3$) in the ocean.

Further, it is balanced by $CO_2$ returned to the atmosphere by volcanoes and by de-carbonation and metamorphic process in the orogenic belts. The flux of $CO_2$ involved in the inorganic carbon cycle (~$10^{19}my^{-1}$) is large compared to the amount of $CO_2$ in the atmosphere and ocean (~$3.2x10^{18}$mole) for which it must be balanced by the fluxes due to the weathering and degassing for an equilibrium concentration of $CO_2$ in the atmosphere (Bickle, 1996). Further, the variations in global weathering rates, operating over a million year time scale, could be supported by a corresponding variation in the supply of $CO_2$ to the atmosphere.

Towards this, the relative significance of various mechanisms of $CO_2$ outgassing is not fully understood on global scale. These studies include mantle degassing at oceanic ridges and at plume related volcanoes, de-carbonation of subducted carbonate and their subsequent release of the $CO_2$ through arc volcanoes and metamorphic belts, in form of geothermal springs. Widespread observations of metamorphic/de-carbonation reactions and their fluxes through geothermal springs in the active orogenic regions provide significance for the $CO_2$ cycle (Barnes et al., 1978, 1984; Ferry, 1991). The active orogen of Himalaya, across a broad region of the south Asia, has also witnessed metamorphism and outgassing of volatiles since its inception. Rapid uplift and exhumation in such mountain belts have been shown to create steep geothermal gradients that can drive hydrothermal circulations (Koons & Craw, 1991; Jenkin et al., 1994; Koons et al., 1998). As a result, the deep-sourced $CO_2$ from decarbonation and oxidation of organic matter mixes with shallow meteoric waters before its degassing from solution near the earth's surface.

Previous studies, based on dissolved inorganic carbon in the geothermal springs from the Nepal Himalaya, have confirmed this process as a significant source of $CO_2$ in atmosphere. Himalayan region have suitable structural conditions and associated thermal gradient which have led to release of $CO_2$ during upward movement of geothermal fluids. Therefore, geothermal systems play a key role in mediating crustal $CO_2$ outgassing to the atmosphere. Realizing their importance, modern researches have been directed towards regional and global-scale $CO_2$ degassing from the deep crust in different part of the Earth (Kerrick & Caldeira, 1998; Evans et al., 2008; Perrier et al., 2008). These studies have shown that $CO_2$ release from both volcanic eruptions and non-eruptive systems affects global atmospheric composition. These non-eruptive systems are generally associated with the zones of geomagnetic anomaly, shallow earthquake, gravity anomalies and high heat flow (Rawat, 2012; Veeraswamy et al., 2010; Azeez & Harinarayana, 2007). Processes assumed to be common among these settings, include the migration of magmatic fluids from the deep to the surface. This results in significant degassing of $CO_2$ and associated changes in the chemical composition of shallow groundwater. Decarbonation and dehydration produce crustal fluids with variable $\delta^{13}C$ at different depths ($CaCO_3+SiO_2 \rightarrow CaSiO_3+CO_2\uparrow$) where high temperature silicate weathering consumes this $CO_2$ to produce alkalinity {$CaSiO_3+2CO_2\downarrow+3H_2O \rightarrow Ca^{+2}+2HCO_3^-+Si(OH)_4$}. This is observed near the surface. In this study, a similar scenario is observed with carbon isotopic composition ($\delta^{13}C_{DIC}$) which provides clear evidences of degassing of $CO_2$ from the northwest Himalaya.

This work presents $\delta^{13}C_{DIC}$ data on Indian Himalayan region for the first time, which is useful to provide insights into the conditions of $CO_2$ degassing along the major thrust zones. Carbon isotope $\delta^{13}C_{DIC}$ in the geothermal waters show a wide range of variation from -8.5 ‰ to +4.0 ‰. The enriched $\delta^{13}C_{DIC}$ compositions are indicative of a process of degassing of volatiles from these regions which has been illustrated with suitable model (Evans et al., 2008). This model depicts that when degassing takes place, carbon isotopes fractionate and the degassed $CO_2$ becomes lighter leaving the remnant water enriched in $\delta^{13}C$. These enriched $\delta^{13}C_{DIC}$ values have been found in several hot springs of the northwest Himalaya which shows about their deeper/magmatic origin. These results are similar and consistent to those in central Nepal Himalaya (Evans et al., 2008). One of the interesting results from this study is that the thermal spring having the highest enriched $\delta^{13}C$ (HS-5, Tapoban) has also the elevated surface temperatures. Therefore the $\delta^{13}C$ of thermal springs may be used as a proxy to depict their origin in terms of meteoric vs. magmatic source.

## 6.2 LITHOSPHERE STRUCTURE AND DEGASSING PROCESS: GEOPHYSICAL STUDIES

Earlier work on structural interpretations and present data on geochemistry and stable isotopes are helpful to understand the process in which the meteoric water enters up to different depths through faults, joints and gets heated before it upwells and releases $CO_2$ on the surface (Schematic model Figs. 6.3, 6.4, and 6.5). It is elaborated with the help of three schematic

models based on the magnetotelluric (MT) studies (Rawat, 2012; Veeraswamy et al., 2010; Azeez & Harinarayana, 2007) from the Garhwal, Himachal and Ladakh geothermal fields. Modeling of magnetotelluric (MT) data of ~150km long N-S oriented profile from Bilaspur-Rohtang pass (Veeraswamy et al., 2010) in Himachal region was found to be considering with several geothermal springs between the Jutogh (MCT) and Vaikrita (MCT). Fluid content in this area seem to have contributed to this conductive anomaly, which finds further support from the presence of geothermal activities in this zone. This fluid reacts with meteoric water at different depths before it upwells on the surface in the form of geothermal spring. Geophysical evidences suggest that the geothermal area of Himachal region is situated in active thrust zone, which have experienced of major Kangra earthquake (1905).

Geophysical investigations especially MT were conducted to infer about crustal electric structure of Puga geothermal field of Ladakh Himalaya (Gupta et al., 1976; Arora et al., 1983; Singh et al., 1983; Mishra et al., 1996). The one-dimensional inversion of the effective impedance data, the two-dimensional inversion of the transverse electric (TE) and transverse magnetic (TM) data (Harinarayana et al., 2006) has confirmed about the presence of a low resistive (5–25 Ω m) near surface layer confined within the 200–300 m thick zone which could sustain these geothermal springs. Harinarayana et al. (2006) has reported an anomalous conductive zone (resistivity < 10 Ωm) at the depth of ~2 km, which could be related to the source of geothermal activity in the Puga and Chumathang area of Ladakh Himalaya. Occurrence of highly

conductive anomalies zones in the part of upper crust of the Himalayan tectonic belt have been revealed from magnetotelluric studies.

## 6.3 EVOLUTION OF METAMORPHIC $CO_2$

The process of metamorphic decarbonation alone may not be invoked for higher $\delta^{13}C_{DIC}$ values observed in many of these springs and therefore, an additional mechanism is required for such enrichment. Towards this, the degassing of $CO_2$ from the thermal water near–surface environment may be a plausible mechanism which can significantly alter the $\delta^{13}C_{DIC}$ of the remnant fluids (Evans et al., 2008).

***Fig 6.1:*** *Field photograph of $CO_2$ rich springs in the Nubra valley (Ladakh) (HS-21). $T_{fluid}$=74˚C, $\delta^{13}C_{DIC}$=+2. HS-21 is surrounded by ($CaCO_3$) deposits.*

When a supersaturated deep fluid reaches the surface, it undergoes degassing and produces $CaCO_3$ in form of travertine (Fig. 6.1). In such systems, $HCO_3^-$ is the dominant form of dissolved $CO_2$ in the near neutral pH environment of the thermal springs where the carbon isotope fractionation factor between the $CO_2$ (g) and dissolved bicarbonate is positive below ~$125^0$C (Mook et al.,

1974). Therefore, at this temperature, an open system degassing would progressively increase the ratio of $\delta^{13}C_{DIC}$ of remaining fluid as the $^{13}C$ depleted $CO_2$ (g) is built up and removed from the system.

## 6.4 DEGASSING FLUX OF METAMORPHIC $CO_2$

Geothermal springs occur mainly along the three mega structural boundaries, which are seismically active. Worldwide, it is observed that $CO_2$ discharge is strongly associated to seismically active zones (Barnes et al., 1978). Pressure of high temperature fluids at depth may be responsible in triggering earthquake by reducing fault strength and controlling the nucleation and recurrence of earthquake rupture (Rice, 1992; Cox, 1995; Sibson, 1992, 2000).

Fast upliftment and exhumation in the Himalayan mountain belts has helped to create steep geothermal gradient that can drive hydrothermal circulation which may an essential component in the thermal budget of this active orogeny. High erosion and uplift of the Himalaya have brought hot rocks to near surface, where contact with water (meteoric origin) produces geothermal springs along the major faults. Thermal gradient in the Himalayan region is suggested to be $100^0$C/km (Chandrasekharam, 2000) having surface temperature of thermal fluids up to $95^0$C. Out gassing flux of $CO_2$ and other volatiles from the geothermal springs from the Nepal Himalayan region have been reported quantitatively (Evans et al. 2008) which is based on isotopic composition of water and volatiles. However, Chaidoni et al., (2000) has used major ions and showed that the large portion of the dissolved inorganic carbon (DIC) in the geothermal waters were derived from the deep source. In the present study the

geochemical (major ions) data of the geothermal springs has been used to estimate the degassing flux of $CO_2$ in the northwest Himalayan region.

## 6.5 RESULT AND DISCUSSION

The results of $\delta^{13}C_{DIC}$ compositions of geothermal springs of Garhwal, Himachal and Ladakh regions are presented in the Table 6.1along with their altitude covering a range of 1033 to 4410 m. The details of discharge, temperature, and other parameters are already given in the *chapter 2.*

***Table 6.1:*** *$\delta^{13}C_{DIC}$ and corresponding altitudes of the geothermal spring of Garhwal, Himachal, and Ladakh regions.*

| Sample no. | Sites name | $\delta^{13}C_{DIC}$ ‰ (VPDB) | Altitude (m, asl) |
|---|---|---|---|
| **HS-1** | Taptkund | 1 | 3089 |
| **HS-2** | *Khiroi* | -7.4 | 2973 |
| **HS-3** | *Bhapkund* | -5.6 | 2680 |
| **HS-4** | *Shaldhar* | 1.6 | 1953 |
| **HS-5** | *Tapoban* | 4.1 | 1890 |
| **HS-6** | *Birahi* | 0.3 | 1190 |
| **HS-7** | *Ganoi* | 3.4 | 1409 |
| **HS-8** | *Langsi* | -0.8 | 1225 |
| **HS-9** | *Helang* | 3.7 | 1210 |
| **HS-10** | *Gaurikund* | 0.8 | 1930 |
| **HS-11** | *Gangnani* | -1.2 | 1900 |
| **HS-12** | *Jhaya* | -8.5 | 1808 |
| **HS-13** | *Bukki* | -3.8 | 1730 |
| **HS-14** | *Thirang* | -1 | 1640 |
| **HS-15** | *Matli* | -5 | 1062 |
| **HS-16** | *Kotimanep* | -0.8 | 1429 |
| **HS-17** | *Suryakund* | 1.4 | 3070 |
| **HS-18** | *Jankichatti* | 2.2 | 2568 |
| **HS-19** | *Banas* | -1.2 | 2210 |
| **HS-20** | *Wozari* | -6.5 | 1630 |
| **HS-21** | *Changlung* | 1.7 | 3410 |
| **HS-22** | *Pulthang* | -1.1 | 3175 |
| **HS-23** | *Panamic* | 0.1 | 3225 |
| **HS-24** | *Gaik* | -6.1 | 3770 |
| **HS-25_1** | *Chumathang* | -2.5 | 4029 |
| **HS-25_2** | *Chumathang* | -3 | 4029 |
| **HS-26** | *Puga* | -3.5 | 4410 |
| **HS-27** | *Sumdo* | -2.4 | 3270 |

| Sample no. | Sites name | $\delta^{13}C_{DIC}$ ‰ (VPDB) | Altitude (m, asl) |
|---|---|---|---|
| **HS-28** | *Thopan* | -8.4 | 2180 |
| **HS-29** | *Tapri* | -5.9 | 1702 |
| **HS-29B** | *Tapri_Handpump* | -8.2 | 1762 |
| **HS-30** | *Naptha* | -4 | 1793 |
| **HS-31** | *Jeori* | -2.8 | 1793 |
| **HS-32** | *Jhakri* | -7.9 | 1130 |
| **HS-33/34** | *Jharar* | -8.3 | 1033 |
| **HS-35** | *Bashist* | -4.2 | 2110 |
| **HS-36** | *Khiral Bihal* | -6.2 | 1750 |
| **HS-37** | *Kalath* | -6.5 | 1730 |
| **HS-38** | *Ramshila Kullu* | -1.2 | 1228 |
| **HS-39** | *Manikaran* | -2.6 | 1662 |
| **HS-40** | *Kasol* | *-8.4* | *1600* |

## 6.6 STABLE CARBON ISOTOPES ($\delta^{13}C_{DIC}$) OF THE SPRINGS

The $\delta^{13}C_{DIC}$ in the geothermal springs of Garhwal, Himachal, and Ladakh regions show a wide range from-8.4 to +4.1 ‰ (Table 6.1, Fig 6.2). Comparison of present work with earlier studies suggests that the spring chemistry as well as isotopic composition of these geothermal springs have not changed much (Giggenbach et al., 1983; Cinti et al., 2009; Jangi & Abrar, 1977 unpublished GSI Report) in decades. Relatively higher $\delta^{13}C_{DIC}$ values are encountered in the springs from northwest Himalaya.

Further, these are similar to springs reported from central Nepal, Himalaya (Evans et al., 2008) and from Yellowstone waters and similar travertines of Utah (Friedman, et al., 1970), Poland (Shipton et al., 2004) and Italy (Dulinski et al., 1995; Pentecost et al., 1995; Guo et al., 1996). Regarding the geothermal springs of the northwest Himalaya, there is no significant source of $CO_2$ for the fluids that have sufficiently enriched $\delta^{13}C_{DIC}$ to account for the higher $\delta^{13}C_{DIC}$ values in them. However, the Lesser Himalaya (LH) contains

few pockets of carbonates with $\delta^{13}C_{carb}$ ranging from -6.23 to -0.7‰ (Fig.6.2). Further, the pelites containing graphite and organic carbon have the $\delta^{13}C_{carb}$ varying from -30 to -19‰ (Evans et al., 2008) in the lesser Himalayan region. Therefore, it is inferred that the source of enriched $\delta^{13}C$ in the thermal water are induced by a sufficient amount of metamorphic fluids during the circulation of meteoric water in these thermal system. Mixing of $CO_2$ rich metamorphic fluid with meteoric water may produce more $CO_2$ concentrations with enriched $\delta^{13}C_{DIC}$ composition while keeping the dominant signature of surface waters values for δD and $\delta^{18}O$.

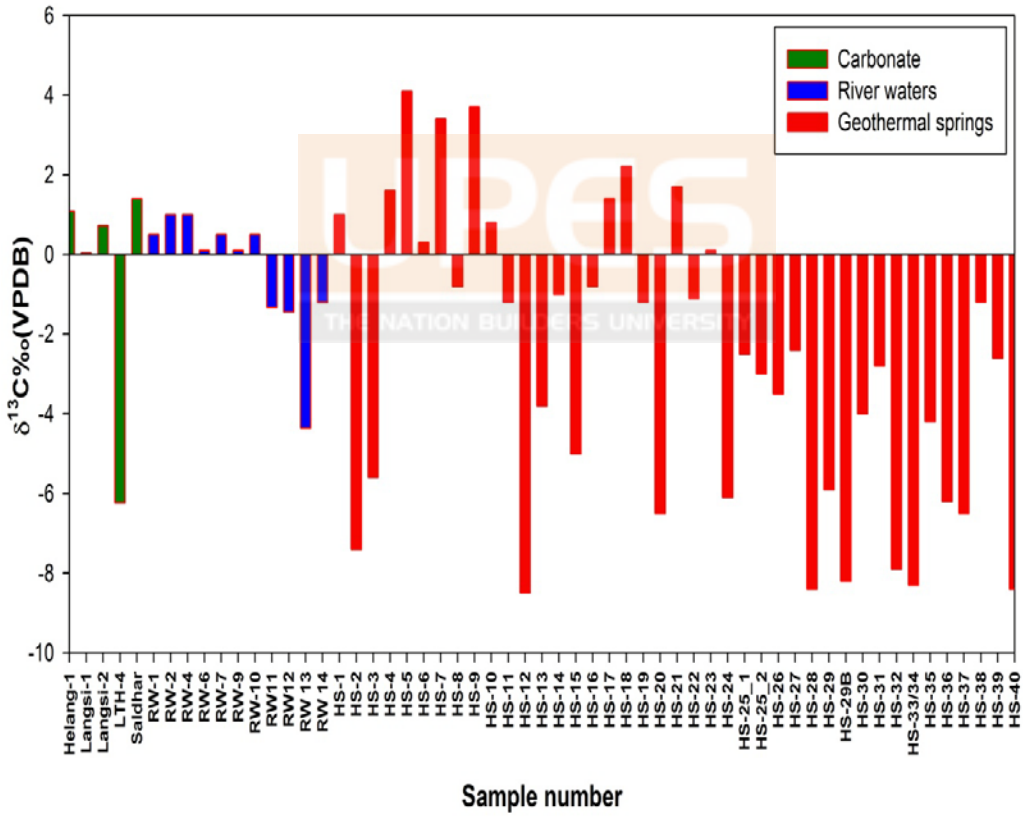


***Fig. 6.2:*** *Scatter plots of $\delta^{13}C_{DIC}$ compositions of geothermal springs, river waters, and carbonates of the northwest Himalaya.*

## 6.7 ENRICHMENT MECHANISM OF $\delta^{13}C_{DIC}$ AND ITS VARIABILITY

Geochemical composition (chloride, bicarbonate, sulphate, and other solutes) of the studied geothermal springs show the affinity towards $HCO_3$: Cl types. Geothermal fluids with a range of $\delta^{13}C_{DIC}$ (-8 to +4) values could be produced by de-carbonation, pyrolysis, and dehydration of the carbonate lithology of lesser Himalaya. The chemistry of the gas phase of geothermal samples show that it is mainly consist of $CO_2$ (>90%) with traces of $N_2$, $O_2$, $CH_4$ and Ar, etc (Giggenbach et al., 1983; Cinti et al., 2009) in some of them. This contains lighter $\delta^{13}C$ of the $CO_2$ gas phase samples which is ~-4‰ with a range of -20 to -7.5‰. The highly enriched values of $\delta^{13}C_{DIC}$ are indicative of metamorphic/ decarbonation reaction for contributing the $CO_2$ to these fluids.



### 6.7.1 MODEL OF METAMORPHIC $CO_2$ DEGASSING

In this work, an attempt has been made for deriving the schematic models of process of metamorphic $CO_2$ through these springs using stable isotopic ($\delta D$, $\delta^{18}O$, $\delta^{13}C_{DIC}$) systems and major & trace elements geochemistry. In addition, electric conductivity imaging (MT data) of subsurface layers along the major thrust zones is also used in combination of degassing model of $CO_2$ (Becker et al., 2008).

#### 6.7.1.1 GARHWAL REGION

Based on twenty active geothermal springs from the Garhwal region, a representative metamorphic $CO_2$ degassing model (Fig. 6.3) is proposed

which utilizes the isotopic and major ions composition. Stable isotope compositions of oxygen and hydrogen of geothermal springs reveal that the origin of waters in thermal springs is mainly derived from meteoric source.

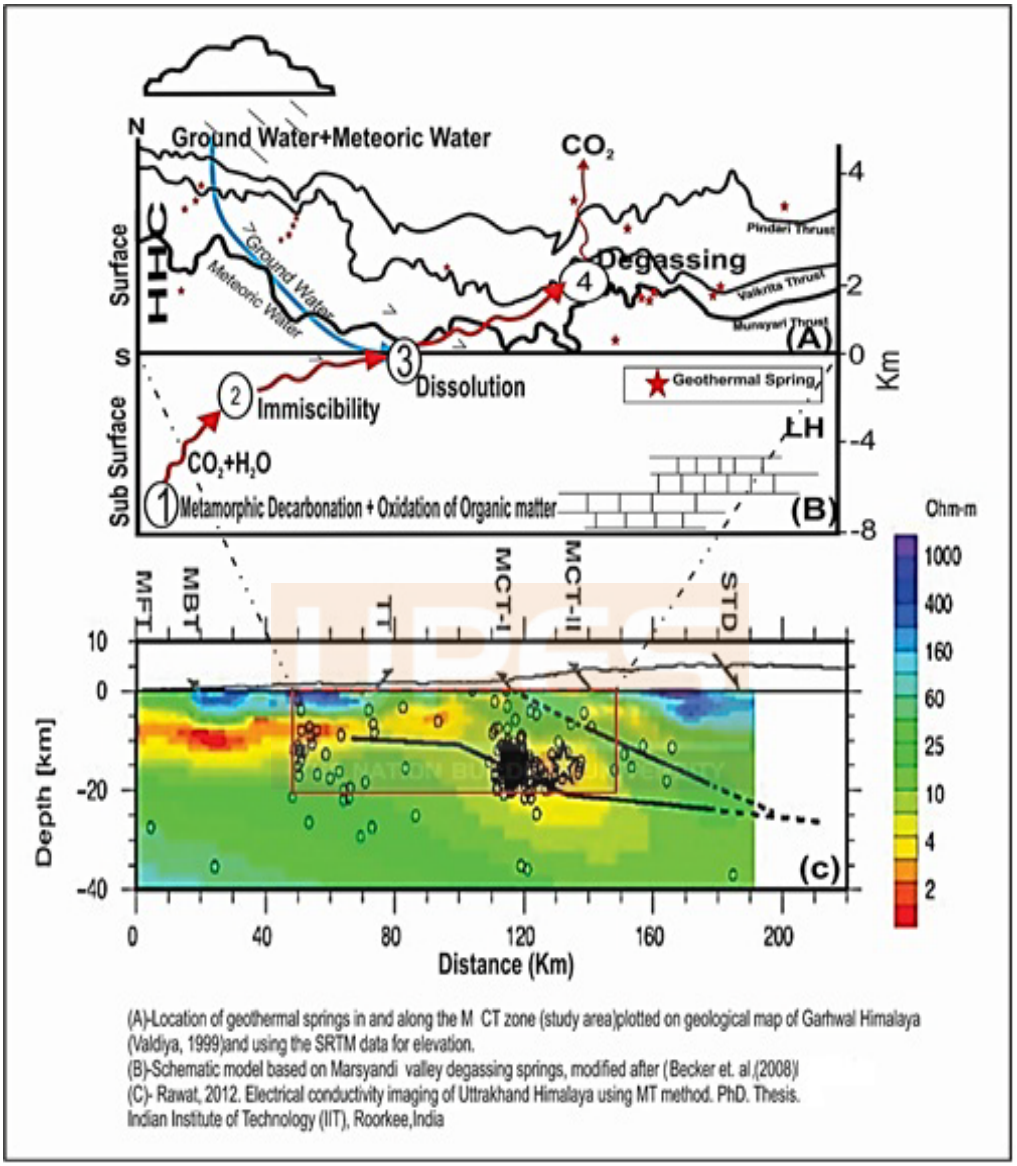


***Fig. 6.3:*** *Schematic model for the process of metamorphic $CO_2$ degassing of geothermal springs of Garhwal region.*

However, $\delta^{13}C_{DIC}$ indicates some input from deeper fluids. This can be explained by invoking a case where dominant meteoric water mixes with magmatic or mantle component with volatiles. Highly conductive zone is also

found to be present in the subsurface of Higher Himalayan crystalline (Fig 6.3, section C) which is inferred from electrical data. Despite the meteoric signature ($\delta^{18}O$ & $\delta D$ line has a slope of 7±0.52 and intercept 0.81±4.9, equation 5.1, table 5.3 of chapter 5) stable isotope of carbon ($\delta^{13}C_{DIC}$) ratio ranges from -8‰ to +4‰ in these geothermal springs. This indicates towards the process of metamorphic decarbonation or oxidation of organic matter beneath the Higher Himalayan crystalline.

### 6.7.1.2 HIMACHAL REGION

Based on fifteen active geothermal springs which are located along the MCT zone of different river valleys namely Sutlej, Parbati, and Beas of the Himachal region, a representative metamorphic $CO_2$ degassing model is proposed. This includes the Manikaran hot springs (HS-39) with highest surface temperature of 95˚C. The regression line drawn for these $\delta D$ and $\delta^{18}O$ in these springs (slope, 8.89±0.99 and intercept 18.2±11.5), shows their similarity with river and surface waters. However, $\delta^{13}C_{DIC}$ reveals about the metamorphic reactions beneath the active geothermal springs (Fig. 6.4, section-C).

To address the subsurface condition of geothermal field of the Himachal region, we have used the deep resistivity model obtained from the joint inversion of TM, impendence and electrical structure across the Himachal region (Veeraswamy et al., 2010). The proposed model for degassing of metamorphic $CO_2$ through thermal springs of Himachal region also suggests significant degassing and presence of subsurface zone of high conductivity.

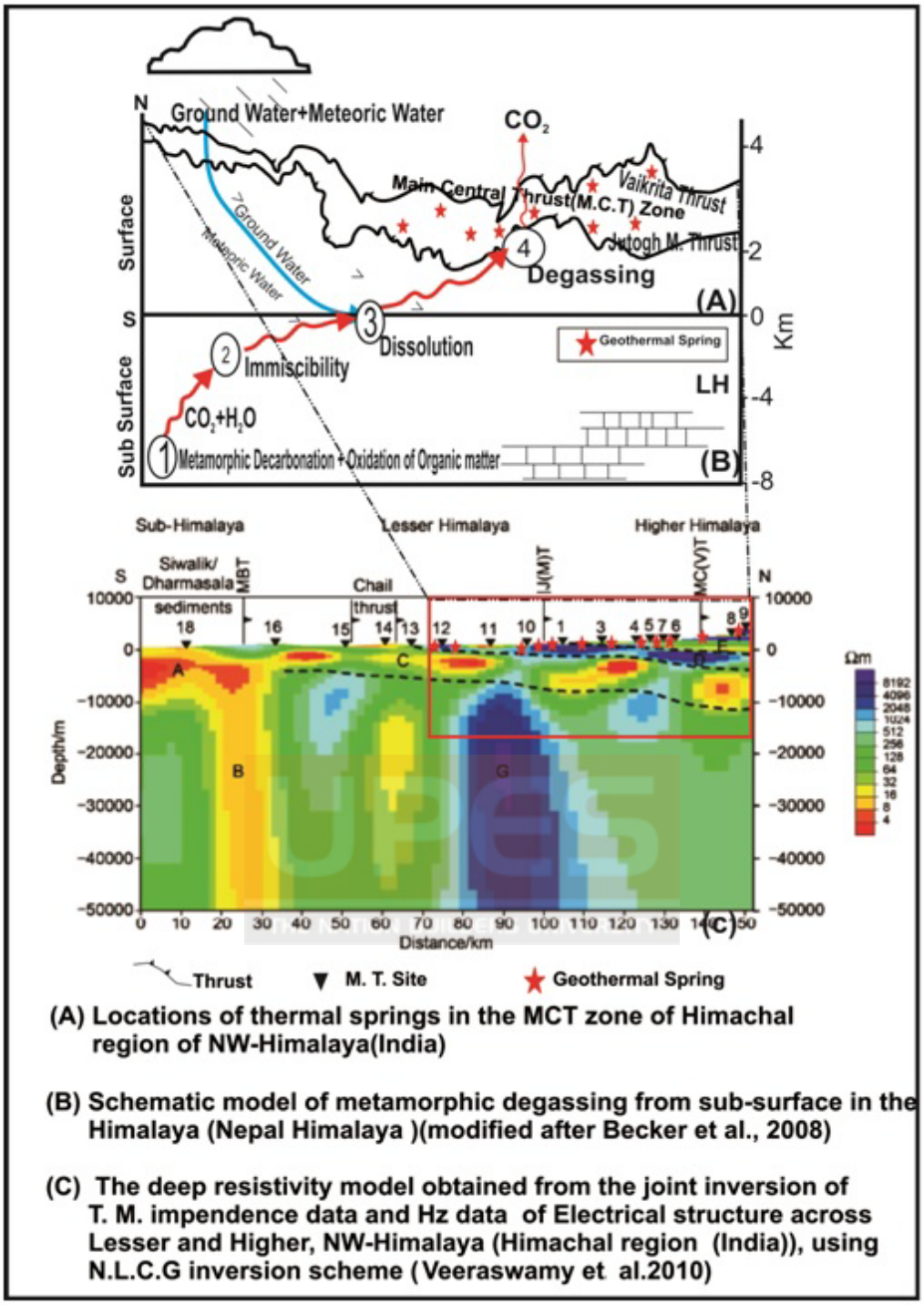


**(A) Locations of thermal springs in the MCT zone of Himachal region of NW-Himalaya(India)**

**(B) Schematic model of metamorphic degassing from sub-surface in the Himalaya (Nepal Himalaya )(modified after Becker et al., 2008)**

**(C) The deep resistivity model obtained from the joint inversion of T. M. impendence data and Hz data of Electrical structure across Lesser and Higher, NW-Himalaya (Himachal region (India)), using N.L.C.G inversion scheme (Veeraswamy et al.2010)**

***Fig. 6.4:*** *Schematic model for the process of $CO_2$ degassing of the geothermal area of Himachal region.*

### 6.7.1.3 LADAKH REGION

There are six active geothermal springs situated in the Ladakh region namely Gaik, Chumathang, and Puga in the Indus valley and Panamik, Changlung & Pulthang in the Nubra valley. Out of which, the Puga and Chumathang geothermal springs are situated along the junction of the Indian and Tibetan plates of Indus Tsangpo Suture Zone. Based on the stable isotopes, major ions and geophysical data of these springs, a representative $CO_2$ degassing model is proposed for the Ladakh region. This shows that both have great potential for the degassing of metamorphic $CO_2$ which is also evident from the fact that these areas exhibit vigorous geothermal activities in the form of hot springs, mud pools, sulphur encrustations and borax deposits. Geothermal springs from Pulthang, Changlung and Panamik have also been found emanating high temperature fluids on the surface. Chemical composition of the springs in this huge thermal activities found along the ITSZ [HS-25 (Chumathang), HS-26 (Puga), and HS-27] reveals that their water characteristics are of volcanic type. In addition, sulphur condensates present at these sites are the independent evidence which represent an old fumarolic activity along hidden fault.

Stable isotope ($\delta D$ and $\delta^{18}O$) correlations of these geothermal springs (Fig 6.5, section-C) show the recharge source of meteoric origin (with slope 8.89±0.99 and intercept 18.2±11.5) falling close to the composition of river and surface water of the region (Pande et al., 2000), whereas enriched $\delta^{13}C_{DIC}$ in these springs suggests about the input of magmatic fluids. In order to correlate with enriched $\delta^{13}C_{DIC}$ with the two dimensional resistivity model for Puga

geothermal springs, field derived inversions of magnetotelluric data (MT) were used (Azeez & Harinarayana, 2007).

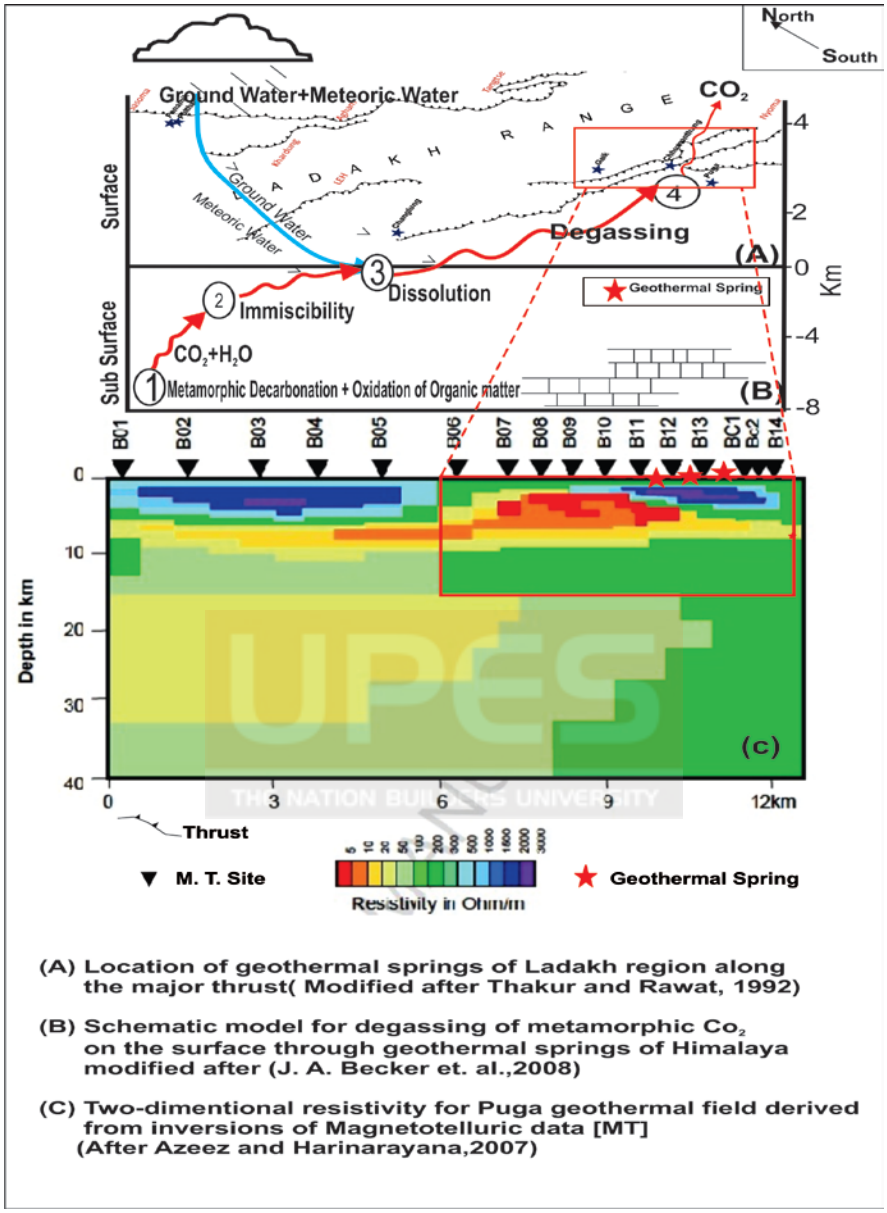


***Fig. 6.5:*** *Schematic model for the process of $CO_2$ degassing of the geothermal area of Ladakh region.*

Further, Harinarayana et al., (2006) has determined an anomalous conductive zone (resistivity less than 10 Ω m) at a depth of ~2 km, which may be related to the source of geothermal activity in the Puga and Chumathang areas of

Ladakh Himalaya. This reveals the occurrences of highly conductive anomaly zones in the upper part of crust in the Ladakh Himalayan region (Fig 6.5, section C) and could be suggestive of magmatic component in these thermal springs.

## 6.8 ESTIMATION OF METAMORPHIC $CO_2$ FLUX

### 6.8.1 GARHWAL REGION

Following the method of Chiodini et al., (2004), the $CO_2$ flux was calculated. It is based on major ions compositions of thermal springs which compare well with the values estimated from isotopic studies (Evans et al., 2008; Becker et al., 2008) of thermal springs and volatiles. Degassing of $CO_2$ and other volatiles from the geothermal springs in the MCT zone of the Nepal Himalayan region have been reported (Derry et al., 2009) in which $CO_2$ emanating flux generated through metamorphism of carbonates have been assessed. Metamorphic $CO_2$ flux is computed in this study with the help of water chemistry, given in table 6.2. It is calculated by deducting the $CO_2$ contribution by near surface water-rock interaction, such as the dissolution of carbonate mineral from the total dissolved inorganic carbon in the solution (Chiodini et al., 2004). Major ion chemistry and $HCO_3^-$ data are taken from the Tables 4.1 and 4.2, *Chapter 4* for the calculation as follows:

$$C_{ex} = DIC-(Ca^{2+}+Mg^{2+})-SO_4^{2-} \text{.....Eqn (6.1)}$$

Towards this, all the concentrations are taken in the moles/liter and $C_{ex}$ (excess Carbon) represents the deep seated carbon source and alkalinity is

assumed to be nearly equal to the DIC (Newell et al., 2008). For this study, direct flux for individual spring was calculated by using total $HCO^-_3$ concentration, discharge measured on site and area computed using geological map of the study area. As the biological sources may also add some carbon in the solution, these should be suitably accounted for. However highly enriched values of $\delta^{13}C_{DIC}$ (-8 to +4‰ $_{VPDB}$) measured in these geothermal waters show that the impact of biological activity is negligible (Newell et al., 2008). Abundances of magnesium and calcium have been taken to account for computing the moles of carbon from the dissolution of carbonate species. In this regard, the dissolution of gypsum is another process which may add calcium without adding carbon to the system and therefore it must be eliminated from total carbon by subtracting the concentration of $SO_4^{2-}$. Towards flux estimation, it is assumed that (i) Lesser Himalayan meta-sedimentaries are the main source of carbon and (ii) the excess carbon is supposed to leave the springs as $CO_2$. The flux from each spring is calculated by multiplying $C_{EX}$ by spring discharge (measured in the field and given in table 2.6, *Chapter 2*).

These estimates show that *geothermal springs of the Garhwal Himalaya have the potential to degas ~7.2x10$^6$ moles of $CO_2$ per year to the atmosphere.* In this study, two geothermal springs (HS-19 & HS-20) have not been included for the flux calculation due to lack of discharge data. Further, one of the springs (Jankichatti, HS-18) shows negative flux which may indicate that it is insignificant in contributing $CO_2$ flux, or it could arise due to uncertainty in the estimation of the areal coverage of springs which is quite dispersed. The

$CO_2$ flux calculated based on $\delta^{13}C$ (Evans et al., 2008) for the Nepal Himalaya gives a robust estimate as it also considers the gas sampling in its calculations. Such calculations were not done in this study as it has no samples of gas/volatiles emanating from springs. The estimated flux from this study is comparable to that derived for the metamorphism release of $CO_2$ during the Cenozoic uplift of the Himalaya (~$10^{11}$mole $a^{-1}$), Kerrick & Calderia (1999) and sub aerial volcanism ($10^{12}$ mol $a^{-1}$; Williams et al., 1992).

***Table 6.2:****Metamorphic $CO_2$ flux for Garhwal region.*

| **Sample ID** | **Sample Name** | **$C_{ex}$ [a](mole/L)** | **Discharge (L/min)** | **Area (m2)** | **$CO_2$ (mole/a)** | **$CO_2$ (mole/$m^2$*a)** |
|---|---|---|---|---|---|---|
| HS-1 | *Taptkund* | 0.02 | 400 | 25 | 4.15E+06 | 1.66E+05 |
| HS-2 | *Khiroi* | 0.002 | 200 | 16 | 2.12E+05 | 1.33E+04 |
| HS-3 | *Bhapkund* | 0.003 | 100 | 16 | 1.53E+05 | 9.58E+03 |
| HS-4 | *Shaldhar* | 0.001 | 300 | 100 | 1.75E+05 | 1.75E+03 |
| HS-5 | *Tapoban* | 0.002 | 50 | 25 | 5.30E+04 | 2.12E+03 |
| HS-6 | *Birahi* | 0.014 | 100 | 400 | 7.45E+05 | 1.86E+03 |
| HS-7 | *Ganoi* | 0.005 | 20 | 4 | 4.78E+04 | 1.19E+04 |
| HS-8 | *Langsi* | 0.006 | 100 | 9 | 2.91E+05 | 3.24E+04 |
| HS-9 | *Helang* | 0.003 | 50 | 4 | 7.68E+04 | 1.92E+04 |
| HS-10 | *Gaurikund* | 0.001 | 200 | 16 | 1.23E+05 | 7.69E+03 |
| HS-11 | *Gangnani* | 0.007 | 100 | 2.25 | 3.92E+05 | 1.74E+05 |
| HS-12 | *Jhaya* | 0.003 | 30 | 1 | 4.38E+04 | 4.38E+04 |
| HS-13 | *Bukki* | 0.013 | 25 | 9 | 1.69E+05 | 1.88E+04 |
| HS-14 | *Thirang* | 0.012 | 60 | 9 | 3.65E+05 | 4.06E+04 |
| HS-15 | *Matli* | 0.002 | 30 | 4 | 3.40E+04 | 8.50E+03 |
| HS-16 | *Kotimanep* | 0.003 | 80 | 4 | 1.14E+05 | 2.84E+04 |
| HS-17 | *Suryakund* | 0.004 | 150 | 25 | 2.76E+05 | 1.11E+04 |
| HS-18 | *Jankichatti* | -0.007 | 70 | 4 | -2.00E+05 | -6.18E+04 |
| HS-19 | *Banas* | 0.002 | nd | 0 | nd | nd |
| HS-20 | *Wozari* | 0.013 | nd | 0 | nd | nd |
| ***Total Flux calculate (Based on eighteen samples)*** | | | **$7.2x10^6$** | | | **$5.3x10^5/m^2$/ year** |

The area of geothermal springs of the Garhwal Himalaya is considered ~10,000 Sq Km (~180 km x 55 km) for this calculation. In addition, this study

assumes that $CO_2$ is degassed to the atmosphere only through the geothermal springs in the Himalaya. In this regard non-volcano regions of Italy have also been found globally significant with $CO_2$ flux of ~$10^{11}$mole $year^{-1}$.

### 6.8.2 HIMACHAL AND LADAKH REGION

Geothermal fields of Himachal Himalaya are spread over an area of ~16000 Sq km (100 km x 160 km) which has thirteen active geothermal springs. Whereas, the Ladakh region contains two geothermal fields namely Puga and Chumathang in a relatively restricted region of ~1200 Sq km (24 km x 50 km). It has three major springs in Puga area and nearly 100 springs outlets in Chumathang dispersed over an area of ~1Sq km. The Geothermal fields of Nubra valley are also distributed over ~450 Sq. km. (15 km x 30 km) area and have three major geothermal springs (Fig 6.6). The flux from each spring of Himachal and Ladakh region are calculated which are presented in table 6.3. *Combining all together, these regions have a potential to degas~2.0x$10^8$ moles of $CO_2$ to the atmosphere.* Out of this ~2.9x$10^6$ moles of $CO_2$ per year may be accounted for Nubra valley alone which include three geothermal springs namely Changlung (HS-21) Pulthang (HS-22) and Panamik (HS-23). Similarly, a flux of (1.8x$10^8$ moles $CO_2$ per year) has been estimated for the Puga and Chumathang, Gaik geothermal fields. A relatively higher flux of 5.3x$10^6$ mole $CO_2$ per year is estimated from the Himachal geothermal field consisting fourteen springs (Table 6.4).

***Table 6.3:****Metamorphic $CO_2$ flux of Ladakh and Himachal regions.*

| Sample no. | Sites name | Cex[a] (Mole/l) | Discharge (L/min) | Area (Sq m) | $CO_2$ (Mole/a) | $CO_2$ (mol/Sq m*a) |
|---|---|---|---|---|---|---|
| **HS-21** | *Changlung* | 0.0109 | 180 | 9 | 1.03E+06 | 1.15E+05 |
| **HS-22** | *Pulthang* | 0.0045 | 160 | 9 | 3.76E+05 | 4.17E+04 |
| **HS-23** | *Panamic* | 0.0048 | 600 | 16 | 1.50E+06 | 9.37E+04 |
| **HS-24** | *Gaik* | 0.0037 | 200 | 4 | 3.88E+05 | 9.69E+04 |
| **HS-25_1** | *Chumatang* | 0.014 | 100 | 225 | 7.34E+05 | 3.26E+03 |
| **HS-25_2** | *Chumatang* | 0.0135 | 100 | 225 | 7.11E+05 | 3.16E+03 |
| **HS-26** | *Puga* | 0.0197 | 18000 | 1000000 | 1.87E+08 | 4.67E+01 |
| **HS-27** | *Sumdo* | 0.0153 | 80 | 9 | 6.43E+05 | 7.15E+04 |
| **HS-28** | *Thopan* | 0.0032 | 50 | 4 | 8.41E+04 | 2.10E+04 |
| **HS-29** | *Tapri* | 0.0015 | 40 | 4 | 3.18E+04 | 7.96E+03 |
| **HS-29B** | *Tapri* | 0.0027 | 100 | 1 | 1.43E+05 | 1.43E+05 |
| **HS-30** | *Naptha* | 0.005 | 200 | 9 | 5.27E+05 | 5.86E+04 |
| **HS-31** | *Jeori* | 0.0101 | 60 | 4 | 3.18E+05 | 7.95E+04 |
| **HS-32** | *Jhakri* | 0.0109 | 100 | 25 | 5.61E+04 | 2.24E+03 |
| **HS-33/34** | *Jharar* | 0.0045 | 50 | 9 | 6.04E+04 | 6.71E+03 |
| **HS-35** | *Bashist* | 0.0048 | 100 | 25 | 2.41E+05 | 9.65E+03 |
| **HS-36** | *Khiral Bihal* | 0.0037 | 50 | 4 | 1.81E+05 | 4.53E+04 |
| **HS-37** | *Kalath* | 0.0109 | 350 | 4 | 1.56E+06 | 3.91E+05 |
| **HS-38** | *Ramshila Kullu* | 0.0045 | 100 | 1 | 9.16E+05 | 9.16E+05 |
| **HS-39** | *Manikaran* | 0.0048 | 300 | 100 | 4.10E+05 | 4.10E+03 |
| **HS-40** | *Kasol* | 0.0037 | 100 | 9 | 1.20E+05 | 1.34E+04 |
| ***Total flux (Based on twenty geothermal samples)*** | | | | | **$2x10^8$** | **$2.12x10^6$** |

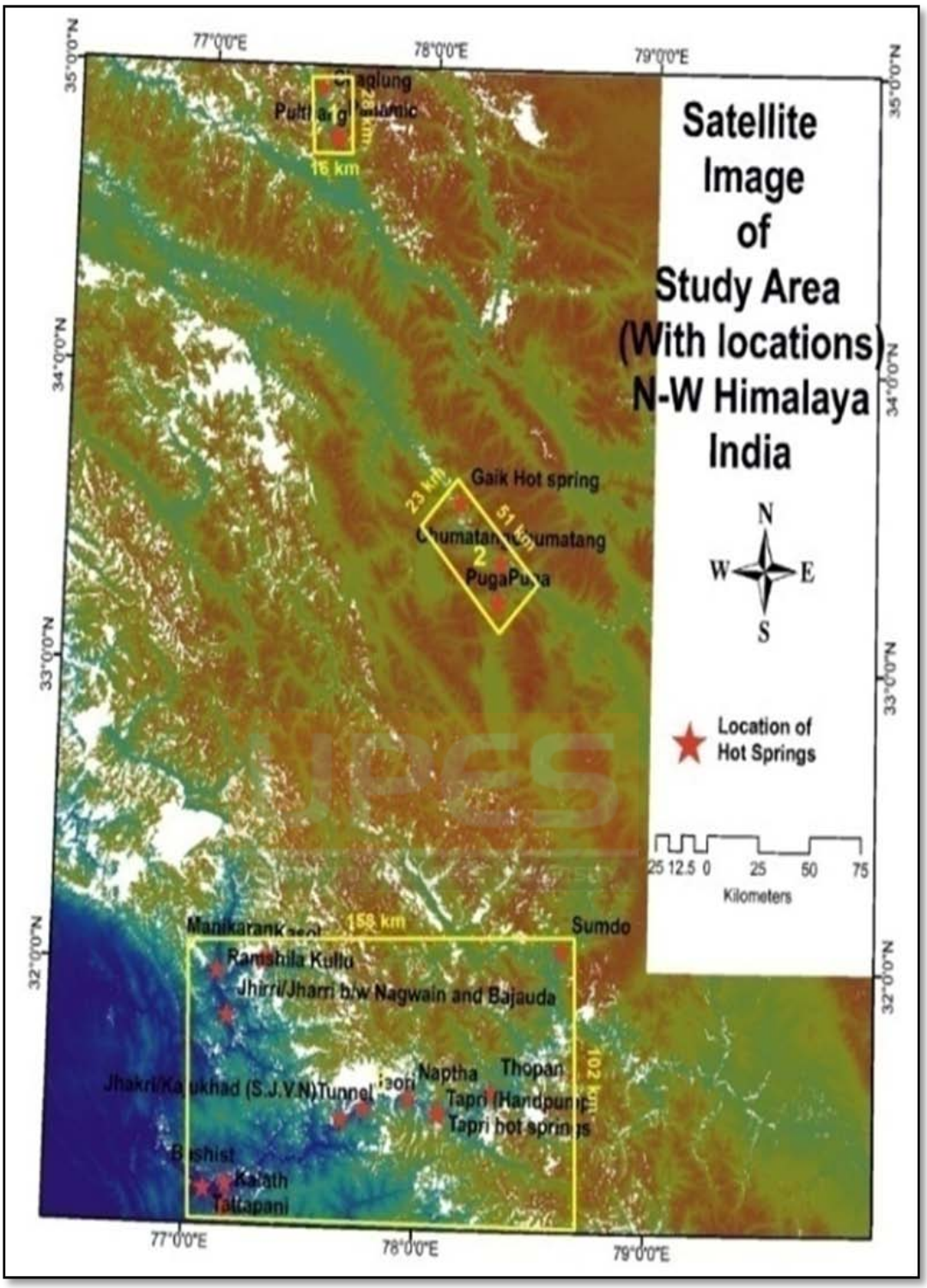


***Figure: 6.6*** *SRTM image of the study area showing the covered area of geothermal springs of Himachal and Ladakh regions.*

$CO_2$ degassing fluxes were estimated based on the studies of forty geothermal springs samples which are also presented in table 6.4 covering the wide region of Himalaya results show that the overall/average calculated $CO_2$ flux from different geothermal fields of northwest Himalaya is ~$2x10^8$moles/ year.

***Table 6.4:*** *Overall metamorphic $CO_2$ fluxes of northwest Himalaya and,* other studies in regions of Nepal Himalaya and Tibet.

| Sites Name. | Width (Km) | Length (Km) | Area ($Km^2$) | No of Springs | $CO_2$ degassing (Mole/a) | References |
|---|---|---|---|---|---|---|
| **Himachal region** | 158 | 102 | 16116 | 14 | $5.3x10^6$ | Present study |
| **Puga valley** | 23 | 51 | 1173 | 3 | $1.89x10^8$ | |
| **Nubra valley** | 16 | 28 | 448 | 3 | $2.9x10^6$ | |
| **Garhwal region** | 178 | 56 | 9968 | 20 | $7.17x10^6$ | |
| **Southern plateau(Tibet)** | 135 | 70 | 9450 | 10 | $1.7x10^6$ | Newell et al., 2008 |
| **Marsyandi valley (Nepal)** | | | 4800 | 28 | $5.4x10^9$ | Becker et al., 2008 |
| **Narayani river valley (Nepal)** | | | 32000 | - | $1.3x10^{10}$ | Evans et. al., 2008 |

In a similar study from the southern Tibet plateau, Newell et al., (2008) has estimated an annual $CO_2$ flux of ~$1.7x10^6$ moles per year by direct measurements of total DIC based on ten geothermal springs spread over~9500 Sq. km of Area. Therefore, it appears that *$CO_2$ flux from northwest Himalaya is higher by two orders of magnitude as compared to Tibetan plateau.* Becker et al., (2008) has reported an annual $CO_2$ flux ~$5.4x10^9$ moles/year. This was based on chloride mass balance distributed over an area of ~4800 Sq km in the Marsyandi valley of Nepal Himalaya. This shows that, *$CO_2$ degassing flux*

*from Nepal Himalaya is ~25 times higher than the combined effect of NW Himalaya.* In a separate study, based on $\delta^{13}C_{DIC}$ in thermal springs of Narayani river basin (Nepal), the total metamorphic $CO_2$ flux was reported to be $1.3x10^{10}$moles/year over a catchment of ~ 32000 Sq km (Evans et al., 2008).

Including all these above studies covering northwest Himalaya, Nepal Himalaya and Tibetan region, a combined estimate of ~$2x10^{10}$ moles/year could be assigned as degassing flux for $CO_2$.This indicates that the Himalayan orogen may be one of the major contributors of $CO_2$ in to the atmosphere.

## 6.9 CONCLUSIONS

The thermal springs of Garhwal, Himachal and Ladakh regions, northwest Himalaya have been extensively sampled and analyzed for their major ions and carbon stable isotope compositions. These measurements have led to the following observations and conclusions:

1. Degassing of metamorphic $CO_2$ from Himalayan region is acting as one of the important donors to the global carbon budget in the atmosphere.

2. Isotopic compositions of dissolved inorganic carbon ($\delta^{13}C_{DIC}$) in the thermal spring waters of Garhwal, Himachal, and Ladakh regions show a wide range of variation from -8.4 to +4.1‰. The $\delta^{13}C_{DIC}$ values of geothermal springs are among the highest reported from the thermal springs from the Northwest Himalaya., These values are similar to those reported from Central Nepal, Himalaya,

3. The metamorphic $CO_2$ flux from forty geothermal springs from northwest Himalaya is estimated to be ~$2.x10^8$ mole/year.

4. $CO_2$ flux from northwest Himalaya is higher by two orders (~25 times) of magnitude as compared to Tibetan plateau.

5. Combining all studies in Himalayan region (NW Himalaya, Nepal Himalaya and Southern Tibet region) together, a total $CO_2$ degassing flux of ~ $2x10^{10}$ moles/year could be assigned. This suggests that Himalayan region acts as one of the major contributors of $CO_2$ in to the atmosphere.

6. However, for a better estimate gas sampling of these spring are highly needed.

# CHAPTER 7

# HYDRO-GEOCHEMICALTHERMOMETRY

# CHAPTER 7:

# HYDRO-GEOCHEMICAL THERMOMETRY

## 7.1 INTRODUCTION

Earth has evolved to its present habitable state from a gaseous object, formed in a hot solar nebula. Since then, the internal energy of the Earth has continuously been coming out inform of heat and the surface manifestation of this energy is visible in the form of geothermal springs. These springs involve the dissolution and precipitation of different substances and their solution characteristics depends upon temperature. Therefore, it is important to understand the temperature induced process in these springs in order to infer about the characteristics of the thermal reservoirs. Geothermometry is a term useful for the determination of equilibrium temperature of natural system including rock, mineral, and liquid phases. In this regard, a geothermometer is an essential proxy to determine the formation temperature of the rock or the equilibrium temperature of a flowing aqueous solution of hydrothermal regime. Therefore geothermometers make the important tools of fluid geochemistry and are widely was used in geothermal energy explorations. In this context, data employed for geothermometers are interpreted carefully under certain assumptions. Thermal fluids are the out pouring from the deep reservoir characterised with water-rock interactions, which mainly depends on the temperature and it influences the chemical compositions.

Geothermal fields of the northwest Himalaya have the potential to act as an abundant resource of energy which has resulted through internal heat of the Earth, accumulated over a longer period of time. It is relatively clean and renewable in nature and hence becoming a preferred choice for an alternative energy resource worldwide. It has a potential to generate 10,600 MW of power in the country like India that can be exploited using latest technologies. However, the potential of geothermal energy is yet to be utilised in India. Studies on the geothermal springs have been limited up to the chemical composition of springs distributed in different part of the country and therefore, it needs to be expanded with other proxies. This work is an attempt to study thermal systems in detail to derive useful information on the reservoir temperature towards their possible use in energy exploration. Geothermometers depend basically on dissolved constituents in the thermal fluid whose concentrations are controlled by the temperature of the fluids. The constituents may be solutes, gases, or isotopes. Towards this, we have measured the major ions, silica, and some of the trace element which have been used to infer about the reservoir temperatures. In addition, stable isotopes have also been measured to characterise these systems and are discussed in chapter 4 and 5, in earlier sections.



## 7.2 GEOCHEMICAL THERMOMETRY

Geochemical thermometers are the experimental formulae which can be utilized to calculate the reservoir temperature. These are based on chemical equilibrium that exists between the rock- water interactions at the different

depths with varying reservoir temperatures. Such thermal estimates are possible using the abundances of its major constituents dissolved in water such as silica (Pasvanoglu et al., 2013; Fournier, 1977, 1979; Fournier & Truesdella, 1973; Arnorsson, 1983; Giggenbach, 1988; Kharaka & Mariner, 1989; Chandrajith et al., 2013). These studies have successfully demonstrated the use of dissolved silica-quartz/chalcedony to estimate the reservoir temperatures in different geothermal terrains. Some of these estimates have certain limitation in which they are affected by chemical processes such as evaporation and mixing. However, dissolved silica based geothermometers consist chalcedony and quartz which are found useful under steam loss and without steam loss conditions (Fournier-1981). This study makes the use of silica concentration to estimate geothermal reservoir temperature in the northwest Himalaya. Generally geothermometers have been categorised in to three groups which include (i) Solute geothermometers (ii) Gas geothermometers and (iii) Isotope geothermometers. Out of these, the first two are known as chemical geothermometers. Several thermometers are in use to estimate the reservoir temperatures of thermal springs using the analyses of its aqueous phases in near surface environments. These include isotope geothermometers based on temperature dependent fractionation and chemical composition (Ellis & Mahon, 1977). The cation based geothermometers have also been used in geothermal springs (Fournier &Truesdell. 1973; Fournier, 1977; Fournier, 1981; Arnorsson, 1983). This study makes use of silica to estimate the reservoir temperature in Himalayan geothermal springs.

## 7.3 DISSOLVED SILICA ($SiO_2$) GEOTHERMOMETRY

Silica geothermometry have become an essential tool for several types of geothermometer models with different characteristics, limitations and uses. In a true sense, silica geothermometers are based upon their temperature dependent water solubility of various polymorphs of silica. It was established by Bodvarsson (1960), who reported an empirical relationship describing silica concentration as a function of surface temperature form Iceland geothermal field. Earlier studies (Fournier & Rowe 1966; Kennedy, 1950 and Morey et al., 1962) used experimental solubility studies of quartz at the different vapour pressures of solution to develop a quantitative silica geothermometer assuming that the quartz is in equilibrium with other silica phases. Mahon (1966) described that silica concentrations in New Zealand geothermal wells (>150$^0$C) were controlled by quartz equilibrium. Quartz is the most stable among silica polymorphs (other varieties of silica) such as meta-stable chalcedony, cristobalite and opal which controls the silica concentrations in thermal water. Silica geothermometer is based on experimentally determined variations in the solubility of various silica species in thermal water which is a function of pressure and temperature.

The general reaction for silica dissolution is described by following equation:

$$SiO_{2(qtz)} + 2H_2O = H_4SiO_4 \text{.....Eqn (7.1)}$$

Geothermal systems with deep fluids at temperature>180$^0$C are found to be in equilibrium with quartz (Fournier, 1977). It is stable up to 870$^0$C and has the least solubility among other silica polymorphs and hence it is common as

primary and secondary minerals of rock forming the hydrothermal systems. Silica polymorphs with a less ordered crystal structure (i.e. chalcedony, opal CT, cristobalite) have higher solubility than quart and form at cooler temperature and therefore they are used for thermometry.

### 7.3.1 QUARTZ GEOTHERMOMETER *(MAXIMUM STEAM LOSS)*

Fournier (1981) has given an equation which compensates for loss of steam from boiling solutions. It also takes care of the resultant increase in the concentration of silica and the cooling of the solution by adiabatic expansion due to decrease in the hydrostatic-hydrodynamic pressure due to heat. This is represented by equation:

$$(T°C) = \frac{1522}{5.75 - logS} - 273.1 < 250°C \ldots\ldots\ldots\ldots\ldots\ldots Eqn(7.2)$$

*Where, T= temperature, S= silica (mg/L).*

### 7.3.2 QUARTZ GEOTHERMOMETER *(NO STEAM LOSS)*

The equation of Quartz *(no steam loss)* geothermometer represents experimentally determined solubilities and applies to the system that cool solely by conduction during ascend of the fluid. The silica quartz conductive cooling geothermometer is best used for geothermal springs at sub boiling temperature and is described as follows:

$$(T°C) = \frac{1309}{5.19 - logS} - 273.1 < 250°C \ldots\ldots\ldots\ldots\ldots\ldots\ldots\ldots\ldots\ldots Eqn\ (7.3)$$

*Where, T= temperature, S= silica (mg/L).*

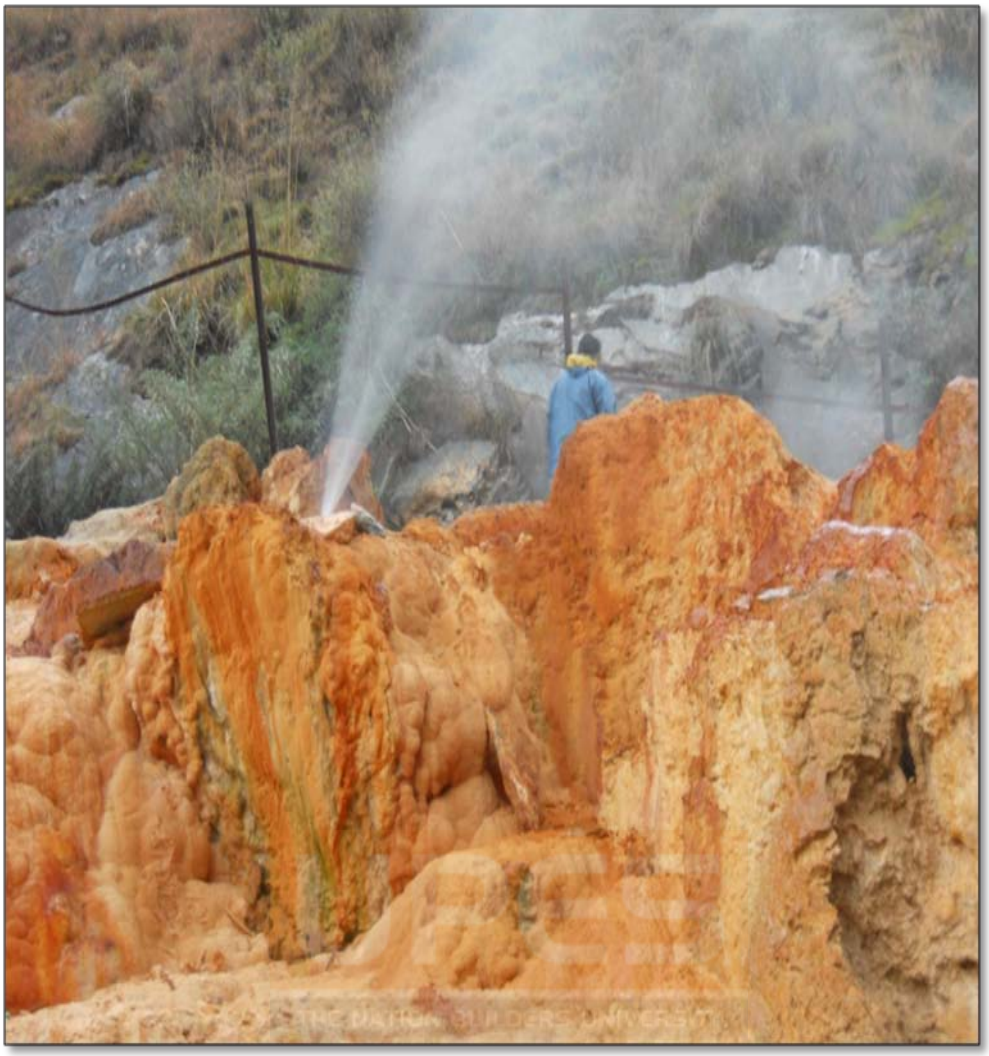

***Fig.7.1:*** *Field photograph of (Shaldhar, HS-04) geothermal spring of the Garhwal region where white yellowish deposits are also seen near the vent.*

### 7.3.3 CHALCEDONY GEOTHERMOMETER

Experimental observation shows that at temperatures ranging between 120-180$^0$C, chalcedony controls silica solubility in thermal waters. Under this situation, chalcedony may be applied for the better estimation of reservoir temperatures, which is described by the following equation.

$$(T°C) = \frac{1032}{4.61 - logS} - 273.1 < 250°C \ldots\ldots\ldots\ldots\ldots\ldots\ldots\ldots Eqn\ (7.4)$$

### 7.3.4 AMORPHOUS SILICA GEOTHERMOMETER

If the reservoir temperature is <100$^0$C, the amorphous silica may dominate the control on the solubility of silica. Under this conditions, geothermal systems with silisic host rocks, the abundance of volcanic gas may enable saturation of a fluid with respect to amorphous silica and will be best characterised by the following equation (Eqn 7.6 given by Arnorssion, 1983).

$$(T°C) = \frac{1112}{4.91 - logS} - 273.15 \quad < 250°C \quad \ldots\ldots\ldots\ldots\ldots\ldots Eqn\ (7.6).$$

Therefore, it depends upon the reservoir temperature which suggests the use of a specific geothermometer for their estimation.

## 7.4 SOURCE OF SILICA IN AQUEOUS SOLUTION

The present study investigates silica-water reactions in the low to moderate surface temperature springs from Garhwal, Himachal, and Ladakh regions of Himalaya with an objective to assess their reservoir temperatures. Data collected for this study consists of chemical analyses of geothermal springs which also include dissolved silica.

In earlier studies (Feth et al., 1964) has described that reactions of dissolved $CO_2$ with primary rock minerals, such as feldspars decides the chemical compositions in the thermal springs. Therefore, the dissolved silica in the geothermal springs may be present due to entirely by such acid attack. This is mediated through dissolved $CO_2$ (or $H_2CO_3$) which attacks the alumino-silicate minerals to releases cations and silica in the solutions. Studies

(Rimstidt & Barnes, 1980) have described that equilibration rates of silica polymorphs are very slow at lower temperature and therefore the use of Silica-quartz/chalcedony method suitable to estimate the temperature of low enthalpy reservoirs in volcanic geothermal terrains.

## 7.5 RESULTS AND DISCUSSION

Results of all the chemical analyses, including dissolved silica in these geothermal springs are mentioned in *Chapter 4*. A region wise discussion for the estimation on reservoir temperature is given as follows;

### 7.5.1 GARHWAL REGION

Reservoir temperatures were estimated based on silica for these waters which are presented in Table 7.1 and Fig. 7.2. The modified silica-quartz with no steam loss method of Fournier (1981) was applied to yield the reservoir temperatures ranging from $69^0$C (Bukki, HS-13) to $149^0$C (JanakiChatti) for this region. For comparison, the silica chalcedony method were also applied and it gave reservoir temperatures ranging from $40^0$C (Bukki, HS-13) to 121 (Jankichatti, Hs-18). Combining both equations used for these springs, the average minimum reservoir temperature for the Garhwal springs is estimated to be $111^0$C with the highest values of $135^0$C for (Jankichatti, HS-18). The estimated reservoir temperatures of the geothermal springs of study area are likely to be the minimum temperature while using silica based thermometers.

Results show that a maximum reservoir temperature is observed in Jankichatti HS-18, which lies near the Main Central Thrust (MCT) zone (Table 7.1& Fig.

7.2). This suggests that structural discontinuities are something to do with high temperatures of these springs and hence linked with magmatic/ deeper component in them.

***Table 7.1:*** *Reservoir temperatures of thermal springs of Garhwal region.*

| **Sites name** | **Sample ID** | **Silica-Chalcedony[a]** | **Silica-quartz *(no steam loss)*[b]** | **Arithmetic mean (°C)** |
|---|---|---|---|---|
| *Taptkund* | HS-1 | 98 | 126 | 112 |
| *Khiroi* | HS-2 | 104 | 132 | 118 |
| *Bhapkund* | HS-3 | 97 | 125 | 111 |
| *Shaldhar* | HS-4 | 99 | 127 | 113 |
| *Tapoban* | HS-5 | 98 | 126 | 112 |
| *Birahi* | HS-6 | 105 | 133 | 119 |
| *Ganoi* | HS-7 | 105 | 133 | 119 |
| *Langsi* | HS-8 | 79 | 108 | 93 |
| *Helang* | HS-9 | 88 | 116 | 102 |
| *Gaurikund* | HS-10 | 117 | 145 | 131 |
| *Gangnani* | HS-11 | 118 | 146 | 132 |
| *Jhaya* | HS-12 | 106 | 134 | 120 |
| *Bukki* | HS-13 | 40 | 69 | 54 |
| *Thirang* | HS-14 | 110 | 139 | 125 |
| *Matli* | HS-15 | 51 | 79 | 65 |
| *Kotimanep* | HS-16 | 120 | 148 | 134 |
| *Suryakund* | HS-17 | 103 | 131 | 117 |
| *Jankichatti* | HS-18 | 121 | 149 | 135 |
| *Banas* | HS-19 | 103 | 131 | 117 |
| *Wozari* | HS-20 | 72 | 101 | 86 |

{[$SiO_2$ (aq) as in mg/L] Silica-Chalcedony[a]: - temperature estimated by chalcedony geothermometer (Arnorsson and Gunnlaugsson, 1983); Silica-quartz (no steam loss) [b]: temperature estimated by quartz geothermometer, no steam loss (Fournier-1981)}.

However, the geothermal springs (Matli, HS-15; Bukki, HS-13; and Wozari, HS-20) lying slightly away from the MCT, show lower reservoir temperature as compared to those from the vicinity of MCT. Such a pattern indicates that the temperature and occurrences of these springs are possibly structurally controlled. However these inferences are open to test with more set of data in other part of the Himalaya before reaching the generalization.

### 7.5.2 HIMACHAL AND LADAKH REGIONS

Dissolved silica based geothermometer was also used for the geothermal springs from Himachal and Ladakh with silica-quartz no steam loss (Fournier, 1981). It yielded varying reservoir temperatures which can be classified into four groups (Table 7.2, Fig. 7.3).

***Table 7.2:*** R*eservoir temperatures of geothermal springs of Ladakh and Himachal regions*

| **Sites name** | **Sample ID** | **Silica-quartz** *(no steam loss)* * |
|---|---|---|
| *Changlung* | HS-21 | 107.2 |
| *Pulthang* | HS-22 | 72.0 |
| *Panamic* | HS-23 | 102.0 |
| *Gaik Hot spring* | HS-24 | 80.8 |
| *Chumatang* | HS-25_1 | 107.3 |
| *Puga* | HS-26 | 106.2 |
| *Sumdo* | HS-27 | 70.9 |
| *Thopan* | HS-28 | 68.3 |
| *Tapri hot springs* | HS-29 | 36.6 |
| *Tapri (Handpump)* | HS-29B | 67.9 |
| *Naptha* | HS-30 | 93.3 |
| *Jeori* | HS-31 | 70.4 |
| *Jhakri(S.J.V.N)Tunnel* | HS-32 | 43.6 |
| *Jharar* | HS-33/34 | 33.3 |
| *Bashist* | HS-35 | 80.9 |
| *KhiralBihal* | HS-36 | 81.7 |
| *Kalath* | HS-37 | 84.6 |
| *RamshilaKullu* | HS-38 | 69.1 |
| *Manikaran* | HS-39 | 83.9 |
| *Kasol* | HS-40 | 69.3 |

{[For all the methods $SiO_2$ (aq) as in mg/l] Silica-quartz (no steam loss)*: - temperature estimated by quartz Geothermometers, no steam loss (Fournier-1981)}.

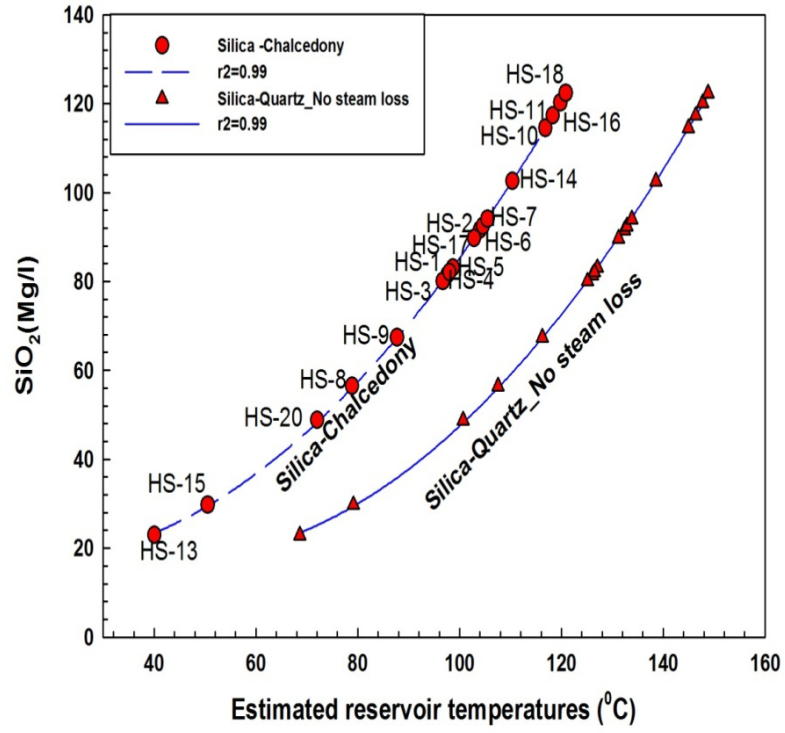


*(a)*

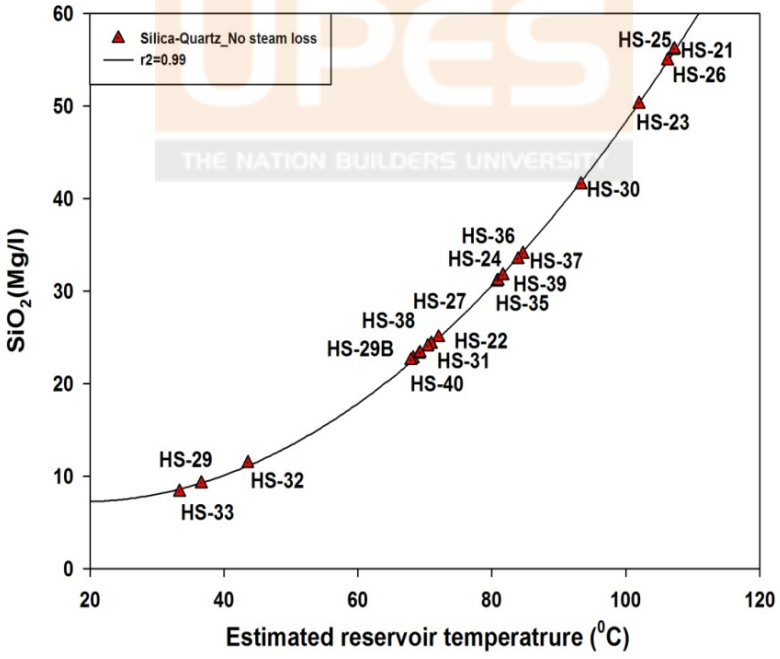


*(b)*

***Fig. 7.2:*** *Scattered regression plots showing the reservoir temperatures (a) Garhwal region, and (b) Himachal and Ladakh region.*

*Group A:* It covers the springs namely HS-29, HS-32, and HS-34 having lower surface temperature and little abundance of dissolved silica. Therefore it represents the reservoir temperature towards lower sides (34 to $68^0$C).

*Group B:* It consists of the geothermal springs namely Pulthang, HS-22; Sumdo, HS-27; Thopan, HS-28; Ramshila-Kullu, HS-38; and Kasol, HS-40 which exhibit moderate reservoir temperatures (~$70^0$C).

*Group C:* It groups the springs Gaik, HS-24; Khiral Bahal, HS-36; Kalath, HS-37, and Manikaran, HS-39 which display relatively higher reservoir temperature.

*Group D:* It shows the highest reservoir temperatures ($107^0$C) which include the Puga and Chumathang geothermal field. Based on this they may be the best sites to be explored for further geothermal exploration.



## 7.6 CONCLUSIONS

Geochemical thermometers constitute a valuable proxy for the exploration of geothermal energy and management of geothermal reservoirs. This work has attempted to estimate the reservoir temperature using dissolved silica geothermometers for all active the geothermal springs covering the Garhwal,

Himachal, and Ladakh regions of northwest Himalaya. These measurements have led to draw the following observations and inferences.

(i) The estimated reservoirs temperatures of geothermal springs of the study area are likely to be minimum temperatures on the surface using silica based thermometry. In the Garhwal region, maximum reservoir temperature of ~135$^0$C was estimated in Jankichatti (HS-18), which is situated close to MCT and seems to be structurally controlled by fault.

(ii) Geothermal springs (Matli-HS-15, Bukki-HS-13 and Wozari-HS-20) situated slightly away from the MCT show relatively lower reservoirs temperature as compared to those from the MCT zone.

(iii) Such a pattern indicates that the temperature and occurrences of these springs are inter-related.

(iv) In the Himachal and Ladakh regions, the average maximum reservoir temperature was observed to be107$^0$C in the group of springs covering Chumathang (HS-25), Puga (HS-26), Panamic (HS-23), and Manikaran (HS-39) which are situated along the ITSZ and MCT.

# *CHAPTER8*

# SYNTHESIS AND FUTURE PROSPECTS

# CHAPTER 8:

# SYNTHESIS AND FUTURE PROSPECTS

This thesis has made efforts to address issues pertaining to the origin of thermal springs in the northwest Himalaya and their role in contributing to $CO_2$ budget to the atmosphere. Towards this, majority of springs from Himalayan region have been demonstrated as source of volatiles with their origin from meteoric waters. These springs have facilitated to use the isotopic data to trace the altitude effects of stable isotopes in Himalayan region. The importance of estimating altitudinal effect lies with the fact that it represents an average precipitation from the region which could give a better estimate than those based on a flash rain sample. The results obtained in this study are summarized and given at the end of each chapter. Therefore, only a brief of their summaries with important conclusions and limitation are given in following paragraphs.

## 8.1 MAJOR AND TRACE ELEMENTS STUDY

Geothermal springs situated along the Alaknanda, Bhagirathi, and Yamuna valleys of Garhwal Himalaya; Sutlej, Parbati, Beas and Spiti valleys of Himachal Himalaya; Indus valley of Ladakh of the northwest Himalaya have

been extensively sampled and analysed for their physical parameters, major ions and trace elements to determine the plausible source of their origin. Manikaran geothermal springs situated in the Parbati valley of Himachal region was found to have the highest surface temperature of $95^0$C, ever recorded in the Himalayan geothermal belt.

Major ions chemistry of geothermal springs of the study area was used to classify the nature of geothermal fluids. The suitable mechanism for the origin of geothermal springs of the northwest Himalaya was suggested. This includes the scenario in which infiltrating water percolates through faults and fractures, and is heated up by a steeper geothermal gradient before it rises to the surface through the permeable zones. These springs also show a strong influence of silicate weathering with elevated abundances of $Na^+$ and $K^+$ contributing the majority of the cation budget. An elevated concentration of Arsenic (As), Boron (B) and Lithium (Li) in these waters suggest high temperature deep fluid mixing as a result of water-rock interaction in geothermal reservoirs.

## 8.2 STABLE ISOTOPES OF OXYGEN AND HYDROGEN

The geothermal spring samples were analyzed for their oxygen and hydrogen stable isotopes (δD and $\delta^{18}O$). These data has been used to infer about their recharge source and other hydrological processes regulating their isotopic compositions. These results combining with those from the Ganga, the Indus and Gaula catchment in the Himalaya were used to understand the altitude effect in the region. δD and $\delta^{18}O$ values in these waters including different

river valleys of Garhwal , Himachal and Ladakh regions , range from -45‰ to -124‰ and from -7.0‰ to -16‰, respectively. This corresponds to the altitude range from 1033 to 4410 m. The isotopic ratios of $\delta^{18}O$ and $\delta D$ in these waters were found to be more depleted towards the higher altitudes. Results show that the recharge source of these geothermal springs is mainly derived from the surface waters, ground waters and precipitations excepting few of them (i.e. Puga, Chumathang and Manikaran etc.) having the magmatic inputs. The "altitude effect" in these geothermal springs of Garhwal, Himachal & Ladakh regions is derived to be 0.25±0.027‰ and 0.24±0.025‰ per 100 m rise in altitude, respectively.

## 8.3 CARBON ISOTOPES ($\delta^{13}C_{DIC}$) & DEGASSING OF $CO_2$

Carbon isotope composition in the dissolved inorganic carbon ($\delta^{13}C_{DIC}$) in geothermal springs shows a wide range from -8.4 to +4.1. The $\delta^{13}C_{DIC}$ values of these geothermal springs are among the highest ratios reported from the northwest Himalaya. These are similar to those values of $\delta^{13}C_{DIC}$ in geothermal springs, reported from central Nepal, Himalaya, Yellowstone waters and associated travertine's, Utah (USA). These results provide evidence for metamorphic $CO_2$ degassing as ongoing process in the Himalaya. It also reveals that majority of them are of meteoric origin. However, few of them like Puga and Chumathang (from Ladakh), Sumdo (from Himachal Pradesh), Helang and Shaldhar (from Garhwal Himalaya) have some magmatic component mixed with them. Based on the major ion composition of 40 springs of different geothermal fields of combined northwest Himalaya (including Ladakh, Himachal, and Garhwal regions), the $CO_2$ flux is estimated

to be $2x10^8$moles/year. Present study show that the $CO_2$ degassing from the Himalayan orogen is one of the important donors to the global carbon budget today and acting as a source of $CO_2$ in the atmosphere.

## 8.4 HYDRO-GEOCHEMICAL THERMOMETRY

These geothermal resources provide an alternative energy source through the earth's internal heat accumulated over a longer period of time. This energy is relatively clean and renewable in nature and hence becoming a preferred choice for an alternative energy resource worldwide. It has a potential to generate 10,600 MW of electricity in India. However, the potential of geothermal energy is unexplored in India. Towards this geothermometers were used to assess the reservoir temperature of these springs. It works basically on dissolved constituents in the thermal fluid whose concentrations are controlled by the temperature of the fluids. These constituents may be solutes, dissolved gases and different isotopes present in them. Dissolved Silica based thermometry was used in these thermal springs to estimate reservoir temperature. Jankichatti geothermal spring shows the maximum reservoir temperature of $135^0$C in the Garhwal region. Results from Himachal and Ladakh regions indicate that high reservoir temperatures exist at Chumathang, Puga, and Panamic which have the potential to generate the geothermal energy in significant quantity. Therefore they could be promising sites for the low cost energy resource for India in future.

## 8.5 LIMITATIONS OF THIS STUDY

In addition to the above points, there are certain limitations which could be taken into considerations in future studies. This work is based on the sampling of spring waters but not the volatiles ($H_2O$, $SO_2$, $H_2S$, and $CO_2$ etc.) which are considered as relatively robust proxy in estimating the $CO_2$ degassing in different geological setups. Further, uses of non-traditional isotopes such as Si, Ge & Si /Ge etc. should be employed which are supposed to be diagnostic in detecting the deeper components contributing to these thermal springs. Keeping these points in view, it may be recommended as a future scope of research on this topic which is as follow;

[1] Volatile/gas sampling using giggenbach procedure to find out the $\delta^{13}C_{DIC}$ ratio of gas phase in thermal springs for a better understanding of carbon isotope fractionations.

[2] Our estimations of metamorphic $CO_2$ degassing are based on alkalinity and needed to be supplemented by analyses of stable and non-traditional isotopes for better estimate of the $CO_2$ flux.

# CHAPTER 9

## References

# CHAPTER 9:

# REFERENCES


Ackerman, T., Erickson, T., Williams, M.W. (2001). Combining GISandGPSto improve our understandingof the spatialdistribution of snow water equivalence, (SWE). *Proceedings of ESRI USERSConference*, San Diego, CA, 2001.

Aggarwal, N.C., & Kumar, G. (1973). Geology of the Upper Bhagirathi and Yamuna Valley, Uttarkashi district. *Him. Geo., (3)*, pp., 1-23.

Alam, A.M. (2002). Hydro geochemistry of thermal springs in Manikaran, Kullu District, Himachal Pradesh (India). *M.Sc. Dissertation (unpublished)*, I.I.T., Bombay, pp., 105.

Allen, E. T.,& Day, A., L. (1935). Hot Springs of the Yellowstone national Park. *Carnegie Institute Washington*, Publ. 466.

Arnorsson, S., & Andresdottir, A. (1995). Processes controlling the distribution of boron and chlorine in natural waters in Iceland. *Geochim. Cosmochim. Acta. 59* (20), pp., 4125-4146.

Arnorsson, S.(1983). The Chemistry of Geothermal waters in Iceland III, Chemical Geothermometry in Geothermal Investigations. *Geochim. Cosmochim. Acta, (47)*, pp.,567-577.

Arora, C. L. (1983). Geophysical exploration of the Puga Valley geothermal field, Ladakh District, Jammu and Kashmir State. *Geological Survey of India Special Publication (2)*, pp., 631-646.

Azeez, K.K.A., &Harinarayana, T. (2007). Magnetotelluric evidence of potential geothermal resource in Puga, Ladakh, NW Himalaya. *Current Geoscience,(93)*, pp., 323-329.

Auden, J. B. (1937). The structure of the Himalaya in Garhwal. *Rec. Geol. Surv. India*, *71*(4), pp., 407-433.

Barbier, E. (2002). Geothermal energy technology and current status: an overview.*Renewable and Sustainable Energy Reviews* (*6.1)*, pp., 3-65.

Barnes, I., Irwin, W. P.,& White, D. E. (1978). Global distribution of carbon-dioxide discharges, and major zones of seismicity, scale 1:40000, 000.*Water Resour. Invest., (11)* pp., *78-39*, open-file report, U.S. Geol. Surv., Washington, DC.

Bartarya, S. K, Bhattacharya S. K., Ramesh R., Somayajulu B. L. K. (1995). $\delta^{18}O$ and $\delta D$ systematics in the surficial waters of the Gaula catchment area, Kumaun Himalaya, India. *Journal of Hydrology*, *(167),* pp., 369–379.

Beaumont, C., Muñoz, J. A., Hamilton, J., & Fullsack, P. (2000). Factors controlling the Alpine evolution of the central Pyrenees inferred from a comparison of observations and geodynamical models. *Journal of geophysical Research: Solid Earth (1978–2012), 105* (B4), pp., 8121-8145.

Becker, J.A., Bickle, M.J., Galy, A., Holland, T.J.B. (2008). Himalayan metamorphic CO2 fluxes: quantitative constraints from hydrothermal springs. *Earth Planetary Science Letters* (*265),* pp., 616–629.

Bhatnagar, N.C. (1961). Hot springs of Kangra district, Punjab. *Unpublished, Geological Survey of India, Report*.

Bhattarai, D.R. (1980). Some geothermal springs of Nepal. *Tectonophysics, (62),* pp.,7-11.

Bhattacharya, A. R., & Siawal, A. (1985). Flattening of folds in the Main Boundary Thrust zone, southern Kumaun. *Geologie Mijnb,(63),*pp.,159-165.

Bhattacharya, S. K., Gupta, S. K., & Krishnamurthy, R. V. (1985). Oxygen and hydrogen isotopic ratios in groundwaters and river waters from India. *Proceedings of the Indian Academy of Sciences-Earth and Planetary Sciences*, *94* (3), 283-295.

Bickle, M. J. (1996). Metamorphic decarbonation, silicate weathering and the long-term carbon cycle. *Terra Nova, 8* (3), pp., 270-276.

Bilham, R., et al. (1997). Indo-Asian Convergence rates in the Nepal Himalaya.*Nature*, (*386),* pp., 61-66.

Bodvarsson, G.(1960). Exploration and exploitation of natural heat in Iceland. *Bulletin of Volcanologique, (23),* pp**.,** 241-250.

Chiodini, G., Cardellini, C., Amato, A., Boschi, E., Caliro, S., Frondini, F., & Ventura, G. (2004). Carbon dioxide Earth degassing and eismogenesisin central and southern Italy. *Geophysical Research Letters,*(*31),*doi:10.1029/2004GL019480.

Chandrajith, R., Johannes, Barth, A. C., Subasinghe, N. D., Dirk Merten, Dissanayake, C. B. (2012). Geochemical and isotope characterization of geothermal spring waters in Sri Lanka: Evidence for steeper than expected geothermal gradients.*Journal of Hydrology, (12).* S0022-1694 00956-0.

Chandrasekharam, D. (2000). Geothermal energy resources of India: country update. *Proceedings World Geothermal Congress, Kyushu-Tohoku, Japan*, pp. 133-138.

Cinti, D., Pizzino, L., Voltattorni, N., Quattrocchi, F., and Walia, V. (2009). Geochemistry of thermal waters along fault segments in the Beas and Parbati valleys (north-west Himalaya, Himachal Pradesh) and in the Sohna town (Haryana), India. *Geochemical Journal, 43*, (2), pp., 65-76.

Clark, I.D. & Fritz, P.(1997). Environmental Isotopes in Hydrology. *Lewis Publishers*, New York, pp. 328.

Cox, S. F. (1995). Faulting processes at high fluid pressures: An example of fault valve behaviour from the Wattle Gully Fault,Victoria,Australia.*J. Geophys. Res., (100)*, 12841–12859.

Craig, H.(1963). The isotopic geochemistry of waters and carbon in geothermal areas. Neuclear Geology on Geothermal Areas. *CNR, Pisa*. pp., 17-53.

Craig, H. (1961a). Isotopic variation in meteoric waters. *Science*, (*133)*, pp., 1702-1703.

Craig, H. (1961, b). *Standard for reporting concentrations of deuterium and oxygen-18 in natural waters. Science, (133), pp.* 1833-34.

Craig, J., Absar, A., Bhat, G., Cadel, G., Hafiz, M., Hakhoo, N., Kashkari, R., Moore, J., Ricchiuto, T.E., Thurow, J., Thusu, B. (2013). Hot springs and the Geothermal Energy potential of Jammu & Kashmir State, N.W. Himalaya, India. *Earth Science Reviews,* doi: 10.1016/j.earscirev.2013.05.004.

Dalai, T. K., Krishnaswami, S., &Sarin, M. M. (2002a). Major ion chemistry in the headwaters of the Yamuna River System: Chemical weathering, its temperature dependence and $CO_2$ consumption in the Himalaya. *Geochimica et Cosmochimica Acta,(66),* pp., 3397-3416.

Dalai, T.K. (2001). Major ions, Stable isotopes, 87Sr/86Sr and Re in the headwaters of the Yamuna: Implications to chemical weathering in the Himalaya.*PhD, Thesis,* M.S.University, Baroda.

Dansgaard, W.(1964). Stable isotopes in precipitation. *Tellus,16,* pp., 436-468.

Derry, L. A., Evans, M. J., Darling, R., France-Lanord, C. (2009). Hydrothermal heat flow near the Main Central Thrust,central Nepal Himalaya.*Earth and Planetary Science Letters, (286),* pp., 101-109,

Despande, R. D., Maurya, A. S.,Bhishm Kumar, Sarkar, A., & Gupta, S. K. (2010). Rain–vapor interaction and vapor source identification using stable isotopes from semiarid western India. *J. Geophy. Res., (115),* D-23311.

Dewey, J. F., & Bird, J. M. (1970). Mountain belts and the new global tectonics. *Journal of Geophysical Research,* (*75),* (14), pp., 2625-2647.

Dewey, J.F., & Burke, K.(1973). Tibetan, Variscan and Precambrian basement reactivation: products of continental collision. *J. of Geol, (81),* pp., 683–692.

Dulinski, M., Grabczak, J., Kostecka, A., Węcławik, S. (1995). Stable-isotope composition of speleancalcites and gaseous $CO_2$ from Tylicz (Polish Carpathians), *Chem. Geol., 125*(3–4), pp., 271–280.

Edmunds, W.M., Guendouz, A. H., Mamou, A., Moulla, A.,Shand, P., Zouari, K.(2003).Groundwater evolution in the Continential Intercalaire aquifer of southern Algeria and Tunisia: trace element and isotopic indicators. *Appl. Geochem., (18),*pp., 805–822.

Ellis, A.J.(1970). Quantitative interpretation of chemical characteristics of hydrothermal systems. *Geothermics (Spec. Iss. 2)*, pp., 516--528.

Ellis A. J.,&Mahon, W.A.J.(1977). Chemistry and Geothermal Systems. New York, Academic *Press INC*,p.392.

Evans, M. J., Derry, L. A., Anderson, S. P., France-Lanord, C. (2001). Hydrothermal source of radiogenic Sr to Himalayan rivers. *Geology*,*29* (9), pp., 803–806.

Evans, M.J., Derry, L.A.(2002). Geothermal fluxes of solutes, heat, and carbon to central Nepal rivers, pp., *225 Cornell University*, Ithaca, N.Y.

Evans, M. J., Derry, L. A. & France-Lanord, C.(2004). Geothermal fluxes of alkalinity in the Narayani river system of central Nepal. *Geochem. Geophys. Geosyst.*(*5)*, pp., 1-21.

Evans, M. J., Derry, L. A. & France-Lanord, C. (2008). Degassing of metamorphic carbon dioxide from the Nepal Himalaya.*Geochem. Geophys. Geosyst., (9),*Q04021, doi:10.1029/2007GC001796.

Ewen, T.L., Weaver, A., J. &Eby, M. (2004).Sensitivity of the inorganic carbon cycle to future climate warming in the U. Vic coupled model. *Atmosphere-Ocean*, (*42)*, pp., 23-42, doi:10.3137/ao.420103.

Ewers, G. R., & Keays, R. R. (1977). Volatile and precious metal zoning in the Broadlands geothermal field, New Zealand. *Econ. Geol., 72*, 1337-1354.

Ferry, J. M., & Dipple, G. M. (1991). Fluid flow, mineral reactions, and metasomatism. *Geology,(19)*, pp., 211–214.

Feth, J.H., Roberson, C.E., & Polzer, W.L. (1964). Sources ofmineral constituents in water from granitic rocks, Sierra Nevada, California and Nevada.*U. S. Geological Survey WaterSupply Paper, (70)*, pp., 1535-1.

Fournier, R. O. (1981). Application of water geochemistry to geothermal exploration and reservoir engineering inGeothermal Systems: Principles and case histories. Ryback Muffler eds., *John Wiley and Sons, N.Y.*, pp., 109-143.

Fournier, A.H.(1979). Geochemical and hydrologic considerations and the use of enthalpy chloride diagrams in the prediction ofunderground conditions in hot spring systems. *J. Vol. Geo. Res. (5),*pp., 1–16.

Fournier, R.O.(1977). Chemical geothermometers and mixing models for geothermal systems. *Geothermics,(5)*, pp., 41-50.

Fournier, R. O., and Rowe, J. J. (1966). Estimation of underground temperatures from thesilica content of water from hot springs and wet-steam wells. *Amer. J. Sci. (264)*, pp., 685-697.

Fournier,R. O., and Truesdella, H. (1973). An empirical Na-K-Ca geothermometer for natural waters. *G.C. A., (37),* pp., 1255-1275.

France, Lanord, C., &Derry, L. A. (1997). Organic carbon burial forcing of the carbon cycle from Himalayan erosion. *Nature, 390,* (6655), pp., 65–67.

Friedman, I. (1970). The isotopicchemistry of a travertine-depositing spring. *Geochim. Cosmochim. Acta, (34),* pp., 1303–1315.

Gaillardet, J., Dupre, B., Allegre, C. J. (1997). Chemical and physical denudation in the Amazon river basin. *Chem. Geol.*,(*142),* pp., 141–173.

Gaillardet, J., & Galy, A. (2008). Himalaya-carbon sink or source?. *SCIENCE-NEW YORK THEN WASHINGTON-*, *320* (5884), 1727.

Galy, A., & France-Lanord, C. (1999). Weathering processes in the Ganges-Brahmaputra basin and the riverine alkalinity budget.*Chemical Geology, (159),* pp., 31-60.

Galy V., France-Lanord C., Beyssac O., Faure P., Kudrass H. and Palhol F. (2007a). Efficient organic carbon burial in the Bengal fan sustained by the Himalayan erosional system.*Nature,* (*450),*pp., 407-410.

Galy, V., Beyssac, O., France-Lanord, C., Eglinton, T. (2008). Recycling of Graphite during Himalayan Erosion: A Geological Stabilization of Carbon in the Crust.*Science, V, 322*.

Gansser, A.(1964). Geology of the Himalayas. Wiley Inter-science, New York, *N.Y., 289*, pp.

Garzione, C. N, Dettman, D. L., Quade, J., DeCelles P. G., Butler R. F. (2000a). High times on the Tibetan Plateau: Palaeoelevation of the Thakkholagraben, *Nepal. Geology (28),*pp., 339-342.

Garzione, C. N., Quade, J., DeCelles P. G., English, N. B. (2000b). Predicting palaeoelevation of Tibet and the Himalaya from $\delta^{18}O$ vs.altitude gradients in meteoric waters across the Nepal Himalaya. *Earth and Planetary Science Letters (183),* pp., 215–229.

Giggenbach, W.F. (1983). Isotope and chemical composition of Parbati valley geothermal discharges Northwest Himalaya, India. *Geothermics (12),* pp., 199-222.

Giggenbach, W.F. (1988). Geothermal solute equilibria: derivation of Na-K-Mg-Ca geoindicators. *Geochim. Cosmochim. Acta, (52),* pp., 2749-2765.

Giggenbach, W. F. (1991). Chemical techniques in geothermal exploration. In D'Amore, F. (coordinator), Application of geochemistry in thermal reservoir development. *UNITAR/UNDP publication, Rome, pp. 119-142*.

Guay, B., Eastoe, C., Bassett, R., & Long, A. (2006). Sources of surface and ground water adjoining the Lower Colorado River inferred by $\delta^{18}O$, $\delta D$ and $^{3}H$. *Hydrogeology Journal, (14),* pp., 146-158.

Guo, L., & Riding, R. (1998). Possible microbial effects on stable carbon isotopes in hot-spring travertines. *J. Sed. Res., 66* (3), pp., 468–473.

Gupta, M. L., Saxena, V. K., & Sukhija, B. S. (1976). An analysis of the hot spring activity of the Manikaran area, Himachal Pradesh, India, by geochemical studies and tritium concentration of spring waters. In:

Proceed. 2nd UN, Symp. *Development and UseofGeothermal Resources, San Francisco, (1),* pp., 741-744.

Geological Survey ofIndia. (1991). Geothermal Atlas of India. *Geol. Surv. India, Sp.Pub. (19),* pp., 143.

Gyanprakash & Raina, C. B. (1975). Report on preliminary geothermal investigation of some hot springs of U.P., Himalaya. *Unpublished, G.S.I, report.*

Han, D. M. (2010). Evaluation of groundwater hydrochemical characteristics and mixing behaviour in the Daying and Qicun geothermal systems, Xinzhou Basin. J. *Volcanol. Geotherm. Res. (189),* pp., 92–104.

Harinarayana, T., Abdul Azeez, K. K., Murthy, D. N., Veeraswamy, K., Eknath Rao, S. P., Manoj, C., and Naganjaneyulu, K. (2006). Exploration of geothermal structure in Puga geothermal field, Ladakh Himalayas, India, by magnetotelluric studies. *J. Appl. Geophys.,(58),* pp., 280–295.

Harrison, T. M., Yin, A., Ryerson, F. J. (1998a). Orographic evolution of the Himalaya and Tibet. In Tectonic Boundary Conditions for Climate Reconstructions, ed. T. J Crowley, K Burke, *pp. 39–72*. New York: *Oxford Univ. Press.*

Harrison, T. M., Copeland, P., Kidd, W. S. F., Yin, A. (1992). Raising Tibet. *Science,(255),* pp., 1663-1670.

Heim, A., & Gansser, A. (1939). Central Himalaya Geological Observation Memories society *Helv. Sci. Nature., (73),* pp., 1-246.

Henley, R. W., Truesdell, A. H., Barton Jr. P. B. (1985). Fluid-Mineral Equilibria in Hydrothermal Systems Robertson J. M. *ed, Society of Economic* Geologists.

Henley, R.W., & Ellis, A. J. (1983). Geothermal Systems Ancient and Modern: A Geochemical Review. *Earth-Science Reviews* ,*(19)*,pp., 1-50.

Henry, P., Le., Pichon, X., Goffe´, B. (1997). Kinematic, thermal and petrological model of the Himalayas; constraints related to metamorphism within the underthrust Indian crust and topographic elevation. *Tectonophysics,273,* (1-2), pp., 31–56.

Hochstein, M. P., & Regenauer, L. K. (1998). Heat generation associated with collision of two plates: The Himalayan geothermal belt. *Jour. of Vol. Geo.*, (*83)*,pp.,75-92.

Hochstein, M. P., & Yang, Z. (1995). The Himalayan Geothermal Belt (Kashmir, Tibet, West Yunnan). In: Terrestrial Heat Flow and Geothermal Energy in Asia. (Eds: Gupta, M. L. and Yamamo, M.) *Oxford and IBH Publishing Co.,* New Delhi, pp., 331-368.

Hochstein, M.P., Yang, Z. & Ehara, S. (1990). The Fuzhou geothermal system (People's Republic of China): Modeling study of a low temperature, fracture zone system. *Geothermics,*(*19),* pp., 43-60.

Jangi, B.L., Gyanprakash, Dua, K. J. S, Tussu, J. L., Dhimri, D. B., & Pathak, C. S. (1976). Geothermal exploration of the Parbati valley geothermal field, Kulu district, Himachal Pradesh, India. In: Proceed. 2nd UN Symp. *Development and Use of Geothermal Resources,* San Francisco, *Vol. (2),* pp., 1085-1094.

Jangi, B. L., & Absar, A. (1977). Report on the stable isotope,radioactive and conventional geochemical studies in the Hydrogeological basin covering Puga-Chumathang Geothermal fields and adjoining areas, Ladakh District, Jammu and Kashmir state with a note on the well head measurements in Puga Valley. *Report of the Geol. Sur. Of India. Unpublished.*

Janik, C. J., Truesdell, A. H., Goff, F., Shevenell, L., Stallard, M. L., Trujillo, P. E., Counce, D. (1991). A geochemical model for the Platanares geothermal systems, Honduras. *J. Vol. Geo. Res., (45), pp., l25*-146.

Jenkin, G. R. T., Craw, D., and Fallick, A. E. (1994). Stable isotopic and fluid inclusion evidence for meteoric fluid infiltration into an active mountain belt; Alpine Schist, New Zealand: *J. of Met. Geo., (12),* pp., 429–444.

Kennedy, G. C. (1950). A portion of the system silica-water. *Economic Geology, (45),* pp., 629-653.

Shivanna, K.,Tirumalesh, K., Noble, J., Joseph T. B., Gursharan, S., Joshi. A. P., Khati, V. S. (2008). Isotopic techniques to identify recharge areas of springs for rainwater harvesting in the mountainous region of Gaucher areas, Chamoli district, Uttarakhand, India. *Current Science, (94),1003*.

Kerrick, D. M., & Caldeira, K. (1998). Metamorphic $CO_2$ degassing from orogenic belts.*Chem. Geol.,145,* (3-4), pp., 213-232.

Kharaka, Y. K., & Mariner, R. H. (2005). Geothermal systems, in Aggarwal, P.K., Gat, J.R., and Froehlich, K.F.O., eds., Isotopes in the Water

Cycle: Past, Present, and Future of a Developing Science,*Springer*, pp,.243-270.

Kharaka, Y. K., Mariner, R. H. (1989). Chemical geothermometers and their application to formation waters from sedimentary basins. In: Naeser, N.D., McCulloch, T. (Eds.), Thermal History of Sedimentary Basins. *Springer Verlag, New York*, pp. 99–117.

Koons, P. O., & Craw, D. (1991). Evolution of fluid driving forces and composition within collisional orogens. *G. R. L., (18),* 5, pp., 935-938.

Koons, P. O., Craw, D., Cox, S., Upton, P., Templeton, A., Chamberlain, C. P. (1998). Fluid flow during active oblique convergence: a southern Alps model from mechanical and geochemical observations. *Geology (26),* pp., 159–162.

Krishnamurthy, R. V., and Bhattacharya, S., K. (1991). Stable Oxygen and hydrogen isotope ratios in shallow groundwater from India and a study of the role of evapotranspiration in the Indian monsoon. S*pl., Publ.,(3),The geochemical society*, pp., 187-193.

Krishnaswami, S., Singh S. K., and Dalai, T. K. (1999). Silicate weatheringin the Himalaya: Role in contributing to major ions and radiogenic Sr to the Bay of Bengal. *Ocean Science, Trends andFuture Directions. Indian National Science Academy and Akademia International*, New Delhi, pp., 23-51.

LeeFort, P. (1975). Himalayas- the collided range-present knowledge of the continents arc. *Am. J. of Sci., A,(275),* pp., 1-44.

Maheo, G., Bertrand, H., Guillot, S., Villa, I. M., Keller, F., & Capiez, P. (2004). The South Ladakh ophiolites (NW Himalaya, India): an intra-

oceanic tholeiitic arc origin with implication for the closure of the Neo-Tethys. *Chemical geology, 203(3),* pp., 273-303.

Maheo, G., Fayoux, X., Guillot, S., Garzanti, E., Capiez, P., &Mascle, G. (2006). Relicts of an intra-oceanic arc in the Sapi-Shergol melange zone (Ladakh, NW Himalaya, India): Implications for the closure of the Neo-Tethys Ocean. *Journal of Asian Earth Sciences, 26* (6), pp., 695-707.

Mahon, W.A.J.(1964). Fluorine in the natural thermal waters of New Zealand. *New Zealand Journal of Science (7),* pp., 3-28.

Mahon, W. A. J. (1966). Silica in hot water disoharge from drillholes at Wairakei, New Zealand. *N.Z. J. Sci.(9), pp.*, 135-144.

Mazor, I., E. (1997). Chemical and isotopic groundwater hydrology: *the applied approach, 2nd , rev. and expand ed., xii, 413* pp., M. Dekker, New York.

Meng, J., Wang, C., Zhao, X., Coe, R., Li, Y., & Finn, D. (2012). India-Asia collision was at 24 [deg] N and 50 [emsp14] Ma: palaeomagnetic proof from southernmost Asia. *Scientific reports, 2*.

Merali, Z., Skinner, B. J., Strahler, A. H., & Strahler, A. H. (2009). *Visualizing Earth Science*. Wiley.

Middlemiss, C. S. (1910). Revision of Silurian-Trias sequence of Kashmir. *Record Geological Survey of India 40(3),* pp., 206–260.

Mishra, H. P. (1996). Geo-electrical studies for demarcating geothermal reservoir in Puga Valley, Ladakh District, Jammu and Kashmir. *Geological Survey of India, Special Publication (45),* pp., 65-68.

Molnar, P., & England, P. (1990). Late Cenozoic uplift of mountain ranges and global climate change: chicken or egg. *Nature, (346),*pp., 29-34.

Molnar, P. (1987). Inversion profile of uplift rates for geometry of dip-slip faults at depth, with example from Alps and Himalaya. *Ann. Geophysicae, (5),* pp., 663-670.

Mook, W.G., Bommerson, J. C., Staverman, W. H. (1974). Carbon isotope fractionation between dissolved bicarbonate and gaseous carbon dioxide. *Earth Plan. Sci. Lett. 22,*(2), pp., 169-176.

Morey, G. W., Fournier, R. O. and Rowe, J. J. (1964). The solubility of amorphous silica at 25°C. *Jour. of Geoph. Res., (69),* pp., 1995-2002.

Naboko, S. I., & Karpov, G.A.(1977). Pore solution metasomatism, sulphide formation. Proc. II Int. Symp. Water-Rock Interaction. *Strasbourg, III*: pp., 46-53.

Newell, D. L., Jessup, J. M, Cottle, M. J., Hilton, R. D, Sharp, Z. D. (2008). Aqueous and isotope geochemistry of mineral springs along the southern margin of the Tibetan plateau: Implications for fluid sources and regional degassing of $CO_2$. *$G^3$ (Q08014, doi: 10.1029/2008GC002021).*

Nicholson, K. (1993). Geothermal Fluids, Chemistry and Exploration Techniques. *Berlin, Springer-Verlag Heidelberg*, New York, 263 p.

Paces, T. (1978). Reversible control ofaqueous aluminum and silica during the irreversible evolution of natural waters. *Geochimica et. Cosmochimica Acta, (42),* pp., 1487-1493.

Pande, K, Padia, J. T, Ramesh, R., Sharma, K., K. (2000). Stable isotope systematics of surface water bodies in the Himalayan and Trans-

Himalayan (Kashmir) region. Proceedings of the Indian Academy of Sciences , *Earth and Planetary Science, (109),*pp., 109–115.

Pasvanoglu, S., and Chandrasekharam, D. (2011). Hydro-geochemical and isotopic study of thermal and mineralized waters from the Nevsehir (Kozakl) area, Central Turkey. *J. of Vo. and Geo. Res., 202,* (3-4): 241-250.

Pentecost, A. (1995). Geochemistry of carbon dioxide in six travertine-depositing waters of Italy. *Jour. of Hydrology, 167* (1–4), 263–278.

Perrier, F., Richon, P., Byrdina, S., France-Lanord, C., Rajaure, S., Koirala, B. P., & Nath Sapkota, S. (2009). A direct evidence for high carbon dioxide and radon-222 discharge in Central Nepal. *Earth and Planetary Science Letters, 278* (3), pp., 198-207.

Piper, A. M. (1944). A graphical procedure in the geochemical interpretation of water analyses, *Eos Trans. AGU, (25),* pp., 914–923.

Plummer, L. N. (2004). Dating of young groundwater, Isotope Hydrology and Integrated Water Resources Management, IAEA-CSP-23.*International Atomic Energy Agency, Vienna,* pp., 19-20

Racoviteanu, A. E. (2007). Evaluating digital elevation models for glaciologic applications: An example from Nevado Coropuna, Peruvian Andes. *Global and Planetary Change, (59),*pp., 110-125.

Ranga Rao, A. (1972). Traverses in the Himalaya of Uttar Pradesh. *Geological Survey of India Miscellaneous publication No. 15*.

Ramesh R., &Sarin, M.M. (1992). Stable isotope study of the Ganga (Ganges) river system. *Journal of Hydrology (139),* pp., 49-62.

Ramstein, G., Fluteau, F., Besse, J., Joussaume, S. (1997). Effect of orogeny, plate motion and land sea distribution on Eurasian climate change over the past 30 million years. *Nature (386)*, pp., 788-795.

Ravishankar, (1988). Heat-flow map of India and discussion on its geo-logical and economic significance. *Indian Miner*, *42*, pp., 89-110.

Rawat, G. (2012). Electrical Conductivity Imaging of Uttarakhand Himalaya Using MT Method. Unpublished Ph.D. Thesis. Indian Institute of Technology (IIT), Roorkee, India.

Rice, J. R. (1992). Fault stress states, pore pressure redistributions, and the weakness of the San Andreas fault, in fault Mechanics and Transport Properties of Rock.Edited by B. Evans and T.-f. Wong, *Academic, San Diego, Calif*, pp., 476-503.

Rimstidt, J. D., & Barnes, H. L. (1980). The kinetics of silica-water reactions. *Geochimica et CosmochimicaActa., (44)*, pp., 1683-1699.

Roy, A. B., & Valdiya, K. S. (1988). Tectonomorphic evolution of Great Himalayan sheet in Garhwal region, Kumaun Himalaya. *Jour. Geol. Soc. Ind., (32)*, pp., 106-124.

Royden, L. H., Burchfiel, B. C., King, R. W., Wang, E., Chen, Z., Shen, F., Liu, Y. (1997). Surface deformation and lower crustal flow in eastern Tibet. *Science (276)*, pp., 788–790.

Rozanski, K., Araguas-Araguas L, Gonfiantini R. (1993). Isotopic patterns in modern global precipitation. In Climate Change in Continental Isotopic Records. *Monograph 78,American Geophysical Union:Washington*, DC; pp., 1–36.

Upadhyay, R. (2001). Middle Cretaceous carbonate build-ups and volcanic seamount in the Shyok suture, northern Ladakh, India. *Curr Sci*, (*81),* pp., 695-699.

Sano, Y.,& Marty, B. (1995). Origin of Carbon in fumarolic gas from island arcs. *Chemical Geology, (119),* Pp., 265-274.

Schotterer, U., Fröhlich, K., Gäggeler, H. W., Sandjordj, S., Stichler, W. (1997). Isotope records from Mongolian and alpine ice core as climate indicator. *Climate Change,(36),*pp., 519-530.

Sehgal, M. L. (1963). Report on geological mapping in Parbati Valley, Kulu subdivision, Kangra district, Punjab, Progress report. 1962-63, *Govt. India*, pp., 1-11.

Searle, M. P., Parrish, R. R., Hodges, K.V., Hurford, A., Ayres, M.W., Whitehouse, M. J. (1997). Shisha Pangma leucogranite, south Tibetan Himalaya: field relations, geochemistry, age origin and emplacements. *J. Geol., (105),*pp., 295-317.

Sharp, Z. (2007). *Principles of stable isotope geochemistry, (p.344).* Upper Saddle River, NJ: Pearson education.

Shipton, Z. K., Evans, J. P., Kirschner, D., Kolesar, P. T., Williams, A. P., & Heath, J. (2004). Analysis of CO2 leakage through 'low-permeability'faults from natural reservoirs in the Colorado Plateau, east-central Utah. *Geological Society, London, Special Publications*, *233*(1), pp., 43-58.

Sibson, R. H. (1992). Fault-valve behaviour and the hydrostatic-lithostatic fluid pressure interface. *Earth Sci. Rev., 32*, pp., 141-144.

Sibson, R. H. (2000). Fluid involvement in normal faulting.*J.Geod,29*,449-469.

Siegenthaler, U., & Matter, H. A. (1983). Dependence of $\delta^{18}O$ and δD in Precipitation on Climatein Paleoclimates and Paleowaters. *A Collection of Environmental Isotope Studies*, IAEA, Vienna,pp., 37-51.

Singh, S. B., Drolia, R. K., Sharma, S. R. & Gupta, M. L. (1983). Application of resistivity surveying to geothermal exploration in the Puga Valley, India. *Geoexploration, (21)*, pp., 1-11.

Smith, T. (2007). A Bright Future for Geothermal Energy. *GEOExPro*, pp., **36-46.**

Tapponnier, P., Xu, Z.Q., Roger, F., Meyer, B., Arnaud, N., Wittlinger, G., Yang, J.S. (2001). Geology-oblique stepwise rise and growth of the Tibet plateau. *Science (294),* pp., 1671-1677.

Tewari, A. P. (1970). General Report for 1966-67, Rec. *Geological Survey of India, Vol. 101*, Pt., 1.

Thakur, V. C., & Rawat, B. S. (1992). Geological Map of Western Himalaya, 1: 1,000,000. *Wadia Inst., of Himalayan Geology*, Dehra Dun, India.

Thakur, V. C., & Misra, D. K. (1984). Tectonic framework of the Indus and Shyok suture zones in eastern Ladakh, northwest Himalaya. *Tectonophysics*, *101* (3), pp., 207-220.

Tong, W., & Zhang, J. (1981). Characteristics of geothermalactivities in Xizang Plateau and their controlling influence on Plateau's tectonic model. In: Geological and Ecological studies of the Quinghai-Xizang Plateau. *Gordon and Breach*, New York, pp., 841-846.

Truesdell, A. H. (1989). Origin and transport of chloride in superheatedgeothermal steam. *Geothermics, (18),* pp., 295-304.

Truesdell, A. H., & Marion, A. M. (1977). Geochemical indications ot boiling in the aquifer of the Cerro Prieto geothermal field. Presented at *Primera Reunion de Intercambio Tecnicosobr eGeotermia,* San Felipe,B.C.

Valdiya, K. S. (1988). Tectonics and evolution of the central sector of the Himalaya. Philosophical Transactions of the *Royal Society of London. Series A (326),* pp., 151– 174.

Valdiya, K. S. (1999). *Indian J. Geol., (71),* pp., 53–63.

Valdiya, K. S., Paul, S. K., Tara Chandra, Bakuni, S. S., & Upadhya, R. (1999). Tectonic and lithological characterization of Himadri (Great Himalaya) between Kali and Yamuna river, Central Himalaya.*Him.Geo, Vol. 20* (2), pp.,1-7.

Veeraswamy, K., Abdul Azeez, K. K., Basava, S., Naidu, D. G., Harinarayana, T. (2010). Electrical structure across lesser and higher N.W., Himalaya, India. *Chinese J. Geophys., 53, (3),*pp., 576-584.

Williams, S. N., Schaefer M. L., Calvache, J. V., Lopez, D. (1992), Global carbon dioxide emission to the atmosphere by volcanoes, *Geo. Cosmo. Acta, 56* (4), pp., 1765-1770.

Williamson, J. H. (1968). Least square fitting of a straight line.*Canadian Journal of Physics (46),* pp., 1845-1847.

Witcher, J.C., King, J.P., Hawley, J.W., Kennedy, J. F., Williams, J., Cleary, M., Bothern, L. R. (2004). Sources of Salinity in the Rio

Grande and Mesilla basin groundwater. *Water Resources Research* Institute Completion Report No. 330.

Yin, A. (2002). Tectonic history of the Al tynTagh fault system in northern Tibet inferred from Cenozoic sedimentation. *Geological Society of America Bulletin (114)*, pp., 1257-1295.

Yin, A. (2006). Cenozoic tectonic evolution of the Himalayan orogen as constrained by along-strike variation of structural geometry, exhumation history, and foreland sedimentation. *E. Sc. Reviews, (76),* pp., 1131.

Yao, T. D. (2000). Amplitude of Climatic Changes in Qinghai-Tibetan Plateau. *Chinese Science Bulletin, 45* (1), pp., 98–106, (in Chinese).

Younger, P. L., & Gluyas, J. G. (2012). Development of deep geothermal energy resources in the U. K. *Proceedings of the Institution of Civil Engineers, Energy (165)*, pp., 19-32.